

MALATYA TURGUT ÖZAL UNIVERSITY

# NATURENGS

MTU Journal of Engineering and Natural Sciences

Volume: 1 Issue: 1-June 2020



<https://dergipark.org.tr/tr/pub/naturengs>  
[www.naturengs.com](http://www.naturengs.com)

MALATYA TURGUT ÖZAL UNIVERSITY



MTU Journal of Engineering and Natural Sciences

Volume: 1 / Issue: 1 / June - 2020

We are delighted to present the first issue of the journal NATURENGS owned by Malatya Turgut Özal University. MTU Journal of Engineering and Natural Sciences – NATURENGS is a double-blind peer-reviewed, open-access international journal which will publish electronically two times in a year by the Malatya Turgut Özal University from June 2020.

We set out with the desire to create an environment where scientific and / or technological studies carried out in universities, industry and other research institutions will be shared. We aim to advance by giving priority to studies involving scientific and / or technological originality.

Manuscripts submitted for publication are analyzed in terms of scientific quality, ethics and research methods in terms of its compliance by the Editorial Board representatives of the relevant areas. Then, the abstracts of the appropriate articles are sent to at least two different referees with a well-known in scientific area. If the referees agree to review the article, full text in the framework of the privacy protocol is sent. By the decisions of referees, either directly or corrected article is published or rejected. Confidential reports of the referees in the journal archive will be retained for ten years. All post-evaluation process is done electronically on the internet.

In the journal's publication policy, we would like to state that we will not compromise on quality. In this process, we know that we have undertaken important tasks, especially the selection of referees and monitoring of evaluations. We will work with the devotion to get our journal into the TR-Index and then the Science Citation Index database as soon as possible.

We would like to thanks our Rector, **Prof. Dr. Aysun Bay KARABULUT**, who encouraged and supported the establishment of our journal.

Also; we would like to express our gratitude and respect to Scientific Board, Authors, Section Editors and Referees.

*Assist. Prof. Aydan AKSOĞAN KORKMAZ  
On behalf of the Editorial Board*

**Volume: 1 / Issue: 1 / June- 2020**

**Owner / Publisher**

**Prof. Dr. Aysun BAY KARABULUT** for Malatya Turgut Özal University

**Editors-in-Chief**

**Prof. Dr. Mehmet ÜLKER**

Malatya Turgut Özal University, 44210 Battalgazi/Malatya,  
TURKEY Phone: +90-422-846 12 55 Fax: +90-422-846 12 25  
e-mail: mulker44@gmail.com

**Co-Editors-in-Chief**

**Assist. Prof. Aydan AKSOĞAN KORKMAZ**

Malatya Turgut Özal University, 44210 Battalgazi/Malatya,  
TURKEY Phone: +90-422-846 12 55 Fax: +90-422-846 12 25  
e-mail: aydan.aksogan@ozal.edu.tr

**Co-Editors-in-Chief**

**Assist. Prof. Harun KAYA**

Malatya Turgut Özal University, 44210 Battalgazi/Malatya,  
TURKEY Phone: +90-422-846 12 55 Fax: +90-422-846 12 25  
e-mail: harun.kaya@ozal.edu.tr

**Contact Information**

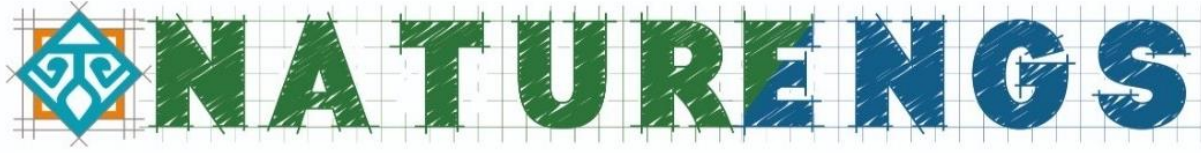
MTU Journal of Engineering and Natural Sciences – NATURENGS,  
Malatya Turgut Özal University, 44210, Battalgazi/Malatya, TURKEY

Phone: +90-422 846 12 55, Fax: +90-422 846 12 25,

e-mail: naturengs@ozal.edu.tr

web: <https://dergipark.org.tr/tr/pub/naturengs>

**MALATYA TURGUT ÖZAL UNIVERSITY**



**MTU Journal of Engineering and Natural Sciences**

**Volume: 1 / Issue: 1 / June - 2020**

**OWNER**

**Aysun BAY KARABULUT, The Rector of Malatya Turgut Özal University**

**EDITORIAL BOARD**

**Mehmet ÜLKER, Editors-in-Chief**

**Aydan AKSOĞAN KORKMAZ, Co-Editors-in-Chief**

**Harun KAYA, Co-Editors-in-Chief**

---

**SECTION EDITORS**

**Aziz AKSOY (Malatya Turgut Özal University, Turkey)**

**Burçin DOĞAN (Malatya Turgut Özal University, Turkey)**

**Deniz KORKMAZ (Malatya Turgut Özal University, Turkey)**

**Eser SERT (Malatya Turgut Özal University, Turkey)**

---

**CONTENTS**

**A Comparison of The Relationship Between Electricity Consumption and Gross Domestic Product According to Development Status of Countries**

Özlem AKAY, Esmâ KAHRAMAN, Ahmet Mahmut KILIÇ ..... 1

**Temperature and Relative Humidity Models of The Malatya City**

Ayşe BİÇER ..... 11

**In Dynamic Systems with Fuzzy A - Cutting Determination of Membership Function Ranges**

Fatih TOPALOĞLU, Hüseyin PEHLIVAN ..... 19

**New Analytical Solutions for Space and Time Fractional Phi-4 Equation**

Ayşegül DAŞCIOĞLU, Sevil ÇULHA ÜNAL, Dilek VAROL BAYRAM ..... 30

**Synthesis of New Bisbenzimidazole Salts and Determination Their Ligand Activities in C-C Coupling Reactions**

Ülkü YILMAZ, Hasan KÜÇÜKBAY ..... 47

**Evaluation of Noise Emission in A Textile Plant**

Zekeriya DURAN, Mehmet GENÇ, Tuğba DOĞAN, Bülent ERDEM ..... 53



## A Comparison of the Relationship Between Electricity Consumption and Gross Domestic Product According to Development Status of Countries

Özlem AKAY<sup>1\*</sup>, Esmâ KAHRAMAN<sup>2</sup>, Ahmet Mahmut KILIÇ<sup>3</sup>

<sup>1</sup> Department of Statistics, Faculty of Science and Letters, Çukurova University, Adana, Turkey.

<sup>2,3</sup> Department of Mining Engineering, Faculty of Engineering, Çukurova University, Adana, Turkey.

(Received: 03.02.2020; Accepted: 18.03.2020)

**ABSTRACT:** Electricity is a requirement for the economic, social and cultural progress for all developed, developing and under-developed countries. This paper examines the relationships between electricity consumption and gross domestic product in 30 countries, using data for the period 1995–2014. These countries are classified according to their developmental status. Widely used tests for the panel unit root, heterogeneous panel cointegration, and panel-based error correction models were employed. The empirical results indicate that electricity consumption and economic growth appear to be cointegrated. The long-run and short-run relationships are estimated using suitable estimations. The results show that the developmental levels of countries differ in their impact on the relationship between electricity consumption and GDP.

**Keywords:** Electricity consumption, Developmental status, Panel data analysis, Long-run, Short-run.

### 1. INTRODUCTION

Energy is considered to be a prime agent in wealth generation and also a significant factor in economic development. The importance of energy in economic development has been recognized universally, with historical data attesting to a strong relationship between the availability of energy and economic activity [1]. In the past decades the world's energy demand and consumption have maintained a steady growth [2].

Economic growth, which is measured by gross domestic product (GDP), is a key determinant in the growth of energy demand. The world's GDP will rise by 3.0% per year from 2015 to 2040. The fastest rates of growth are projected to be for the emerging, non-OECD regions, where combined GDP increases of 3.8% per year, driving the fast-paced growth in future energy consumption among those nations. In the OECD regions, GDP will grow at a much slower rate of 1.7% per year between 2015 and 2040, at least in part, because of slow or declining population growth in those regions [3].

\*Corresponding Author: oakay@cu.edu.tr

ORCID number of authors: <sup>1</sup>0000-0002-9539-7202, <sup>2</sup>0000-0002-4326-7202, <sup>3</sup>0000-0002-2082-749X

According to the International Energy Outlook Report, (EIA, 2017) world net electricity generation will increase by 45%, rising from 23.4 trillion kilowatt-hours (kWh) in 2015 to 34.0 trillion kWh in 2040. Electricity is the world's fastest-growing form of end-use energy consumption, as it has been for many decades. Power systems continue to evolve from isolated, noncompetitive grids to integrated national and international markets. The strongest growth in electricity generation is projected to occur among the developing, non-OECD nations. Increases in electricity generation in non-OECD countries average 1.9% per year (Reference case (IEO 2017)) in International Energy Outlook 2017). As rising living standards increase the demand for home appliances and electronic devices, and for commercial services, including hospitals, schools, office buildings, and shopping malls increases. In the OECD nations, where infrastructures are more mature and population growth is relatively slow or declining, electric power generation will increase by an average of 1.0% per year from 2015 to 2040 in the IEO 2017 Reference case [3].

The purpose of this article was to examine the relationship between electricity consumption and gross domestic product (GDP) in 30 countries. These countries were divided into three groups: developed, developing and under-developed countries. These countries were chosen because electricity consumption and gross domestic product data in these countries are regular and complete.

Electricity consumption has been increasing day by day alongside the development of industry and population increase. This situation has led researchers to investigate the relationship between the economy and energy.

Some research has shown country-specific causality between energy consumption and economic growth and can provide insight for designing future energy policy. Bah and Azam (2017) investigated the causal relationship between electricity consumption, economic growth, financial development, and CO<sub>2</sub> emissions for South Africa over the period 1971–2012, validating the existence of cointegration among the included variables [4]. Shahbaz and Lean (2012) showed a relationship between electricity consumption and economic growth in Pakistan, They found bi-directional Granger causality between electricity consumption and economic growth [5]. Odhiambo (2009) examined the causal relationship between electricity consumption and economic growth in South Africa by using the causality framework. Empirical results showed that there was a distinct bidirectional causality between electricity consumption and economic growth and employment in South Africa [6]. Yuan et. al (2008) tested the energy consumption and economic growth relationship for China using a neo-classical aggregate production model at both aggregated total energy and disaggregated levels of coal, oil, and electricity consumption [7]. Aqeel and Butt (2001) showed that there was a relationship between energy consumption and economic growth in Pakistan. Their paper investigated the causal relationship between energy consumption and economic growth and energy consumption and employment in Pakistan by applying techniques of co-integration and Hsiao's version of Granger causality [8].

Other researchers have shown that, by combining some countries causality studies between energy consumption and economic growth, they can provide a wider perspective for determining future energy policy. Fotis et all. (2017) showed that there was a relationship between energy demand and real Gross Domestic Product (GDP) growth and per capita Final

Energy Consumption (FEC) in 34 countries during the period from 2005 to 2013 [9]. Oztürk et al. (2011) investigated energy consumption and GDP for 51 countries, using annual data from 1971 to 2005, by classifying countries according to national income. The populations studied were divided into three groups: low-income group, lower-middle-income group, and upper-middle-income group [10].

They found a relationship between energy consumption and economic growth for all income groups considered in this study. Wolde-Rufael (2006) tested the causal relationship between electricity consumption per capita and real gross domestic product (GDP) per capita for 17 African countries, for the period 1971–2001. Empirical evidence showed that there was a long-running relationship between electricity consumption per capita and real GDP per capita for only 9 countries and Granger causality for only 12 countries [11]. Soytaş and Sarı (2003) investigated the Energy consumption and GDP causality relationship in G-7 countries and emerging markets. They found bi-directional causality in Argentina, causality running from GDP to energy consumption in Italy and Korea, and from energy consumption to GDP in Turkey, France, Germany, and Japan [12]. Bozoklu and Yılcı (2003) examined the causal relationship between energy consumption and economic growth for 20 OECD countries and according to their findings, economic activity depends on energy usage and increases in energy consumption may stimulate real GDP in these countries [13].

The purpose of this article was to examine the relationship between consumption of electricity (EC) and gross domestic product (GDP) in 30 countries. These countries were divided into three groups: developed, developing and under-developed countries. These countries were chosen because the consumption of electricity and gross domestic product data in these countries are regular and complete.

## **2. MATERIAL AND METHODS**

### **2.1. Material**

The data set used in this paper comprises annual data, 1995-2014, for several developed, developing and under-developed countries. We divided 30 countries according to the gross domestic product classification as either developed countries, developing countries, or under-developed countries. The developed countries are Belgium, Austria, Portugal, Denmark, Germany, Ireland, Greece, Spain, France, Italy. The developing countries are Bulgaria, Turkey, Ukraine, Bosnia and Herzegovina, Azerbaijan, India, Moldova, Macedonia, Hungary, Croatia. The under-developed countries are Zambia, Sudan, Nepal, Senegal, Zimbabwe, Tanzania, Togo, Haiti, Mozambique, Kenya. The variables used in this study are electricity consumption [14] (EC) and Gross Domestic Product [15] (GDP). All the variables were used as natural logarithmical values in the model. Electricity consumption and GDP data are taken from the World Development Indicators database of the World for the period between 1995-2014 (Table 1) [16].

**Table 1.** List of Variables

<b>Variables</b>	<b>Abbreviation</b>	<b>Description</b>	<b>Period</b>	<b>Source</b>
Electricity Consumption	EC	Electric consumption for each country (kWh per capita)	Annual	WDI
Gross Domestic Product	GDP	A measure of a country's economic output that accounts for its population. (current US\$)	Annual	WDI

## 2.2. Methods

We investigate the causal relationship between EC and GDP according to the development status of countries. Firstly, we identify the order of integration of the series using panel unit root tests. Secondly, we employ panel cointegration tests to examine the existence of a long-run relationship between the series. Finally, we estimate the long-run and short-run relationships using suitable estimations.

### 2.2.1. Panel Unit Root Tests

In panel data analysis, the panel unit root test must be taken first in order to identify the stationary properties of the relevant variables. There exist a number of methods for panel unit root tests, such as the Levin-Lin Chu (LLC) test [17], the Im-Pesaran-Shin (IPS) test [18], and the Hadri test [19]. The LLC test takes into account the heterogeneity of various sections, but it has low power in small samples because of the serial correlation, which cannot be eliminated. The IPS test considers the heterogeneity among the sections and also eliminates the serial correlation, and thus has a strong ability of testing small samples, while the Hadri test is different in that the null should be reversed to be the stationary hypothesis in order to have a stronger power test.

### 2.2.2. Panel Cointegration Tests

A method for testing the null of no cointegration in dynamic panels with multiple regressors are developed by Pedroni [20].

Having established the panel unit root test, a prerequisite condition for the cointegration test is that all variables must be of order  $I(1)$ . Once this condition is fulfilled, the next step is to test for the existence of a long-run cointegration of the specified variables using panel cointegration tests suggested by Pedroni [20] which comprise seven panel cointegration statistics in determining the fitness of the tests after normalizing the panel statistics with correction terms.

The tests allow for considerable heterogeneity among individual members of the panel, including heterogeneity in both the long-run cointegrating vectors as well as heterogeneity in the dynamics associated with short-run deviations from these cointegrating vectors [20].

### 2.2.3. Panel Granger Causality Tests

Granger Causality is a statistical hypothesis test that verifies whether one time series is capable of forecasting another [21]. Granger causality becomes a powerful tool to investigate the causal effect and functional relation from numerous temporal data which are easy to source today [22].

An underlying assumption of Granger causality is that a variable X Granger causes Y if Y can be better predicted using the histories of both X and Y than it can use the history of Y alone. Engle and Granger [23] explained that if co-integration exists between two variables in the long run, and then there must be either unidirectional or bi-directional Granger Causality between these two variables.

### 3. EMPIRICAL RESULTS

To test whether there exist any long-run and short-run relationships between electricity consumption (EC) and gross domestic product (GDP) related to the classified countries, panel unit root analysis, panel cointegration analysis, panel causality analysis, panel pooled mean group (PMG) and mean group (MG) estimates were employed in this study. The statistical software package Stata version 13.0 was used for this analysis.

Table 2 presents descriptive statistics for the log-transformed variables of interest. The second and third columns are the mean and standard deviation for each of the variables and the other columns show the correlation matrix. The correlation between electricity consumption (EC) and gross domestic product (GDP) was positive.

**Table 2.** Descriptive Statistics of the Log Transformed Variables

Countries	Variable	Obs	Mean	Std. Dev.	EC	GDP
Developed	EC	200	8.710	0.221	1	
	GDP	200	10.294	0.424	0.69	1
Developing	EC	200	7.738	0.612	1	
	GDP	200	7.898	1.067	0.598	1
Under-developed	EC	200	4.959	0.996	1	
	GDP	200	6.258	0.534	0.3328	1

Table 3 presents the panel unit root tests of all variables for three groups tested both for levels and for first differences. According to Levin-Lin Chu (LLC), the EC variables are stationary for developed countries while these variables include the unit root for developing and under-developed countries. In addition to this the GDP variables are stationary for developing countries, but these variables include the unit root for developed and under-developed countries. The Im-Pesaran-Shin (IPS) test results show that the EC variables are stationary for developed countries but these variables include the unit root for developing and under-developed countries. Furthermore; the GDP variables include the unit root for all three groups. The null hypothesis of the Hadri tests is that no unit root exists in the series and the alternative hypothesis is that a unit root exists. For the three groups the unit root hypothesis is rejected when the variables EC and GDP are in level form. Therefore, the difference in the series was taken. According to the results of the unit roots test namely (LLC) and (IPS), the first difference of these variables is that they are stationary. When the first differences are taken using the Hadri tests, the GDP variables for developing countries and the EC variables for underdeveloped countries are stationary.

**Table 3.** Panel unit root test results for developed status countries

Countries	Variables	LLC test		IPS test		Hadri test	
		Level	First Difference	Level	First Difference	Level	First Difference
Developed	EC	-4.409 (0.000)	-	-2.483 (0.006)	-	25.064 (0.000)	13.478 (0.000)
	GDP	-0.361 (0.358)	-6.072 (0.000)	2.031 (0.978)	-4.275 (0.000)	31.544 (0.000)	1.785 (0.037)
Developing	EC	-0.686 (0.246)	-8.169 (0.000)	0.715 (0.763)	-6.421 (0.000)	31.178 (0.000)	1.856 (0.031)
	GDP	-1.799 (0.036)	-	2.181 (0.985)	-5.740 (0.000)	35.217 (0.000)	1.509 (1.509)
Under-developed	EC	-0.207 (0.418)	-9.832 (0.000)	2.004 (0.977)	-10.110 (0.000)	30.040 (0.000)	0.707 (0.239)
	GDP	1.350 (0.911)	-9.376 (0.000)	4.257 (1.000)	-5.186 (0.000)	33.008 (0.000)	1.664 (0.048)

It can be seen from Table 3 that all the variables are integrated of order one, which meets the requirements of the cointegration test. In this paper the procedure proposed by Pedroni (1999) was used because it allows for the investigation of heterogeneous panels, in which heterogeneous slope coefficients, fixed effects and individual specific deterministic trends are permitted [20]. This framework provides cointegration tests for both heterogeneous and homogenous panels with seven regressors based on seven residual-based statistics. These statistics are composed of the panel cointegration tests that include four statistics and the group cointegration tests that include three statistics. Table 4 shows the results of panel co-integration tests for developed status countries.

**Table 4.** Results of panel co-integration tests for developed status countries

Countries	Panel (within dimension)			Group (between dimension)		
	Statistics	Value	Prob.	Statistics	Value	Prob.
Developed	Panel v-stat.	2.997	0.998	Group rho-stat.	0.1346	0.553
	Panel rho-stat.	-0.960	0.168			
	Panel PP-stat.	-3.677	0.000			
	Panel ADF-stat.	-3.562	0.000			
Developing	Panel v-stat.	2.247	0.987	Group rho-stat.	1.129	0.870
	Panel rho-stat.	-0.129	0.448			
	Panel PP-stat.	-1.944	0.025			
	Panel ADF-stat.	-2.211	0.013			
Under-developed	Panel v-stat.	0.102	0.540	Group rho-stat.	1.004	0.842
	Panel rho-stat.	-0.162	0.435			
	Panel PP-stat.	-2.29	0.011			
	Panel ADF-stat.	-0.800	0.211			
				Group PP-stat.	-2.12	0.017
				Group ADF-stat.	-0.6316	0.263

It can be seen from Table 4 that for developed countries, three panel statistics reject the null hypothesis of no cointegration and two statistics that admit that there is no cointegration between the variables, i.e. the panel v-statistic and panel rho-statistic. In the group cointegration tests, two group statistics reject the null hypothesis and one admits it. For developing countries, two panel statistics reject the null hypothesis of no cointegration and two statistics admit there is no cointegration between the variables, i.e. the panel v-statistic and panel rho-statistic. In group cointegration tests, one group statistics rejects the null hypothesis and two admit it. For

under-developed countries, Panel PP- statistic and Group PP- statistic reject the null hypothesis of no cointegration.

Having established cointegration in the long-run by Pedroni (1999) in Table 4, we examine the direction of causality between GDP and EC in a Panel context which is based on the following regressions:

$$\Delta \ln EC_{it} = \varphi_{1i} + \sum_p \varphi_{11ip} \Delta \ln EC_{it-p} + \sum_p \varphi_{12ip} \Delta \ln GDP_{it-p} + \psi_{1i} ECM_{t-1} \tag{1}$$

$$\Delta \ln GDP_{it} = \varphi_{2i} + \sum_p \varphi_{21ip} \Delta \ln GDP_{it-p} + \sum_p \varphi_{22ip} \Delta \ln EC_{it-p} + \psi_{2i} ECM_{t-1} \tag{2}$$

Eqs. (1) and (2) are estimated using the pooled mean group estimator (PMGE) and mean group estimator (MGE). In order to be able to choose the appropriate estimator, the Hausman test was conducted and long-run homogeneity was tested. Causality is tested based on  $H_0: \varphi_{12ip} = 0$  and  $H_0: \varphi_{22ip} = 0$  for all  $i$  and  $p$ , where  $p$  is the lag length for the differenced variables of the respective equations.

Eq (1) gives the estimates of the panel correction model of the variables according to development status by the mean group estimator and the pooled mean group estimator. Results of the Hausman test show that the mean group estimator for the developed (Chi-square: 3818.74 (0.000)) and developing (Chi-square: 24.65 (0.000)), according to the test results, is valid, whereas for the under-developed countries (Chi-square: 0.27 (0.605)) the pooled group estimator is appropriated.

Eq (2) gives the results of the Hausman test and show that, according to the test results, the mean group estimator for the developed countries (Chi-square: 78.86 (0.000)) and under-developed countries (Chi-square: 57.74 (0.000)) is valid, whereas for the developing countries (Chi-square: 1.13 (0.2869)) pooled group estimator is appropriated. The panel Granger causality test results are reported in Table 5.

**Table 5.** Causality test results

Countries	Dependent Variable	Source of causation (independent variable)				
		Short-run		Long run		
		EC	GDP	EC	GDP	ECM
Developed	EC	-	-0.0367**	-	0.038***	0.894***
	GDP	0.893***	-	-1.07***	-	0.841***
Developing	EC	-	0.091***	-	-0.347*	0.552***
	GDP	-0.0265	-	-1.75***	-	0.721***
Under-developed	EC	-	0.246***	-	0.156***	0.614***
	GDP	0.313*	-	-0.428*	-	0.834***

\*and \*\*\* represent significance at 10% and 1%, respectively.

According to the Granger causality test results, there is a long-run Granger causality running from GDP to EC for the three groups of countries and vice versa. It shows that electricity consumption is determined by economic growth. Any shock to the electricity supply will have effects on economic growth and vice versa.

For developed countries the error correction parameter is 0.894 and is positive and significant. There is a long-run relationship between the two variables. This parameter indicates the rate at

which the short-run deviations resulting from the non-stationary series will impact on equilibrium in the next period. The results show that about 89% of imbalances in a period will be corrected in the next period. This will ensure a long-run equilibrium approach. Moreover, the long-run parameter of gross domestic product is 0.038 and is statistically significant; the short-run parameter is -0.036 and is statistically significant and negative. A 1% increase in gross domestic product in the short-run will result in a 0.03% decrease in electricity consumption.

For developing countries, the error correction parameter is 0.552, positive and significant. This parameter indicates the rate at which the short-run deviations resulting from the non-stationary series will impact on equilibrium in the next period. The results show that about 55% of imbalances in a period will be corrected in the next period. This will ensure a long-run equilibrium approach. Moreover, the long-run parameter of gross domestic product is -0.34 and is statistically significant and negative, and the short-run parameter is 0.091 and is statistically significant and positive. A 1% increase in gross domestic production in the short-run will result in a 1% increase in electricity consumption.

For under-developed countries, the error correction parameter is 0.614, which is positive and significant. This parameter indicates the rate at which the short-run deviations resulting from the non-stationary series will impact on equilibrium in the next period. The results show that about 61% of imbalances in a period will be corrected in the next period. This will ensure a long-run equilibrium approach. Moreover, the long-run parameter of gross domestic product is 0.156, and the short-run parameter is 0.24 are both statistically significant and positive. A 1% increase in gross domestic product in the short run will result in a 2% increase in electricity consumption.

#### **4. CONCLUSIONS**

Electricity consumption depends on many factors, such as income levels of countries, technological developments, literacy status of people, and conscious usage of energy resources habits.

In this study we used the panel data of electricity consumption and GDP for 30 countries, using annual data from 1995 to 2014. The countries studied were divided into three groups: developing, developed and under-developed countries. The aim of this study was to investigate whether there is a relationship between electricity consumption and per capita GDP; to examine the causality between these variables and to determine the significance of this relationship. The relationship between electricity consumption and GDP was determined by employing Pedroni (1999) panel cointegration method. The empirical results of the panel cointegration test indicated that electricity consumption and GDP are cointegrated for all three groups. Also, panel causality test results revealed that there is a long-run Granger causality running from GDP to EC for the three groups and vice versa. The results obtained are consistent with the findings of other researches [10,12].

The overall results of this study show that there is a relationship between EC and GDP. In the short-run, this relationship is negative for developed countries but positive for developing and under-developed countries. In the long-run, this relationship is negative for developing

countries but positive for developed and under-developed countries. This clearly indicates that electricity consumption differs according to the developmental level of the countries.

The short-term relationship in developed countries is negative. This is due to the continued increase in GDP despite the stagnation of electricity consumption. In terms of technology and industrialization, these countries are thought to have attained sufficient saturation.

In the developing countries, the long-term relationship has been observed to be negative. This shows that developing countries will reach fullness in terms of technology and industrialization in the long run.

For under-developed countries, technology and industrialization are not expected to reach saturation in the near future.

## REFERENCES

- [1] Kaygusuz, K. (2003). Energy policy and climate change in Turkey. *Energy Conversion and Management*, 44(10): 1671–1688.
- [2] Suganthi, L. And Samuel, A. A. (2012). Energy models for demand forecasting- a review, *Renewable Sustain Energy Rev*, 16(2): 1223–1240.
- [3] U.S. Energy Information Administration EIA, [https://www.eia.gov/outlooks/ieo/pdf/0484\(2017\).pdf](https://www.eia.gov/outlooks/ieo/pdf/0484(2017).pdf) (accessed December 11, 2017).
- [4] Bah, M. and Azam, M. (2017). Investigating the relationship between electricity consumption and economic growth: evidence from South Africa, *Renewable and Sustainable Energy Reviews*, 80: 531-537.
- [5] Shahbaz, M. and Lean H., H. (2012). The dynamics of electricity consumption and economic growth: A revisit study of their causality in Pakistan, *Energy*, 39(1): 146-153.
- [6] Odhiambo, N. M. (2009). Electricity consumption and economic growth in South Africa: a trivariate causality test, *Energy Economics*, 31(5): 635-640.
- [7] Yuan, J. H., Kang, J., G., Zhao, C., H. and Hu, Z. G. (2008). Energy consumption and economic growth: evidence from China at both aggregated and disaggregated levels, *Energy Economics*, 30(6): 3077-3094.
- [8] Aqeel, A. and Butt, M. S. (2001). The relationship between energy consumption and economic growth in Pakistan, *Asia-Pacific Development Journal*, 8(2): 101-110.
- [9] Fotis, P., Karkalakos, S. and Asteriou, D. (2017). The relationship between energy demand and real GDP growth rate: the role of price asymmetries and spatial externalities within 34 countries across the globe, *Energy Economics*, 66: 69-84.
- [10] Ozturk, I., Aslan, A. and Kalyoncu, H. (2010). Energy consumption and economic growth relationship: Evidence from panel data for low and middle income countries, *Energy Policy*, 38(8): 4422-4428.
- [11] Wolde-Rufael, Y. (2006). Electricity consumption and economic growth: a time series experience for 17 African countries, *Energy Policy*, 34(10): 1106-1114.
- [12] Soytas, U. and Sari, R. (2003). Energy consumption and GDP: causality relationship in G-7 countries and emerging markets, *Energy Economics*, 25(1): 33-37.

- [13] Bozoklu, S. and Yılancı, V. (2013). Energy consumption and economic growth for selected OECD countries: further evidence from the granger causality test in the frequency domain, *Energy Policy*, 63: 877-881.
- [14] EC, Electricity Consumption. <https://data.worldbank.org/indicator/EG.USE.ELEC.KH.PC> (accessed April 20, 2018)
- [15] GDP, Gross Domestic Product. <https://data.worldbank.org/indicator/NY.GDP.PCAP.CD> (accessed April 20, 2018).
- [16] WDI, World Development Indicators. <https://data.worldbank.org/products/wdi> (accessed April 20, 2018).
- [17] Levin, A., Lin, C., F. and Chu, C. S. J. (2002). Unit root tests in panel data: Asymptotic and finite-sample properties, *Journal of Econometrics*, 108(1): 1–24.
- [18] Im, K.S., Pesaran, M., H. and Shin, Y. (2003). Testing for unit roots in heterogeneous panels, *Journal of Econometrics*, 115(1): 53–74.
- [19] Hadri, K. (2000). Testing for stationarity in heterogeneous panel data, *The Econometrics Journal*, 3(2): 148-161.
- [20] Pedroni, P. (1999). Critical values for cointegration tests in heterogeneous panels with multiple regressors, *Oxford Bulletin of Economics and Statistics*, 61(1): 653-670.
- [21] Granger, C.W.J. 1969. Investigating causal relations by econometric models and cross spectral methods, *Econometrica*, 37: 424-438.
- [22] Lay, E., Chye, X.-H. and Choong, C.H.-K. 2011. Energy-growth causality: a panel analysis, *International Conference on Applied Economics e ICOAE 2011*.
- [23] Engle, R.F. and Granger, C.W.J. 1987. Cointegration and error correction: representation, estimation, and testing, *Econometrica*, 55: 251-276.



## Temperature and Relative Humidity Models of the Malatya City

Ayşe BİÇER

Department of BioEngineering, Faculty of Engineering and Natural Sciences, Malatya Turgut Özal University, Malatya, Turkey.

(Received: 15.04.2020; Accepted: 02.05.2020)

**ABSTRACT:** In this study, the temperature changes Malatya provinces located in the Euphrates Basin are analyzed and modeled based on 24 years of observation process (1996-2019). Relative humidity models were analyzed by observing the yearly mean temperatures of provinces, the lowest mean temperatures of winter months (December, January and February) and the highest mean temperatures of summer months (June, July and August). With the help of these models; temperature and humidity estimations can be made for future years and these models can be used in energy-related studies

**Keywords:** Temperature, Relative humidity, Meteorological data, Modelling.

### 1. INTRODUCTION

Meteorological data are of great importance in determining the energy potential of a region in the past and present, and developing ways to solve its problems [1, 2]. The need for energy is directly related to climate and weather conditions. Climate data is of great importance in the design of buildings, in the planning of agricultural production, in the design of the energy and installations needed for heating residential and industrial areas in cold weather and cooling in hot weather. [3, 4].

Outdoor temperature values of cities and towns in Turkey were identified in the 1950s, yet they are not in compliance with the present day conditions. Population increase, green areas, industrialization and lakes and ponds created in the cities affect the climate structures of the cities and cause the change of the outdoor temperature parameter. Five large dams were constructed on the *Firat River*, which is one of the important rivers of Eastern Anatolia, from the border to the exit gateway for both energy production and irrigation. The *Firat River* is born on the *Murat River* and the *Karasu River* at an altitude of 3290 meters and flows through the cities of Erzincan, Tunceli, Elazığ, Malatya, Diyarbakir, Adiyaman, Gaziantep and Sanliurfa and flows into the Persian Gulf. Its length is 2800 km and a total of 6396 MW of electrical energy is produced from five HEPPs through the river. This power is 30,8% of the electricity produced from hydroelectric power plants in Turkey, meeting 8,3% of the total electricity consumption. In addition to ensuring the energy generation of these dams, it also caused the change of the climate structure of the region.

\*Corresponding Author: [ayse.bicer@ozal.edu.tr](mailto:ayse.bicer@ozal.edu.tr)

ORCID number of authors: 0000 -0003-4514-5644

Many studies have been done on the subject, especially in the country. These studies can be grouped into two groups. The first group of studies are mainly related to climate structures. Some examples of these studies are summarized below:

Bakırcı et al [1] conducted energy studies for Erzurum province using meteorological data. Çobanyılmaz and Yüksel [2] presented the case study of Ankara by examining the harms that cities can experience due to climate change. Turkey's climate classification structure was made by the General Directorate of Meteorology [3] -Department of Climatology. Dönmez [4] carried out studies involving cities' air conditioners and climates. Geymen and Dirican [5] analyzed sea-level changes due to climate change. Apple et al. [6] and Şen [7] developed weather forecasting models using meteorological values. Al-Garni et al. [8] examined the climatic structures of the eastern regions of Saudi Arabia and modeled the wind power of the region. Akpınar et al. [9] investigated the weather conditions and wind power of some provinces in the Eastern Anatolia Region. Bicer [10] established the temperature and humidity models using meteorological data for certain provinces in the Euphrates Basin.

The second group of studies deals with the effects of the artificial lakes or ponds on the climate of the region. Dam lakes in the region can be seen in Figure 1. Some of these studies are summarized below:

Şengün [11] examined the changes caused by Keban Dam Lake in Elazığ climate within 30 years before and after 1975 and evaluated the results. Özkan [12] investigated the effect of Keban dam lake on Elazığ climate conditions. He examined climate variables in the periods before and after the dam construction. After the dam was constructed, significant increases were observed in the winter months, as well as a certain amount of decreases in the temperatures in the summer months. Yeşilata et al. [13] investigated the change in the dam lake caused by temperature and humidity parameters in the GAP Region. Apart from these studies, Emiroğlu et al. [14], Tonbul [15] and Kadioğlu [16] investigated the effect of Keban Dam Lake on the climate structure of Şanlıurfa province, Elazığ province, Biçer and Yıldız [17]. Bacanlı and Tuğrul [18] examined the effect of Gökpınar Dam Lake on the climate structure of the provinces.

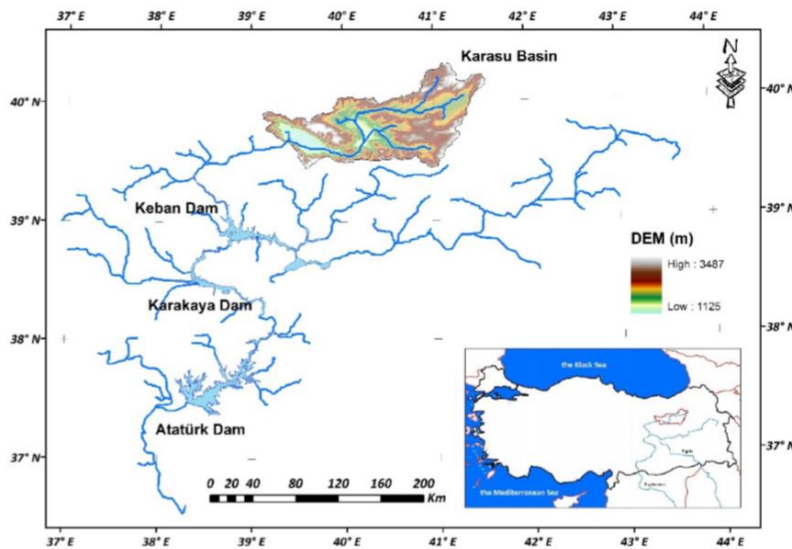


**Figure 1.** Some of the dam lakes in the Upper Euphrates basin [19]

The aim of this study is to examine the weather parameters such as temperature and humidity of Malatya province by using meteorological values for a 24-year observation period, as well as presenting a preliminary idea for future studies by determining regression equations.

## 2. MATERIAL AND METHODS

### 2.1. Materials

The outdoor temperature parameter (T) of Malatya province, along with the monthly lowest and highest average temperature values were taken from the results of the meteorological measurement of the General Directorate of State Meteorological Affairs for the 1996-2019 observation process [20].

### 2.2. Methods

#### 2.2.1. Temperature

The average of the lowest monthly average of temperatures ( $T_{dmin}$ ) for the winter months (December, January and February) of the province is calculated by Equation (1) and the average of the lowest temperature averages (EDSO) for the observation process [21].

$$T_{dmin}=(T_{min \text{ December}} + T_{min \text{ January}} + T_{min \text{ February}}). (1/3) \quad (1)$$

$$T_{EDSO}=(1/n). \sum T_{dmin} \quad (2)$$

Similarly, for the summer season (June, July and August), the average of the highest temperature values of the province ( $T_{dmax}$ ), Equation (3) and the average of the highest temperature values for the observation process (TEYSO) were calculated by Equation (4) [21].

$$T_{dmaks}=(T_{max \text{ June}} + T_{max \text{ July}} + T_{maks \text{ August}}). (1/3) \quad (3)$$

$$T_{EYSO}=(1/n). \sum T_{dmax} \quad (4)$$

Using the meteorological values of each province, the average of the lowest temperature averages (SO) of the 12 months of the year for the 24-year observation period was calculated through Equation (5)...

$$T_{SO}=(1/n). \sum T_{yearly} \quad (5)$$

#### 2.2.2. Relative Humidity

The monthly average values of the relative humidity parameter of the province were calculated through the annual meteorological measurement results of the General Directorate of State Meteorological Affairs for the 1996-2019 observation process [20].

### 3. RESULTS AND DISCUSSION

The average change of EDSO, EYSO and SO temperature averages of the province is shown in Figure 2 for the monthly period and 24-year observation period. For this process, the average temperature, January, February and December temperature average values (EDSO), June, July and August temperature average values (EYSO) and 12-month average temperature values (SO) are shown in Table 1 as allocated by provinces.

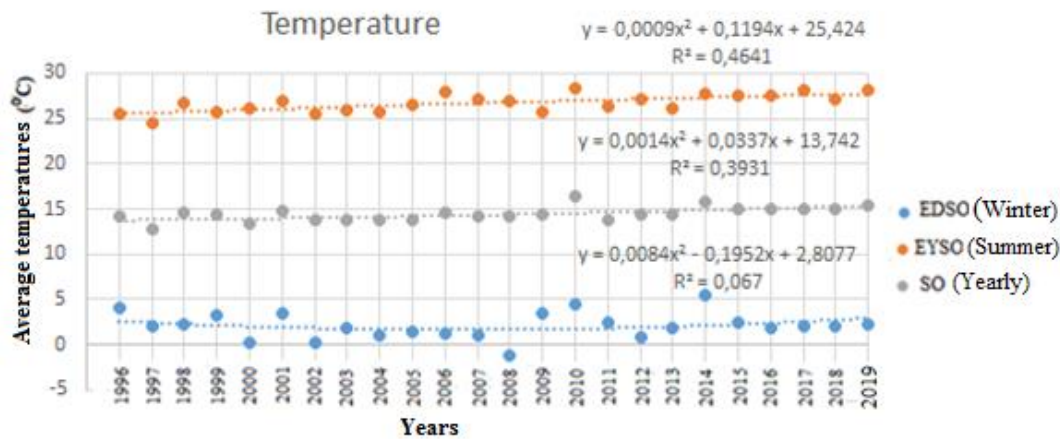


Figure 2. Linear regression of average temperature values of Malatya province

Table 1. Average temperature values of Malatya province (°C)

Average temperature values		
EDSO	EYSO	SO
2.07	26.7	14.4

Examining Figure 2, it can be seen that the smallest value of EDSO was observed in 2008 (-1.23 °C), the highest value in 2010 (4.57 °C), the lowest value of EYSO in 1997 (24.47 °C) and the highest value in 2010 (28.43 °C). Likewise, the smallest value for SO was observed in 1997 (12.81 °C) and the highest value in 2010 (16.34 °C). The regression equations of these three parameters over the years show a rising graph, albeit very small. Keban Dam, which formed a lake field in 1975, and Karakaya Dam Lake in 1988 brought cooling to Elazig province for 4-5 °C in winter conditions and 2-3 °C in summer conditions [10]. However, both global warming and the explosions in the Sun caused a temperature rise across the world. For this reason, during the observation, the average temperature of Malatya province has risen slightly in 24 years.

EDSO, EYSO and SO temperature variation models of the province were determined by linear regression relations on the computer. The temperature changes of the province were examined as linear, exponential, polynomial and logarithmic models, and the equation with the largest  $R^2$  value among the models was determined as the model of the relevant parameter of that province. Table 2 shows the models shown collectively and  $R^2$  of the model. In this table, the model suitable for the changes in the average temperatures of the province is stated in bold. Examining these models, it can be seen that EDSO, EYSO and SO exchange models of the province are polynomial models

**Table 2.** Temperature values linear regression relations of Malatya province

Model type	SO	EDSO	EYSO
<b>Linear</b>	$T_{SO} = 0,07*Y+13,6$ $R^2=0,3868$	$T_{EDSO} = 0,015*Y +1,89$ $R^2=0,0049$	$T_{EYSO} = 0,097*Y + 25,6$ $R^2=0,4626$
<b>Exponential</b>	$T_{SO} =13,59*e^{0,0048*Y}$ $R^2=0,3832$	-	$T_{EYSO} =25,527*e^{0,0036*Y}$ $R^2=0,4625$
<b>Polynomial</b>	$T_{SO}=0,001*Y^2+0,03*Y+13$ $R^2=0,3931$	$T_{EDSO}=0,009*Y^2-0,2*Y +2$ $R^2=0,0741$	$T_{EYSO}=0,001*Y^2+0,12*Y+25$ $R^2=0,4641$
<b>Logarithmic</b>	$T_{SO}=0,52*Ln(Y)+13,3$ $R^2=0,2969$	$T_{EDSO}=0,13*Ln(Y)+2,8$ $R^2=0,0053$	$T_{EYSO}=0,76*Ln(Y)+24,97$ $R^2=0,4024$

T=Temperature, , Y=Year

Relative humidity is the ratio of the humidity in the air to the maximum humidity at that temperature. The relative humidity must exceed 100% in order for precipitation to occur somewhere. The relative humidity decreases as the temperature increases. The reason for this is that the increase in the volume of the heated air will increase the humidity it can take. As relative humidity decreases, evaporation increases, while, on the other hand, relative humidity increases, evaporation decreases. Examining Table 3, the smallest and largest average relative humidity values between 1996-2019 can be seen as 46.55% - 57.51% for Malatya province. The average relative humidity change by years is shown in the graph in Figure 3.

**Table 3.** Average relative humidity values of the Malatya province

Years	Relative humidity	Years	Relative humidity
1996	56.94	2008	52.56
1997	53.83	2009	56.7
1998	53.13	2010	50.06
1999	49.17	2011	49.63
2000	48.08	2012	50.05
2001	47.4	2013	46.65
2002	<b>57.51</b>	2014	46.88
2003	58.45	2015	50.78
2004	56.67	2016	46.59
2005	56.21	2017	<b>46.55</b>
2006	54.23	2018	46.56
2007	54.09	2019	46.60

In the average relative humidity equations and curves shown in Figure 3, it can be conferred that the appropriate model is polynomial type as in the temperature parameter and the equation shows a decreasing trend with the (-) sign at the beginning of the equation (Table 4).

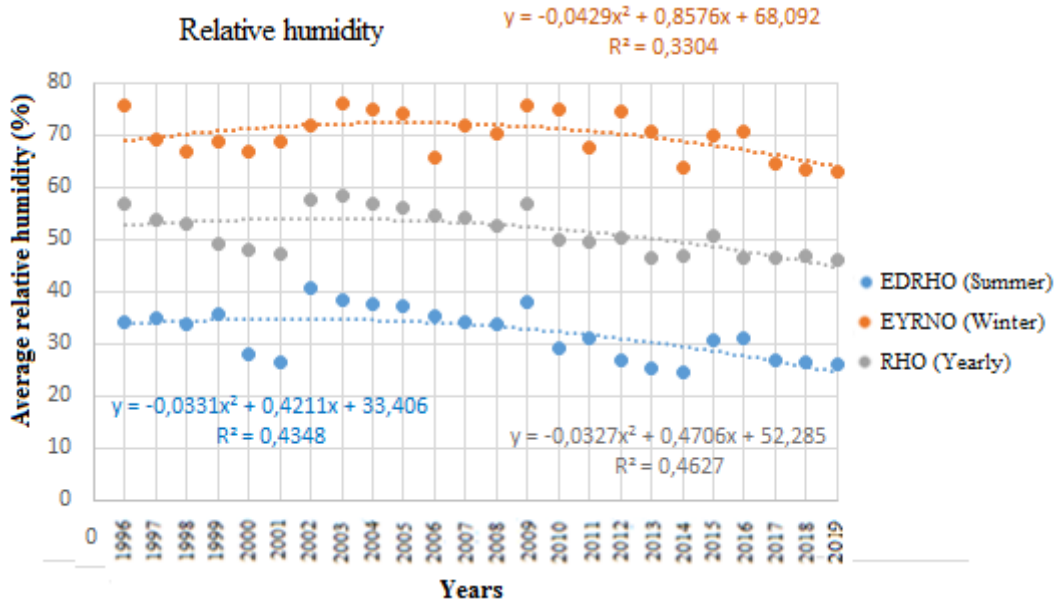


**Figure 3.** Linear regression of the relative humidity values of Malatya province

Here; EDRHO: the smallest average relative humidity, EYRHO; the largest average relative humidity and RHO: the relative humidity averages of the 12 months (yearly)

**Table 4.** Average relative humidity values of the province, linear regression equations

Model type	RHO	EDRHO	EYRHO
<b>Linear</b>	$RHO = -0,35*Y + 55,8$ $R^2 = 0,3456$	$EDRHO = -0,406*Y + 36,99$ $R^2 = 0,347$	$EYRHO = -0,215*Y + 72,7$ $R^2 = 0,1312$
<b>Exponential</b>	$RHO = 55,87 * e^{-0,007*Y}$ $R^2 = 0,3523$	$EDRHO = 37,13 * e^{-0,013*Y}$ $R^2 = 0,3554$	$EYRHO = 72,746 * e^{-0,003*Y}$ $R^2 = 0,1374$
<b>Polynomial</b>	$RHO = -0,03*Y^2 + 0,5*Y + 52,3$ $R^2 = 0,4627$	$EDRHO = -0,03*Y^2 + 0,42*Y + 33,4$ $R^2 = 0,4348$	$EYRHO = -0,04*Y^2 + 0,9*Y + 68,1$ $R^2 = 0,3304$
<b>Logarithmic</b>	$RHO = -2,37 * \ln(Y) + 57$ $R^2 = 0,2223$	$EDRHO = -2,61 * \ln(Y) + 37,9$ $R^2 = 0,1979$	$EYRHO = -1,32 * \ln(Y) + 73$ $R^2 = 0,4024$

The models that are found in compliance among the temperature and humidity models examined in the province are given collectively in Table 5.

**Table 5.** Linear regression relations of the city's temperature and relative humidity values

Climate Parameter	Season	Linear regression models
<b>Temperature (°C)</b>	SO	$T_{SO} = 0,0014*Y^2 + 0,0337*Y + 13,742$
	EDSO	$T_{EDSO} = 0,0088*Y^2 - 0,2028 + 2,8327$
	EYSO	$T_{EYSO} = 0,0009*Y^2 + 0,1194*Y + 25,42$
<b>Relative humidity (%)</b>	RHO	$RHO = -0,0327*Y^2 + 0,47*Y + 52,28$
	EDRHO	$RDRHO = -0,0331*Y^2 + 0,4211*Y + 33,406$
	EYRHO	$T_{EYNO} = -0,0429*Y^2 + 0,8576*Y + 68,092$

## 4. CONCLUSIONS

In this study, using the meteorological data for the 24-year observation process of the Malatya province in the Upper Euphrates basin, the models of the change of the temperature average and relative humidity parameters of the provinces were determined.

✓ A polynomial equation model has been determined for the average of average annual temperature and humidity in winter, as well as the lowest, the highest in summer and 12 months during the city's observation.

✓ The average temperature of the province shows a rising change while the relative humidity shows a lowering change.

✓ With these equations, it will be possible to estimate the temperature averages and relative humidity parameters of the province in the coming years and to determine the effects of these predicted weather conditions on the environment.

✓ Outdoor temperature parameter, which is an important parameter in the design of heating installations, has been calculated based on very old data. Outdoor temperature parameters must be updated due to the increase in the winter months of the province considering the dam lakes in the region and the global warming. This study will help update the outdoor temperature parameter for the summer and winter seasons across the country.

✓ Both construction costs and energy costs will be reduced with the design of the heating installations to be prepared with the new outdoor temperature parameter to be updated.

**Thanks to:** I would like to take this chance to thank the “General Directorate of State Meteorological Affairs” for their interest and assistance for the provision of meteorological measurement data used in the study.

## REFERENCES

- [1] Bakırcı, K., Özyurt, Ö., Yılmaz, M. and Erdoğan, S. (2006). Erzurum ili enerji çalışmaları için iklim ve meteoroloji verileri, *Tesisat Mühendisliği Dergisi*, 9: 19-26.
- [2] Çobanyılmaz, P. And Yüksel, Ü.D. (2013). Kentlerin iklim değişikliğinden zarar görebilirliğinin belirlenmesi: Ankara Örneği, *Süleyman Demirel Üniversitesi Fen Bilimleri Enstitüsü Dergisi*, 17(3): 389-50.
- [3] İklim Sınıflandırmaları, (2017). Meteoroloji Genel Müdürlüğü, Klimatoloji Şube Müdürlüğü, Kalaba, 1-16, Ankara, Türkiye.
- [4] Dönmez, Y. (1984). *Umumi klimatoloji ve iklim çalışmaları* İ.T.Ü. Yayın No: 2506.
- [5] Geymen, A. and Dirican, A.Y. (2016). İklim değişikliğine bağlı deniz seviyesi değişiminin coğrafi bilgi sistemleri kullanılarak analiz edilmesi, *Harita Teknolojileri Elektronik Dergisi*, 8(1): 65-74.
- [6] Apple, L.S.C., Chow, T.T., Square, K.F.F. and Lin, J.Z. (2006). Generation of a typical meteorological year for Hong Kong. *Energy Conversion and Management*, 47: 87–96.

- [7] Sen, Z. (1999). Simple nonlinear solar irradiation estimation model. *Renewable Energy*, 32:342–350.
- [8] Al-Garni, A.Z., Şahin, A.Z. and Al-Farayedhi, A. (1999). Modelling of weather characteristics and wind power in the Eastern Part of Saudi Arabia, *International Journal of Energy Research*, 23: 805-812.
- [9] Akpınar, E.K., Biçer, Y., Erdoğan, B. and Çetinkaya, F. (2005). Doğu Anadolu Bölgesindeki bazı illerin hava şartları ve rüzgar gücünün araştırılması. 15. *Ulusal Isı Bilimi ve Tekniği Kongresi* 7-9 Eylül, Karadeniz Teknik Üniversitesi, Trabzon.
- [10] Bicer, A. (2019). Fırat havzasında bulunan bazı illerin sıcaklık ve nem modelleri, *Bartın University International Journal of Natural and Applied Sciences*, 2(1): 50-58.
- [11] Şengün, M.T. (2007). Son değerlendirmeler ışığında Keban Barajı'nın Elazığ İklimine etkisi. Doğu Anadolu Bölgesi Araştırmaları, 116-121.
- [12] Özkan, F. (1996). Keban Baraj Gölü'nün Elazığ Bölgesi iklim şartlarına etkisinin araştırılması, Yüksek Lisans Tezi, Fırat Üniversitesi Fen Bilimleri Enstitüsü, Elazığ.
- [13] Yeşilata, B., Bulut, H. and Yeşilnacar, M.İ. (2004). GAP Bölgesinde sıcaklık ve nem parametrelerindeki baraj gölü kaynaklı değişim trendinin araştırılması. *Tesisat Mühendisliği Dergisi*, 83: 21-31.
- [14] Emiroğlu, M. E., Özkan, F. and Öztürk, M. (1996). Keban Barajı Rezervuarı'nın Elazığ ili iklim şartlarına etkisi üzerine bir araştırma. *GAP I. Mühendislik Kongresi Bildiriler Kitabı*, Sayfa 167-174, Harran Üniversitesi, Şanlıurfa.
- [15] Tonbul, S. (1986). Elazığ ve çevresinin, iklim özellikleri ve Keban barajının yöre iklimi üzerine olan etkileri. *Fırat Üniversitesi Coğrafya Sempozyumu*, 14-15 Nisan, Elazığ.
- [16] Kadioğlu, M. (1994). Keban Barajı öncesi ve sonrasında çevre ikliminin Franktal analizi. *Bayındırlık ve İskan Bakanlığı DSİ Genel Müdürlüğü Su ve Toprak Kaynaklarının Geliştirilmesi Konferansı Bildirileri* 3: 1087-1098, Ankara.
- [17] Biçer, Y. and Yıldız, C. (1994). Atatürk Barajı Rezervuarının Şanlıurfa ili dış sıcaklık parametresine etkisinin araştırılması, 3. *Ulusal Soğutma ve İklimlendirme Kongresi*, Sayfa 333-340, 4-6 Mayıs Çukurova Üniversitesi, Adana.
- [18] Bacanlı, Ü.G. and Tuğrul, A.T. (2016). Baraj göllerinin iklimsel etkisi ve Vali Recep Yazıcıoğlu Gökınar Baraj gölü örneği. *Pamukkale Üniversitesi Muh Bilim Dergisi* 22(3): 154-159.
- [19] Uysal, G., Şorman, A.A. and Şensoy, A. (2016). Streamflow Forecasting Using Different Neural Network Models with Satellite Data for a Snow Dominated Region in Turkey, *Procedia Engineering* 154: 1185-1192.
- [20] MGM, (2019). Devlet Meteoroloji İşleri Genel Müdürlüğü, aylık ve yıllık meteorolojik ölçüm değerleri, 23 Şubat 2019.
- [21] Gülferi, İ. (1976). Meteorolojik değerler yardımıyla kış için dış hesap sıcaklığının bulunmasında yeni bir istatistiki metot. Doktora Çalışması, İTÜ Fen Bilimleri Enstitüsü.



## In Dynamic Systems with Fuzzy A - Cutting Determination of Membership Function Ranges

Fatih TOPALOĞLU<sup>1\*</sup>, Hüseyin PEHLİVAN<sup>2</sup>

<sup>1</sup> Department of Computer Engineering, Faculty of Engineering and Natural Sciences, Malatya Turgut Özal University, Malatya, Turkey.

<sup>2</sup> Department of Computer Engineering, Faculty of Engineering, Karadeniz Technical University, Trabzon, Turkey.

(Received: 01.05.2020; Accepted: 10.05.2020)

**ABSTRACT:** Uncertainties and inaccuracies in the membership function value ranges defined by the expert in dynamic systems cause serious errors in system output. In this study, the fuzzy  $\alpha$ -cutting technique was used to determine the ranges of membership functions on the universal cluster and neighborhood values of normal values were calculated for different  $\alpha$  cutting coefficients and then neighborhood values were adjusted according to determined step values. Thus, while determining the value range of membership function in dynamic systems, it will be possible to talk about its neighborhood in the values that serve the same purpose. Operation in the dynamic process as wind power installation for Turkey wind energy interval value set in the potential atlas used and  $\alpha$  cutting techniques of the gap on the universal set of the determined value with re-calculation and determination are provided.

**Keywords:** Dynamic systems,  $\alpha$  - Cutting technique, Fuzzy cluster, Membership function.

### 1. INTRODUCTION

The concept of the fuzzy cluster was proposed by Zadeh in his classic article in 1962. Fuzzy sets and fuzzy logic provide methods and tools for accurate and precise data analysis and processing [1]. Fuzzy logic also has certain limits, and these limits vary depending on the situation. What distinguishes it from classical logic is that these limits are more flexible. Thanks to this flexibility, fuzzy logic gives much more sensitive results in every field it is applied [2]. Although the membership function value range is flexible, it is mostly determined based on the experience of the expert.

In fuzzy modeling, the correct determination of membership functions is of primary importance for the success of the model. It is possible to encounter many approaches in the literature about the selection of membership functions [3-15]. The fact that the value ranges that are close to the value determined in the approaches to determine the membership function value range also affects the system and has caused the need to be evaluated in the system at their neglected values.

\*Corresponding Author: fatih.topaloglu@ozal.edu.tr

ORCID number of authors: <sup>1</sup> 0000-0002-2089-5214, <sup>2</sup> 0000-0002-0672-9009

The method used for this need is the Fuzzy alpha cutting (FAC) technique. It is used to describe the uncertainty or error in the parameters of the FAC fuzzy set theory. Relations in the method can be extended to include fuzzy arguments. This principle can be used analytically in simple arithmetic operations. It is also used to perform arithmetic analysis at intervals [16].

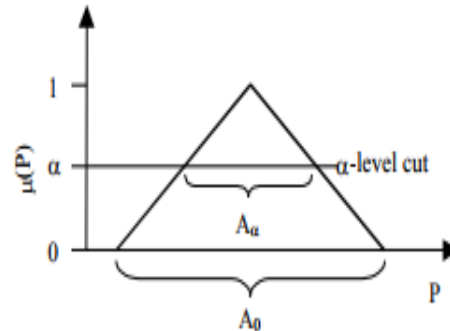


**Figure 1.** Fuzzy number support and cut

The membership function is truncated horizontally from a limited number of  $\alpha$  levels from 0 to 1, as in Figure 1. The model is run to determine the minimum and maximum possible values of the output for each level of the parameter. This information is used to create the corresponding fuzziness of the outputs used as a measure of uncertainty [16].

The study, which required the installation of wind turbines wind speed, power density and capacity Electrical Power Resources Survey and Development Administration for meteorological parameters consisting of factors and the General Directorate of Meteorology Turkey wind energy potential atlas prepared by (REPA) with a range of over universal set of specified values It is provided to calculate and determine with  $\alpha$  - cutting technique.

In the article, firstly, mathematical equations that form the basis of  $\alpha$  - cutting technique application are presented, then  $\alpha$  - cutting technique application is applied to membership functions determined by expert experience. Finally, the new membership function value ranges are shown in the findings section.

## 2. MATERIAL AND METHODS

### 2.1. Mathematical Infrastructure and Used Equations

Mathematically, the fuzzy cluster is the assignment of a value that indicates the degree of membership to any entity in the discourse universe. The purpose of the fuzzy sets theory is to determine the degree of membership in the concepts to determine the uncertainty, which is difficult to define or difficult to define.

In classical set theory, an object is either an element of that set or not. Partial membership is not possible. If the object's membership value is 1, it is the element of the set, and 0 is not the element. In fuzzy sets, an object is an element that determines a certain level of membership.

Generally, the curve that changes according to the values of the elements of the set is called the membership function. In other words, the related characteristic function that has a value between [0,1] created by the fuzzy set is the membership function. Accordingly, the membership level is the value of the change between 0 and 1 for each item. The fuzzy cluster theory developed by Zadeh assigns each object to some extent as a membership in a particular cluster [17].

**Definition 2.1:** If  $A = [a_1, a_3]$  is in the value range, the membership function  $\mu_A(x)$  can be shown as in equation 1.

$$\mu_A(x) = \begin{cases} 0, & x < a_1 \\ 1, & a_1 \leq x \leq a_3 \\ 0 & x > a_3 \end{cases} \tag{1}$$

**Definition 2.2:** The relation used for the  $\mu_A(x)$  triangle membership function is given in equation 2 and equation 3.

$$\mu_A(x) = \begin{cases} 0, & x < a_1 \\ \frac{x - a_1}{a_2 - a_1}, & a_1 \leq x \leq a_2 \\ \frac{a_3 - x}{a_3 - a_2}, & a_2 \leq x \leq a_3 \\ 0, & x > a_3 \end{cases} \tag{2}$$

$$A_\Delta = \max\left(\min\left(\frac{x - x_1}{x_T - x_1}, \frac{x_2 - x}{x_2 - x_T}\right), 0\right) \tag{3}$$

**Definition 2.3:** According to equation 2, set,  $A = \{a_1, a_2, a_3\}$  is defined.  $a_2$  is considered a regular value membership. It is stated here that, depending on a  $\alpha$  coefficient, it will have the same meaning as  $a_2$  value at values close to  $a_2$ . In other words, the uncertainty in  $a_2$  can be tolerated with a  $\alpha$  coefficient to be determined. The specified neighborhood relationship is shown in Figure 2.

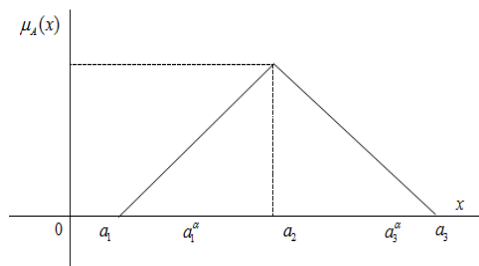


**Figure 2.** Neighborhood of numbers

**Definition 2.4:** In fuzzy logic applications,  $\alpha$  value is defined as the cutting coefficient. The numbers  $a_1^\alpha$  and  $a_3^\alpha$  are the lower and upper limit values of the values assumed to have the same meaning as the  $a_2$  value.  $a_1^\alpha$  and  $a_3^\alpha$  values can be found with the help of equations 4 and 5.

$$\frac{a_1^\alpha - a_1}{a_2 - a_1} = \alpha \tag{4}$$

$$\frac{a_3 - a_3^\alpha}{a_3 - a_2} = \alpha \tag{5}$$

**Definition 2.5:** For  $\forall \alpha \in [0,1]$  from Equations 4 and 5, the  $A_\alpha = [a_1^\alpha, a_3^\alpha]$  value range can be defined. The values of  $a_1^\alpha$  and  $a_3^\alpha$  can be calculated as in equations 6 and 7.

$$a_1^\alpha = \alpha(a_2 - a_1) + a_1 \tag{6}$$

$$a_3^\alpha = a_3 - (a_3 - a_2)\alpha \tag{7}$$

Artificial neural networks, intuition, genetic algorithm, angled fuzzy cluster, and inference fuzzy logic are among the methods used to determine membership functions [18]. Membership functions used in fuzzy logic applications are trapezoid, triangle, Gaussian, S membership function,  $\Pi$  membership function and bell curve membership functions [19].

### 2.2. $\alpha$ -Cutting Technique Application

In the study, the ranges of the membership functions prepared for the meteorological parameters that are planned to be used as input values in the installation of wind energy turbines on the universal cluster Meteorology General and Renewable Energy Office Headquarters located in Turkey wind atlas of Figure 3 is derived from five different topographical 50 m wind potential ranges of values are determined based on the height.

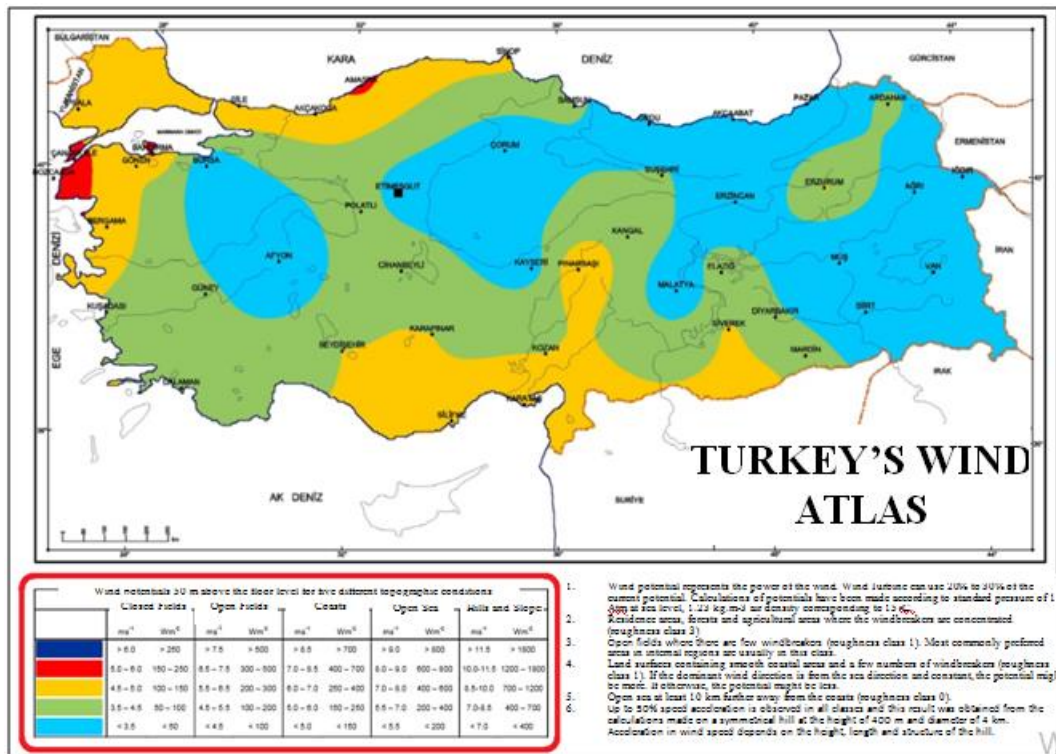


Figure 3. Turkey wind energy potential atlas [20].

In the study Matlab program designed meteorolojik\_fuzz In the system, average wind speed X1, average power density X2 and capacity factor X3 introduction despite the values Y1 produces an output value.

Meteorological based parameters It is assessed meteorolojik\_fuzzy fuzzy logic model in Figure 4, each used membership function Figure 3 for with the help of identified ranges and linguistic Variables Figure 5, Figure 6 and In Figure 7 It is shown.

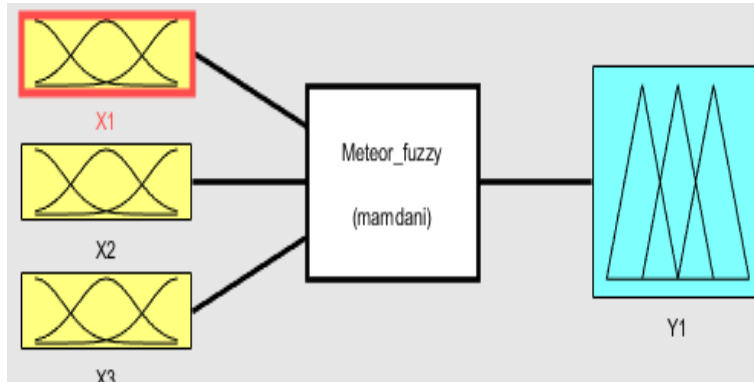


Figure 4. Meteorological fuzzy

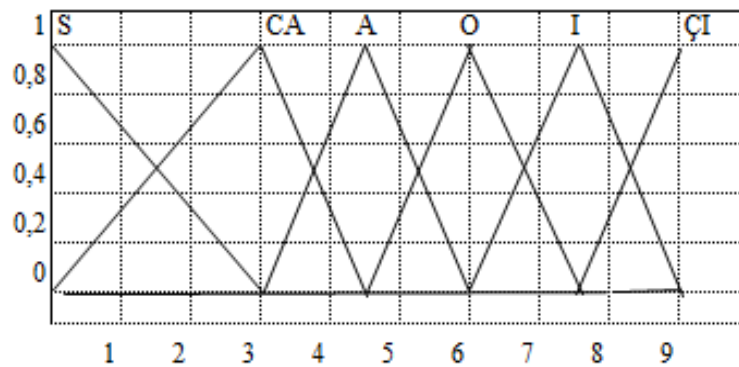


Figure 5. Average wind speed

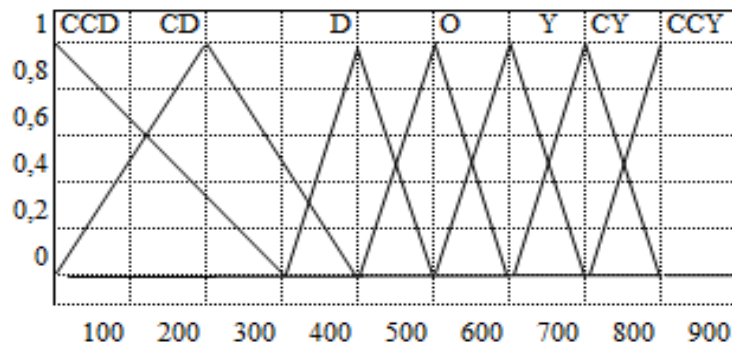


Figure 6. Average power density

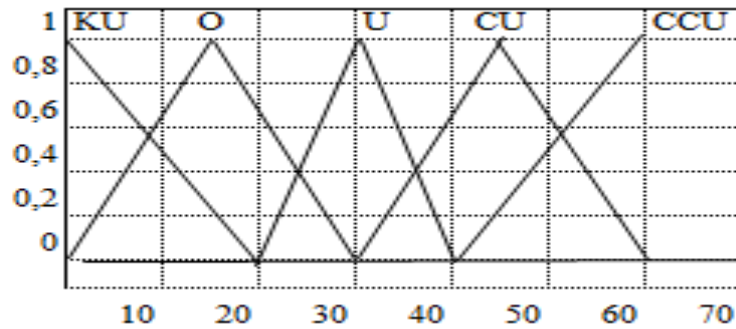


Figure 7. Capacity factor

When the wind speed and direction data obtained from the measurement stations and the power density and capacity factor values calculated through these data are examined, it is observed that there are serious accumulations above and below the specified membership function intervals.

While determining the value ranges of the membership function, the values close to these value ranges are considered to be statistically insignificant. Therefore, the correct values for the system designed by considering these accumulations determine our It is desired to calculate a flexible value range that will provide. For this, recalculation and determination of membership function value range prepared based on wind potential atlas with fuzzy  $\alpha$  cutting technique will be provided.

In the sample mathematical calculation for the first value range of the average wind speed membership function in study 3 the normal value was selected and the following triangular membership function was created in the fuzzy set (0 3 4,5).

$$\mu_A(x) = \begin{cases} 0, & x < 0 \\ \frac{x-0}{3-0}, & 0 \leq x \leq 3 \\ \frac{4,5-x}{4,5-3}, & 3 \leq x \leq 4,5 \\ 0, & x > 4,5 \end{cases} \quad (8)$$

In this function,  $a_1 = 0$ ,  $a_2 = 3$  and  $a_3 = 4,5$  are accepted and the following formulas are obtained for the neighborhood of 3 normal values.

$$a_1^\alpha = 3.\alpha \quad (9)$$

$$a_3^\alpha = 4,5 - 1,5.\alpha \quad (10)$$

The neighborhood values of the normal values of the intervals of the average wind speed membership function for different  $\alpha$  cutting coefficients were calculated with the help of formulas 9 and 10. In the calculation, the neighborhoods obtained for the different  $\alpha$  cutting coefficients and the neighborhoods corrected according to the step value being 0.025 are shown in Table 1.

**Table 1.** Average wind speed membership function intervals calculated for different  $\alpha$  cutting coefficients

$\alpha$ Coefficient	Neighbourhood of the Normal Values						Corrected Interval					
	0	3	4,5	6	7,5	9	0	3	4,5	6	7,5	9
0,98	0 - 0,06	2,99 - 3,03	4,47 - 4,53	5,97 - 6,03	7,47 - 7,53	8,97 - 9,03	0 - 0,05	2,975 - 3,025	4,50 - 4,575	6 - 6,075	7,425 - 7,575	8,925 - 9,075
0,97	0 - 0,09	2,99 - 3,04	4,45 - 4,54	5,95 - 6,04	7,45 - 7,54	8,95 - 9,04	0 - 0,075	2,975 - 3,025	4,50 - 4,575	5,975 - 6,075	7,425 - 7,575	8,925 - 9,075
0,95	0 - 0,15	2,97 - 3,07	4,42 - 4,57	5,92 - 6,07	7,42 - 7,57	8,92 - 9,07	0 - 0,15	2,95 - 3,075	4,475 - 4,60	5,95 - 6,10	7,375 - 7,60	8,90 - 9,10
0,93	0 - 0,21	2,97 - 3,10	4,39 - 4,60	5,89 - 6,10	7,39 - 7,60	8,89 - 9,10	0 - 0,225	2,95 - 3,075	4,475 - 4,65	5,95 - 6,125	7,35 - 7,625	8,975 - 9,125
0,91	0 - 0,27	2,97 - 3,13	4,36 - 4,63	5,86 - 6,13	7,36 - 7,63	8,86 - 9,13	0 - 0,25	2,95 - 3,10	4,475 - 4,65	5,925 - 6,15	7,325 - 7,65	8,95 - 9,15
0,89	0 - 0,33	2,96 - 3,16	4,33 - 4,66	5,83 - 6,16	7,33 - 7,66	8,83 - 9,16	0 - 0,325	2,925 - 3,125	4,45 - 4,675	5,925 - 6,20	7,325 - 7,65	8,925 - 9,175
0,87	0 - 0,39	2,96 - 3,19	4,30 - 4,69	5,80 - 6,19	7,30 - 7,69	8,80 - 9,19	0 - 0,40	2,925 - 3,125	4,425 - 4,70	5,90 - 6,225	7,275 - 7,675	8,925 - 9,20
0,85	0 - 0,45	2,95 - 3,22	4,27 - 4,72	5,77 - 6,22	7,27 - 7,72	8,77 - 9,22	0 - 0,475	2,90 - 3,15	4,40 - 4,70	5,825 - 6,325	7,25 - 7,75	8,875 - 9,275
0,82	0 - 0,54	2,94 - 3,27	4,23 - 4,77	5,73 - 6,27	7,23 - 7,77	8,73 - 9,27	0 - 0,575	2,90 - 3,175	4,35 - 4,80	5,80 - 6,375	7,25 - 7,80	8,90 - 9,30
0,79	0 - 0,63	2,93 - 3,31	4,18 - 4,81	5,68 - 6,31	7,18 - 7,81	8,68 - 9,31	0 - 0,625	2,875 - 3,20	4,275 - 4,85	5,725 - 6,45	7,225 - 7,875	8,925 - 9,325

The average power density for different  $\alpha$  cut-off coefficients was calculated with the help of the 9th and 10th formulas of the normal values of the ranges of the membership function. In the calculation, the neighborhoods obtained for the different  $\alpha$  cutting coefficients and the neighborhoods corrected according to the step value of 1.25 are shown in Table 2.

**Table 2.** Power density membership function ranges calculated for different  $\alpha$  cutting coefficients

$\alpha$ Coefficient	Neighbourhood of the Normal Values							Corrected Interval						
	0	200	400	500	600	700	800	0	200	400	500	600	700	800
0,98	0 - 0,6	199,6 - 200,4	399,8 - 400,2	499,8 - 500,2	599,8 - 600,2	699,8 - 700,2	799,8 - 800,2	0 - 1,25	198,75 - 201,25	398,75 - 401,25	497,5 - 502,5	597,5 - 602,5	697,5 - 702,5	797,5 - 802,5
0,97	0 - 0,9	199,4 - 200,6	399,7 - 400,3	499,7 - 500,3	599,7 - 600,3	699,7 - 700,3	799,7 - 800,3	0 - 1,25	198,75 - 201,25	398,75 - 401,25	497,5 - 502,5	597,5 - 602,5	697,5 - 702,5	797,5 - 802,5
0,95	0 - 1,5	199 - 201	399,5 - 400,5	499,5 - 500,5	599,5 - 600,5	699,5 - 700,5	799,5 - 800,5	0 - 2,5	197,5 - 202,5	397,5 - 402,5	496,25 - 503,75	596,25 - 603,75	696,25 - 703,75	796,25 - 803,75
0,93	0 - 2,1	198,6 - 201,4	399,3 - 400,7	499,3 - 500,7	599,3 - 600,7	699,3 - 700,7	799,3 - 800,7	0 - 2,5	197,5 - 202,5	396,25 - 403,75	495 - 505	595 - 605	695 - 705	795 - 805
0,91	0 - 2,7	198,2 - 201,8	399,1 - 400,9	499,1 - 500,9	599,1 - 600,9	699,1 - 700,9	799,1 - 800,9	0 - 3,75	196,5 - 203,75	396,25 - 403,75	495 - 506,25	593,75 - 606,25	693,75 - 706,25	793,75 - 806,25
0,89	0 - 3,3	197,8 - 202,2	398,9 - 401,1	498,9 - 501,1	598,9 - 601,1	698,9 - 701,1	798,9 - 801,1	0 - 3,75	196,5 - 203,75	395 - 405	493,75 - 506,25	592,5 - 606,25	692,5 - 706,25	792,5 - 806,25
0,87	0 - 3,9	197,4 - 202,6	398,7 - 401,3	498,7 - 501,3	598,7 - 601,3	698,7 - 701,3	798,7 - 801,3	0 - 5,0	195 - 203,75	393,75 - 406,25	493,75 - 507,5	590 - 607,5	691,25 - 707,5	791,25 - 807,5
0,85	0 - 4,5	197 - 203	398,5 - 401,5	498,5 - 501,5	598,5 - 601,5	698,5 - 701,5	798,5 - 801,5	0 - 5,0	193,75 - 205	393,75 - 406,25	492,5 - 507,5	588,75 - 608,75	690 - 708,75	790 - 808,75
0,82	0 - 5,4	196,4 - 203,6	398,2 - 401,8	498,2 - 501,8	598,2 - 601,8	698,2 - 701,8	798,2 - 801,8	0 - 6,25	192,5 - 206,25	392,5 - 408,75	488,75 - 508,75	586,25 - 610	687,5 - 710	787,5 - 810
0,79	0 - 6,3	195,8 - 204,2	397,9 - 402,1	497,9 - 502,1	597,9 - 602,1	697,9 - 702,1	797,9 - 802,1	0 - 7,5	191,25 - 207,5	391,25 - 410	487,5 - 511,25	583,75 - 611,25	686,25 - 711,25	786,25 - 811,25

The neighborhood values of the normal values of the ranges of the capacity factor membership function for different  $\alpha$  cutting coefficients were calculated with the help of formulas 9 and 10. In the calculation, the neighborhoods obtained for the different  $\alpha$  cutting coefficients and the neighborhoods corrected according to the step value of 0.25 are shown in Table 3.

**Table 3.** Capacity factor membership function ranges calculated for different  $\alpha$  cut coefficients

$\alpha$ Coefficient	Neighbourhood of the Normal Values					Corrected Interval				
	0	15	30	45	60	0	15	30	45	60
0,98	0 - 0,04	14,99 - 15,03	29,98 - 30,02	44,97 - 45,03	59,96 - 60,04	0 - 0,25	14,5 - 15,5	29,5 - 30,5	44,5 - 45,5	59,5 - 60,5
0,97	0 - 0,06	14,98 - 15,04	29,97 - 30,03	44,95 - 45,04	59,94 - 60,06	0 - 0,25	14,5 - 15,5	29,5 - 30,5	44,5 - 45,5	59,5 - 60,5
0,95	0 - 0,1	14,97 - 15,07	29,95 - 30,05	44,92 - 45,07	59,90 - 60,1	0 - 0,50	14,25 - 15,75	29,25 - 30,75	44,25 - 45,75	59,25 - 60,75
0,93	0 - 0,14	14,96 - 15,10	29,93 - 30,07	44,89 - 45,10	59,86 - 60,14	0 - 0,50	14 - 15,75	29 - 30,75	44 - 45,75	59 - 60,75
0,91	0 - 0,18	14,95 - 15,13	29,91 - 30,09	44,86 - 45,13	59,82 - 60,18	0 - 0,50	13,75 - 16,25	28,75 - 31,25	43,75 - 46,25	58,75 - 61,25
0,89	0 - 0,22	14,94 - 15,16	29,89 - 30,11	44,83 - 45,16	59,78 - 60,22	0 - 0,50	13,5 - 16,5	28,5 - 31,5	43,5 - 46,5	58,5 - 61,5
0,87	0 - 0,26	14,93 - 15,19	29,87 - 30,13	44,80 - 45,19	59,74 - 60,26	0 - 0,75	13,25 - 16,75	28,25 - 31,75	43,25 - 46,75	58,25 - 61,75
0,85	0 - 0,3	14,92 - 15,22	29,85 - 30,15	44,77 - 45,22	59,70 - 60,30	0 - 1,0	13 - 17	28 - 32	43 - 47	58 - 62
0,82	0 - 0,36	14,91 - 15,27	29,82 - 30,18	44,73 - 45,27	59,64 - 60,36	0 - 1,5	12,75 - 17,25	27,75 - 32,25	42,75 - 47,25	57,75 - 62,25
0,79	0 - 0,42	14,89 - 15,31	29,79 - 30,21	44,68 - 45,31	59,58 - 60,42	0 - 2,0	12,25 - 17,75	27,25 - 32,75	42,25 - 46,75	57,25 - 62,75

### 3. RESULTS AND DISCUSSION

When the wind speed and direction data obtained from the measurement stations and the power density and capacity factor values calculated through these data are examined, it is observed that there are serious accumulations in some value ranges. Although these accumulations have a similar effect in the decision process, the determined value ranges in the applications do not include them in the decision process.

In the studies made on the data obtained in the study, the  $\alpha$  coefficient that best represents the accumulation level was determined as 0.91. As a result of the calculations, the average wind speed, average power density and the capacity factor and membership function structure and value ranges of the capacity factor are given in Figure 8, Figure 9 and Figure 10, respectively.

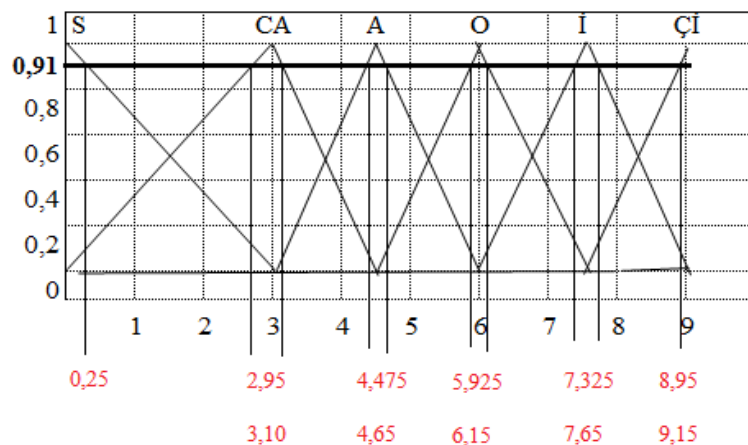


**Figure 8.** Average wind speed membership function defined by  $\alpha$  cutting coefficient

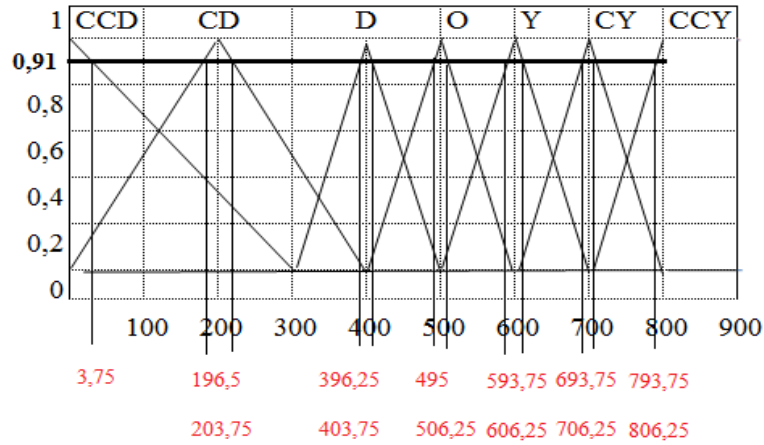


Figure 9. Average power density membership function defined by  $\alpha$  cutting coefficient

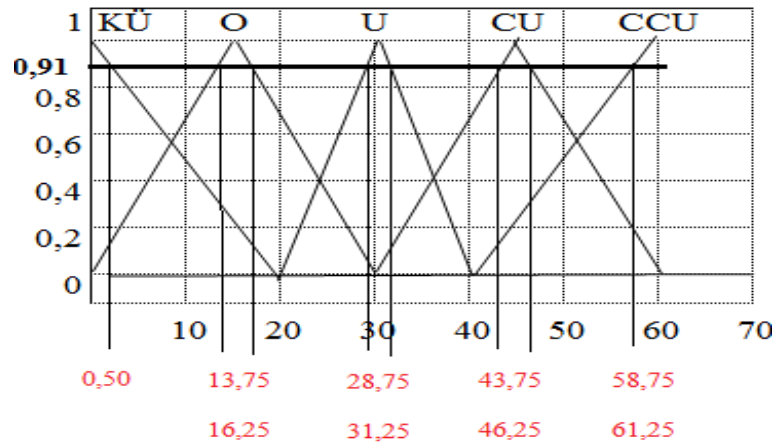


Figure 10. Capacity factor membership function defined by  $\alpha$  cutting coefficient

#### 4. CONCLUSIONS

In this study, the normal value neighborhoods for different  $\alpha$  cutting coefficients and corrected neighborhoods for the determining step values were calculated in the wind turbine installation model determined as a dynamic process. According to the width of the accumulation around the membership functions value ranges defined for the meteorological parameters in the wind turbine model designed using these calculated tables, the appropriate  $\alpha$  cut-off coefficient has been selected and thus, the most suitable value ranges have been calculated for the system designed by considering these accumulations.

As a result of the calculations, the membership functions of the average wind speed, average power density and capacity factor determined as the input value are given in Figure 11, Figure 12 and Figure 13, respectively.

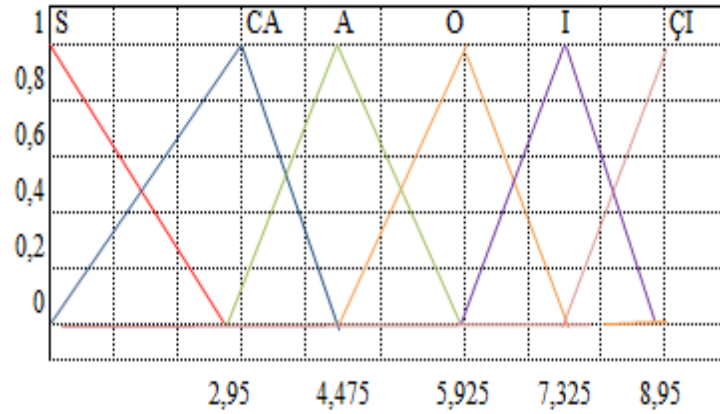


Figure 11. Calculated average wind speed

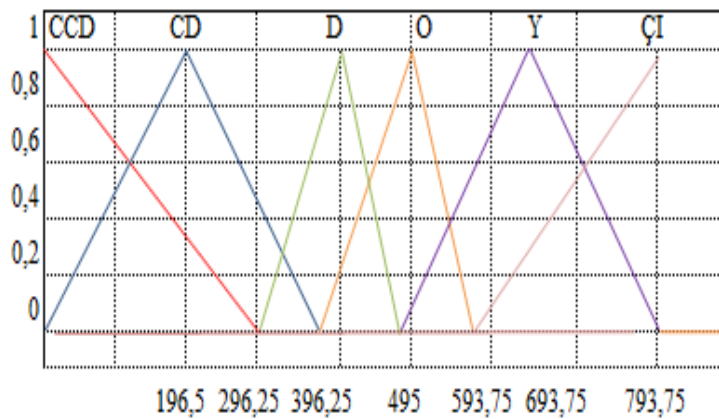


Figure 12. Calculated average power density

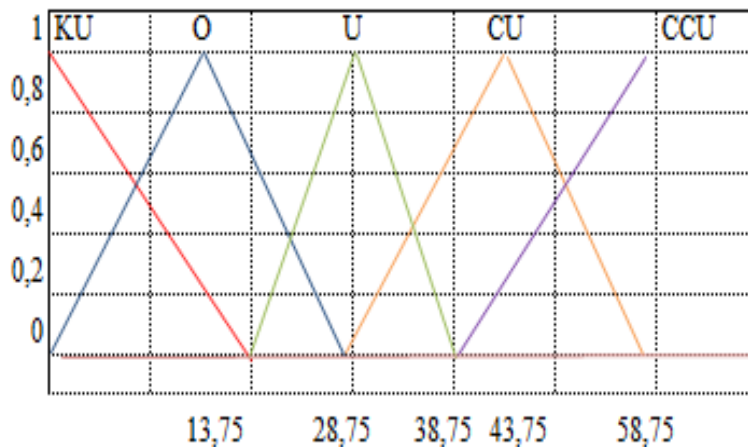


Figure 13. Calculated capacity factor

In the study, the values that serve the same purpose with the redefined membership functions were entered into the system. The findings obtained as a result of the application are intended to form a scale that will be based on the studies to be carried out for the wind power plant installation problem.

## REFERENCES

- [1] Kandil, A., El-Tantawy, O.A., El-Sheikh, S.A., El-Sayed, Sawsan S.S. (2017). Fuzzy soft connected sets in fuzzy soft topological spaces II, *Journal of the Egyptian Mathematical Society*, 25, 171–177.
- [2] Alan, A.Y. (2003). *Nispi Mantik (Fuzzy Logic)*, International Seminar Group, Ludwigshaven, Germany
- [3] Kissi, M., Ramdani, M., Tollabi, M. and Zakarya, D. (2004). Determination of fuzzy logic membership functions using genetic algorithms: application to structure-odor modeling, *Journal of Molecular Modeling*, 10 (5-6): 335-341.
- [4] Kim, J.W., Kim, B.M. and Kim, J.Y. (1998). Genetic algorithm simulation approach to determine membership functions of fuzzy traffic controller, *Electronics Letters*, 34 (20): 1982- 1983.
- [5] Mondelli, G., Castellano, G., Attolico, V. and Distanto, C. (1998). Parallel genetic evolution of membership functions and rules for a fuzzy controller, *High-Performance Computing and Networking Lecture Notes in Computer Science*, 1401, 922-924.
- [6] Kim, J.H., Seo, J.Y. and Kim, G.C. (1996). Estimating membership functions in a fuzzy network model for part-of-speech tagging, *Journal of Intelligent & Fuzzy Systems*, 4 (4): 309-320.
- [7] Singpurwalla, N.D. (2004). Membership functions and probability measures of fuzzy sets – Rejoinder, *Journal of the American Statistical Association*, 99 (467): 884-889.
- [8] Lindley, D.V. (2004). Membership functions and probability measures of fuzzy sets – Comment, *Journal of the American Statistical Association*, 99 (467): 877-879.
- [9] Simon, D. (2002). Sum normal optimization of fuzzy membership functions, *International Journal of Uncertainty fuzziness and Knowledge-Based Systems*, 10 (4): 363-384.
- [10] Sancho-Royo, A. and Verdegay, J.L. (1999). Methods for the construction of membership functions, *International Journal of Intelligent Systems*, 14 (12): 1213-1230.
- [11] Chen, S.M., Kao, C.H. and Yu, C.H. (2002). Generating fuzzy rules from training data containing noise for handling classification problem, *Cybernetics and Systems*, 33 (7): 723-748.
- [12] Cho, Y., Lee, K., Yoo, J. and Park, M. (1998). Autogeneration of fuzzy rules and membership functions for fuzzy modelling using rough set theory, *IEE Proceedings-Control Theory and Applications*, 145 (5): 437-442.
- [13] Lin, C.J. and Ho, W.H. (2005). An asymmetry-similarity- measure-based neural fuzzy inference system, *Fuzzy Sets and Systems*, 152 (3): 535- 551.
- [14] Wu, T.P. and Chen, S.M. (1999). A new method for constructing membership functions and fuzzy rules from training examples, *IEEE Transactions on Systems Man and Cybernetics Part B-Cybernetics*, 29 (1): 25-40.
- [15] Halgamuge, S.K., Poehmueller, W. and Glesner, M. (1995). An alternative approach for generation of membership functions and fuzzy rules based on radial and cubic basis functions networks, *International Journal of Approximate Reasoning*, 12 (3-4): 279-298.
- [16] Abebe, A. J., GUÏNOT, V. and Solomatine, D. P. (2000). Fuzzy alpha-cut vs. Monte Carlo techniques in assessing uncertainty in model parameters, *Proc. 4-th International Conference on Hydroinformatics*, Iowa City, USA.
- [17] Turnbull, H. and Omenzetter, P. (2017). Fuzzy finite element model updating of a laboratory wind turbine blade for structural modification detection, *Procedia Engineering*, 199, 2274–2281.
- [18] Bojadziev, G. and Bojadziev, M. (1991). *Fuzzy Sets, Fuzzy Logic, Applications*, World Scientific, London.
- [19] Bai, Y. and Wang, D. (2006). *Fundamentals of Fuzzy Logic Kontrol Fuzzy Sets, Fuzzy Rules and Defuzzifications*, Advanced Fuzzy Logic Technologies InIndustrial Applications, Springer.
- [20] Internet: General Directorate of Meteorology, (2017). <https://www.mgm.gov.tr/genel/ruzgar-atlasi.aspx>



## New Analytical Solutions for Space and Time Fractional Phi-4 Equation

Ayşegül DAŞCIOĞLU<sup>1</sup>, Sevil ÇULHA ÜNAL<sup>2\*</sup>, Dilek VAROL BAYRAM<sup>3</sup>

<sup>1,2,3</sup> Department of Mathematics, Faculty of Science and Arts, Pamukkale University, Denizli, Turkey.

(Received: 03.03.2020; Accepted: 18.05.2020)

**ABSTRACT:** In this paper, the largest set in the literature of space, time and space-time conformable fractional Phi-4 equations is found by utilizing an analytical method based upon the Jacobi elliptic functions. These solutions are obtained in a general form including trigonometric, rational, complex and hyperbolic functions. Some problems are presented to illustrate the practical application of the proposed method and some of the solutions are also demonstrated with the two-dimensional and three-dimensional graphics.

Mathematics Subject Classification: 35G20, 35L05, 35R11, 33E05.

Keywords: Jacobi elliptic functions; Space-time fractional Phi-4 equation; Conformable fractional derivative; Analytic method.

### 1. INTRODUCTION

The Phi-4 equation which is a particular form of Klein-Gordon equation and has used in particle and nuclear physics is defined by

$$u_{tt} - au_{xx} - bu + \lambda u^3 = 0$$

where  $a$ ,  $b$  and  $\lambda$  are constants. This equation has also been the subject of intensive investigation for classical and quantized field theory, and it has kink-like solutions which are not solitons [1]. Besides, the Phi-4 equation has been mostly examined as the easiest nontrivial relativistic invariant field theoretical model [2]. If  $\lambda = 0$ , the above equation turns into a linear differential equation.

Recently, various methods have been used to solve the integer order Phi-4 equation. The solution methods for this equation are sine-cosine [3], sine-cosine ansatz [4], tanh [4], generalized tanh [5], modified extended tanh-function [6], Weierstrass elliptic function [7], Jacobi-Gauss-Lobatto collocation [8], variational [9], modified simple equation [10,11], homotopy perturbation [12], homotopy analysis [12], Adomian decomposition [12],  $(G'/G, 1/G)$ -expansion [13], trigonometric B-Spline collocation [14] generalized Kudryashov [15] and improved  $F$ -expansion [16].

In recent years, searching solutions of the fractional differential equations have drawn remarkable interest not only for applied mathematicians but also for the other scientists. So far, various solutions of the time fractional Phi-four equation have been founded by utilizing the tanh function [17], modified residual power series [18], modified Kudryashov [19], exponential

\*Corresponding Author: sevilclh@gmail.com

ORCID number of authors: <sup>1</sup> 0000-0001-8931-6930, <sup>2</sup> 0000-0001-7447-9219, <sup>3</sup> 0000-0002-5158-5614

function [19], extended direct algebraic [20], mapping [21], modified mapping [21],  $q$ -homotopy analysis transform ( $q$ -HATM) [22], and generalized Kudryashov [23] methods. The solutions of space-time conformable fractional Phi-four equation is also gained by using the  $(G'/G, 1/G)$ -expansion [24] method. Among these methods, exponential function, the modified Kudryashov, extended direct algebraic, mapping, modified mapping and generalized Kudryashov methods contain the fractional derivatives with respect to time in the conformable sense, while the  $(G'/G, 1/G)$ -expansion method includes the fractional derivatives with respect to space and time in the conformable sense. However, a solution method for space fractional Phi-4 equations is not yet available in the literature. On the other side, although there has not found any method involving the Jacobi elliptic functions for the solutions of the conformable space-time fractional Phi-4 equation, Jacobi elliptic functions have been used to obtain the exact solutions of different conformable fractional partial differential equations [25-34].

In this study, Jacobi elliptic functions have been used to improve an analytic method for the space, time, and space-time conformable fractional Phi-4 equations is presented. Our goal is to find the possible largest set of exact solutions of the space-time conformable fractional Phi-four equation in the form

$$D_t^\alpha D_t^\alpha u - a D_x^\beta D_x^\beta u - bu + \lambda u^3 = 0, \quad 0 < \alpha, \beta \leq 1. \tag{1}$$

Here,  $D_x^\beta$  and  $D_t^\alpha$  stand for the conformable fractional derivative of the unknown function  $u(x, t)$  with respect to  $x$  and  $t$ , respectively.

The rest of the paper has been organized as follows: In the second section, conformable fractional derivative and some properties of Jacobi elliptic functions are presented. The exact solutions of the conformable space-time fractional Phi-four equation are obtained in terms of Jacobi elliptic functions in the third section. In the fourth section, to illustrate the practical application of the proposed method, four problems are presented and some solutions are demonstrated by the 2D and 3D graphics. Finally, the paper has been concluded in the fifth section.

## 2. PRELIMINARIES

Recently, Khalil et al. [35] has described the conformable fractional derivative. Since it is similar to the definition of the usual derivative this definition of the fractional derivative is the simplest way compared to the other fractional derivatives. Thus, the fractional Phi-4 equation is examined in the conformable sense in this paper. The definition and some of the properties of the mentioned conformable fractional derivative can be given as follows and other properties of it can be seen in [35] and [36].

**Definition [35]:** Let  $f: [0, \infty) \rightarrow \mathbb{R}$  be a function. The conformable fractional derivative of  $\alpha$ -the order of the function  $f$  is described by

$$T_\alpha(f)(t) = \lim_{\varepsilon \rightarrow 0} \frac{f(t + \varepsilon t^{1-\alpha}) - f(t)}{\varepsilon}, \quad \alpha \in (0,1), \quad t > 0.$$

If the function  $f$  is  $\alpha$ -differentiable in conformable sense and  $\lim_{t \rightarrow 0^+} f^{(\alpha)}(t)$  exists, then

$$f^{(\alpha)}(0) = \lim_{t \rightarrow 0^+} f^{(\alpha)}(t).$$

**Theorem 1 [35]:** Let the functions  $f$  and  $g$  be  $\alpha$ -differentiable in conformable sense for  $t > 0$  such that  $\alpha \in (0,1]$ . Then, the following properties are satisfied:

- 1)  $T_\alpha(af + bg) = aT_\alpha(f) + bT_\alpha(g); \quad \forall a, b \in \mathbb{R}.$
- 2)  $T_\alpha(t^p) = pt^{p-\alpha}; \quad \forall p \in \mathbb{R}.$
- 3)  $T_\alpha(\lambda) = 0,$  where  $\lambda$  is a constant.
- 4)  $T_\alpha(fg) = fT_\alpha(g) + gT_\alpha(f).$
- 5)  $T_\alpha\left(\frac{f}{g}\right) = \frac{gT_\alpha(f) - fT_\alpha(g)}{g^2}.$
- 6) If  $f$  is differentiable, then  $T_\alpha(f)(t) = t^{1-\alpha} \frac{df}{dt}(t).$

**Theorem 2 [36]:** Assume that the functions  $f, g : (0, \infty) \rightarrow \mathbb{R}$  be  $\alpha$ -differentiable in conformable sense and  $0 < \alpha \leq 1$ . Suppose that  $h(t) = f(g(t))$ , then the composite function  $h(t)$  is  $\alpha$ -differentiable in conformable sense also. For non-zero  $t$  and  $g(t) \neq 0$ , we obtain

$$T_\alpha(h)(t) = T_\alpha(f)(g(t)) \cdot T_\alpha(g)(t) \cdot g(t)^{\alpha-1}.$$

If  $t = 0$ , we get

$$T_\alpha(h)(0) = \lim_{t \rightarrow 0} T_\alpha(f)(g(t)) \cdot T_\alpha(g)(t) \cdot g(t)^{\alpha-1}.$$

The basic Jacobi elliptic functions are

$$\operatorname{sn}\xi = \operatorname{sn}(\xi|m^2), \quad \operatorname{cn}\xi = \operatorname{cn}(\xi|m^2), \quad \operatorname{dn}\xi = \operatorname{dn}(\xi|m^2)$$

where  $m$  is a complex number and it represents the modulus of the elliptic function. If this modulus is a real number, it can always be set up as  $0 < m^2 < 1$ . Besides these three well-known elliptic functions, there are nine other elliptic functions named as ns, nc, nd, sc, sd, cd, cs, ds and dc which are determined by taking reciprocals and quotients [37]. Twelve Jacobi elliptic functions are examined in four groups, and the notations can be clear from Table 1.

**Table 1.** Jacobi elliptic functions

1	$\operatorname{sn}\xi$	$\operatorname{cn}\xi$	$\operatorname{dn}\xi$
2	$\operatorname{sd}\xi = \frac{\operatorname{sn}\xi}{\operatorname{dn}\xi}$	$\operatorname{cd}\xi = \frac{\operatorname{cn}\xi}{\operatorname{dn}\xi}$	$\operatorname{nd}\xi = \frac{1}{\operatorname{dn}\xi}$
3	$\operatorname{sc}\xi = \frac{\operatorname{sn}\xi}{\operatorname{cn}\xi}$	$\operatorname{nc}\xi = \frac{1}{\operatorname{cn}\xi}$	$\operatorname{dc}\xi = \frac{\operatorname{dn}\xi}{\operatorname{cn}\xi}$
4	$\operatorname{ns}\xi = \frac{1}{\operatorname{sn}\xi}$	$\operatorname{cs}\xi = \frac{\operatorname{cn}\xi}{\operatorname{sn}\xi}$	$\operatorname{ds}\xi = \frac{\operatorname{dn}\xi}{\operatorname{sn}\xi}$

These double periodic functions satisfy the properties in Table 2. Moreover, when  $m = 0$  and  $m = 1$ , Jacobi elliptic functions transform trigonometric and hyperbolic functions, respectively. The derivatives and the other properties of these functions can be seen in Ref. [38].

**Table 2.** The relations of Jacobi elliptic functions

1	$\text{sn}^2\xi + \text{cn}^2\xi = 1$	$\text{dn}^2\xi + m^2\text{sn}^2\xi = 1$	$\text{dn}^2\xi - m^2\text{cn}^2\xi = 1 - m^2$	$\text{cn}^2\xi + (1 - m^2)\text{sn}^2\xi = \text{dn}^2\xi$
2	$\text{nd}^2\xi - m^2\text{sd}^2\xi = 1$	$\text{cd}^2\xi + (1 - m^2)\text{sd}^2\xi = 1$	$m^2\text{cd}^2\xi + (1 - m^2)\text{nd}^2\xi = 1$	$\text{cd}^2\xi + \text{sd}^2\xi = \text{nd}^2\xi$
3	$\text{nc}^2\xi - \text{sc}^2\xi = 1$	$\text{dc}^2\xi - (1 - m^2)\text{sc}^2\xi = 1$	$\text{dc}^2\xi - (1 - m^2)\text{nc}^2\xi = m^2$	$\text{nc}^2\xi - m^2\text{sc}^2\xi = \text{dc}^2\xi$
4	$\text{ns}^2\xi - \text{cs}^2\xi = 1$	$\text{ns}^2\xi - \text{ds}^2\xi = m^2$	$\text{ds}^2\xi - \text{cs}^2\xi = 1 - m^2$	$m^2\text{cs}^2\xi + (1 - m^2)\text{ns}^2\xi = \text{ds}^2\xi$

### 3. EXACT SOLUTIONS OF THE SPACE-TIME FRACTIONAL PHI-4 EQUATION

In this part of the paper, the space and time conformable fractional Phi-four equation (1) is considered. Utilizing the following change of the variables

$$\xi = k \frac{t^\alpha}{\alpha} + l \frac{x^\beta}{\beta}$$

such that  $k$  and  $l$  are arbitrary constants and using the chain rule, Eq. (1) becomes an ordinary differential equation in the form

$$(k^2 - al^2) \frac{d^2u}{d\xi^2} - bu + \lambda u^3 = 0 \tag{2}$$

where  $k^2 - al^2 \neq 0$ . When  $\lambda = 0$ , Eq. (2) becomes a linear ordinary differential equation, and the solution can be founded easily. In this study, the solutions are investigated for the nonlinear case.

The main purpose of this analytical method is to gain the solutions  $u(\xi)$  in the form

$$u(\xi) = \sum_{j=0}^N c_j F^j(\xi).$$

Here,  $c_j$  are the coefficients to be determined and  $F(\xi)$  are the solutions of the auxiliary nonlinear ordinary differential equation given by

$$(dF/d\xi)^2 = PF^4(\xi) + QF^2(\xi) + R \tag{3}$$

where  $P, Q$  and  $R$  are constants. The solutions of this auxiliary equation are in terms of Jacobi elliptic functions. Depending on the selected values of the constants  $P, Q$  and  $R$ , the set of these Jacobi elliptic function solutions of Eq. (3) are given in Table 3. Some of them can be seen also in Ref. [31-34].

**Table 3.** The solution  $F$  for  $P$ ,  $Q$  and  $R$

	$P$	$Q$	$R$	$F$
1	$m^2$	$-(m^2 + 1)$	1	$\pm sn\xi, \pm cd\xi$
2	1	$-(m^2 + 1)$	$m^2$	$\pm ns\xi, \pm dc\xi$
3	$-m^2$	$-(m^2 + 1)$	-1	$\pm isn\xi, \pm icd\xi$
4	-1	$-(1 + m^2)$	$-m^2$	$\pm ins\xi, \pm idc\xi$
5	1	$-m^2 + 2$	$1 - m^2$	$\pm cs\xi, \pm idn\xi$
6	$-m^2 + 1$	$-m^2 + 2$	1	$\pm sc\xi, \pm ind\xi$
7	-1	$2 - m^2$	$m^2 - 1$	$\pm ics\xi, \pm dn\xi$
8	$-1 + m^2$	$-m^2 + 2$	-1	$\pm isc\xi, \pm nd\xi$
9	$1 - m^2$	$2m^2 - 1$	$-m^2$	$\pm nc\xi, \pm imsd\xi$
10	$-m^2$	$2m^2 - 1$	$1 - m^2$	$\pm cn\xi, \pm \frac{i}{m} ds\xi$
11	$m^2 - 1$	$2m^2 - 1$	$m^2$	$\pm inc\xi, \pm msd\xi$
12	$m^2$	$2m^2 - 1$	$m^2 - 1$	$\pm icn\xi, \pm \frac{1}{m} ds\xi$
13	$m^4 - m^2$	$2m^2 - 1$	1	$\pm \frac{i}{m} nc\xi, \pm sd\xi$
14	1	$2m^2 - 1$	$m^4 - m^2$	$\pm imcn\xi, \pm ds\xi$
15	$-m^4 + m^2$	$2m^2 - 1$	-1	$\pm \frac{1}{m} nc\xi, \pm isd\xi$
16	-1	$2m^2 - 1$	$-m^4 + m^2$	$\pm mcn\xi, \pm ids\xi$
17	$\frac{1}{4}$	$\frac{1 + m^2}{2}$	$\frac{(1 - m^2)^2}{4}$	$ds\xi \pm cs\xi, -ds\xi \mp cs\xi,$ $i(mcn\xi \pm dn\xi), -i(mcn\xi \pm dn\xi)$
18	$\frac{(1 - m^2)^2}{4}$	$\frac{1 + m^2}{2}$	$\frac{1}{4}$	$\frac{1}{1 - m^2} (ds\xi \pm cs\xi), \frac{-1}{1 - m^2} (ds\xi \pm cs\xi),$ $\frac{i}{1 - m^2} (mcn\xi \pm dn\xi), \frac{-i}{1 - m^2} (mcn\xi \pm dn\xi)$
19	$-\frac{1}{4}$	$\frac{1 + m^2}{2}$	$-\frac{(1 - m^2)^2}{4}$	$i(ds\xi \pm cs\xi), -i(ds\xi \pm cs\xi),$ $mcn\xi \pm dn\xi, -mcn\xi \mp dn\xi$
20	$-\frac{(1 - m^2)^2}{4}$	$\frac{1 + m^2}{2}$	$-\frac{1}{4}$	$\frac{i}{1 - m^2} (ds\xi \pm cs\xi), \frac{-i}{1 - m^2} (ds\xi \pm cs\xi),$ $\frac{1}{1 - m^2} (mcn\xi \pm dn\xi), \frac{-1}{1 - m^2} (mcn\xi \pm dn\xi)$
21	$\frac{-m^2 + 1}{4}$	$\frac{m^2 + 1}{2}$	$\frac{-m^2 + 1}{4}$	$nc\xi \pm sc\xi, -nc\xi \mp sc\xi,$ $i(msd\xi \pm nd\xi), -i(msd\xi \pm nd\xi),$
22	$\frac{-1 + m^2}{4}$	$\frac{m^2 + 1}{2}$	$\frac{-1 + m^2}{4}$	$i(nc\xi \pm sc\xi), -i(nc\xi \pm sc\xi),$ $msd\xi \pm nd\xi, -msd\xi \mp nd\xi,$
23	$\frac{1}{4}$	$\frac{m^2 - 2}{2}$	$\frac{m^4}{4}$	$ns\xi \pm ds\xi, -ns\xi \mp ds\xi,$ $dc\xi \pm \sqrt{1 - m^2}nc\xi, -dc\xi \mp \sqrt{1 - m^2}nc\xi$

24	$\frac{m^4}{4}$	$\frac{m^2 - 2}{2}$	$\frac{1}{4}$	$\frac{1}{m^2}(\text{ns}\xi \pm \text{ds}\xi), \frac{-1}{m^2}(\text{ns}\xi \pm \text{ds}\xi),$ $\frac{1}{m^2}(\text{dc}\xi \pm \sqrt{1 - m^2}\text{nc}\xi), \frac{-1}{m^2}(\text{dc}\xi \pm \sqrt{1 - m^2}\text{nc}\xi)$
25	$-\frac{1}{4}$	$\frac{m^2 - 2}{2}$	$-\frac{m^4}{4}$	$i(\text{ns}\xi \pm \text{ds}\xi), -i(\text{ns}\xi \pm \text{ds}\xi),$ $i(\text{dc}\xi \pm \sqrt{1 - m^2}\text{nc}\xi), -i(\text{dc}\xi \pm \sqrt{1 - m^2}\text{nc}\xi)$
26	$-\frac{m^4}{4}$	$\frac{m^2 - 2}{2}$	$-\frac{1}{4}$	$\frac{i}{m^2}(\text{ns}\xi \pm \text{ds}\xi), \frac{-i}{m^2}(\text{ns}\xi \pm \text{ds}\xi),$ $\frac{i}{m^2}(\text{dc}\xi \pm \sqrt{1 - m^2}\text{nc}\xi), \frac{-i}{m^2}(\text{dc}\xi \pm \sqrt{1 - m^2}\text{nc}\xi)$
27	$\frac{m^2}{4}$	$\frac{m^2 - 2}{2}$	$\frac{m^2}{4}$	$\text{sn}\xi \pm \text{icn}\xi, -\text{sn}\xi \mp \text{icn}\xi,$ $\text{cd}\xi \pm i\sqrt{1 - m^2}\text{sd}\xi, -\text{cd}\xi \mp i\sqrt{1 - m^2}\text{sd}\xi$
28	$-\frac{m^2}{4}$	$\frac{m^2 - 2}{2}$	$-\frac{m^2}{4}$	$\text{cn}\xi \pm \text{isn}\xi, -\text{cn}\xi \mp \text{isn}\xi,$ $\sqrt{1 - m^2}\text{sd}\xi \pm \text{icd}\xi, -\sqrt{1 - m^2}\text{sd}\xi \mp \text{icd}\xi$
29	$\frac{1}{4}$	$\frac{1 - 2m^2}{2}$	$\frac{1}{4}$	$\text{ns}\xi \pm \text{cs}\xi, -\text{ns}\xi \mp \text{cs}\xi,$ $\text{msn}\xi \pm \text{idn}\xi, -\text{msn}\xi \mp \text{idn}\xi,$ $\text{dc}\xi \pm \sqrt{1 - m^2}\text{sc}\xi, -\text{dc}\xi \mp \sqrt{1 - m^2}\text{sc}\xi,$ $\text{mcd}\xi \pm i\sqrt{1 - m^2}\text{nd}\xi, -\text{mcd}\xi \mp i\sqrt{1 - m^2}\text{nd}\xi$
30	$-\frac{1}{4}$	$\frac{1 - 2m^2}{2}$	$-\frac{1}{4}$	$i(\text{ns}\xi \pm \text{cs}\xi), -i(\text{ns}\xi \mp \text{cs}\xi),$ $\text{dn}\xi \pm \text{imsn}\xi, -\text{dn}\xi \mp \text{imsn}\xi,$ $i(\text{dc}\xi \pm \sqrt{1 - m^2}\text{sc}\xi), -i(\text{dc}\xi \pm \sqrt{1 - m^2}\text{sc}\xi),$ $\sqrt{1 - m^2}\text{nd}\xi \pm \text{imcd}\xi, -\sqrt{1 - m^2}\text{nd}\xi \mp \text{imcd}\xi$

By applying a balancing procedure to the highest orders of nonlinear and linear terms, we obtain the number  $N = 1$ . Hence, the solution of Eq. (2) can be stated as

$$u(\xi) = c_0 + c_1F.$$

Since the ordinary differential equation (2) is a second order differential equation, we differentiate this solution two times and using the derives form of Eq. (3), we have

$$u''(\xi) = c_1QF + 2c_1PF^3. \tag{4}$$

Substituting Eq. (4) into Eq. (2), a third order polynomial in  $F$  is gained. After that, setting its coefficients to be zero, the following equations system arises

$$\begin{aligned} -bc_0 + \lambda c_0^3 &= 0 \\ k^2Qc_1 - al^2Qc_1 + 3\lambda c_0^2c_1 - bc_1 &= 0 \\ 3\lambda c_0c_1^2 &= 0 \\ 2k^2Pc_1 - 2al^2Pc_1 + \lambda c_1^3 &= 0. \end{aligned}$$

Solving this system, we get  $c_0 = 0$ ,  $c_1 = \mp\sqrt{-2bP/(\lambda Q)}$  and  $c_0 = \mp\sqrt{b/\lambda}$ ,  $c_1 = 0$  such that

$$Q = b/(k^2 - a^2). \tag{5}$$

If we take  $A = \sqrt{b/\lambda}$ , the solutions of Eq. (2) become

$$u = \pm A \sqrt{\frac{-2P}{Q}} F, \quad u = \pm A.$$

Substituting the function  $F$  from Table 3 into the above solution and taking inverse transformation, the solutions of Eq. (1) are obtained. Moreover, the elementary function solutions of Eq. (2) can be found by utilizing the Jacobi elliptic functions for  $m = 0$  and  $m = 1$ . Some of these solutions are constant such that  $u = 0$  and  $u = \pm A$ , the other solutions are listed in Table 4.

**Table 4.** Nonconstant solutions of Eq. (2) when  $m = 0$  and  $m = 1$

$m = 0$	$m = 1$
$u = \pm\sqrt{2}A\sec\xi$	$u = \pm\sqrt{2}A\operatorname{sech}\xi$
$u = \pm\sqrt{2}A\operatorname{csc}\xi$	$u = \pm i\sqrt{2}A\operatorname{csch}\xi$
$u = \pm iA\tan\xi$	$u = \pm A\tanh\xi$
$u = \pm iA\cot\xi$	$u = \pm A\coth\xi$
$u = iA(\sec\xi \pm \tan\xi)$	$u = A(i\operatorname{sech}\xi \pm \tanh\xi)$
$u = -iA(\sec\xi \pm \tan\xi)$	$u = -A(i\operatorname{sech}\xi \pm \tanh\xi)$
$u = iA\left(\frac{\sin\xi}{1 \pm \cos\xi}\right) = iA(\operatorname{csc}\xi \mp \cot\xi)$	$u = A\left(\frac{\sinh\xi}{\cosh\xi \pm 1}\right) = A(\coth\xi \mp \operatorname{csch}\xi)$
$u = -iA\left(\frac{\sin\xi}{1 \pm \cos\xi}\right) = -iA(\operatorname{csc}\xi \mp \cot\xi)$	$u = -A\left(\frac{\sinh\xi}{\cosh\xi \pm 1}\right) = -A(\coth\xi \pm \operatorname{csch}\xi)$

#### 4. APPLICATIONS

In that part of the paper, four different types of examples are considered. These examples are composed of time, space and space-time fractional types of Phi-4 Eq. (1). The solutions of the given examples are also demonstrated by graphics. In all figures, the solutions are drawn by the Mathematica 11.3.

**Example 1.** Consider the conformable space-time fractional Phi-4 Eq. (1) for  $a = 1$ ,  $b = 1$ ,  $\lambda = 1$  and  $\alpha = 0.5$ ,  $\beta = 1$ ; that is

$$D_t^{1/2} D_t^{1/2} u - u_{xx} - u + u^3 = 0. \tag{6}$$

This equation is called the time fractional Phi-4 equation. The solutions of Eq. (6) are

$$u = \pm \sqrt{\frac{-2P}{Q}} F, \quad u = \pm 1$$

such that  $A = 1$ . When  $m = 1$ , condition (5) is satisfied for  $k = 1/2$  and  $l = \sqrt{3}/2$ , then transformation becomes  $\xi = \sqrt{t} + (\sqrt{3}/2)x$ . In Table 4, when  $m = 1$ , the solutions in case 1 and 3 become  $u = \pm \tanh(\sqrt{t} + (\sqrt{3}/2)x)$ . These solutions are illustrated for  $-20 \leq x \leq 20$  and  $0 \leq t \leq 20$  in Figure 1 and Figure 2. The  $(\pm)$  signs correspond to localized soliton solutions that move with opposite screw senses. They have also named a kink soliton and an antikink soliton, respectively [39]. Thus, Figure 1 represents the kink type travelling wave solution, while Figure 2 represents the antikink type travelling wave solution. Besides, Figure 3 and Figure 4 illustrate the same solutions with a two-dimensional plot for  $-20 \leq x \leq 20$  at time  $t = 2$ .

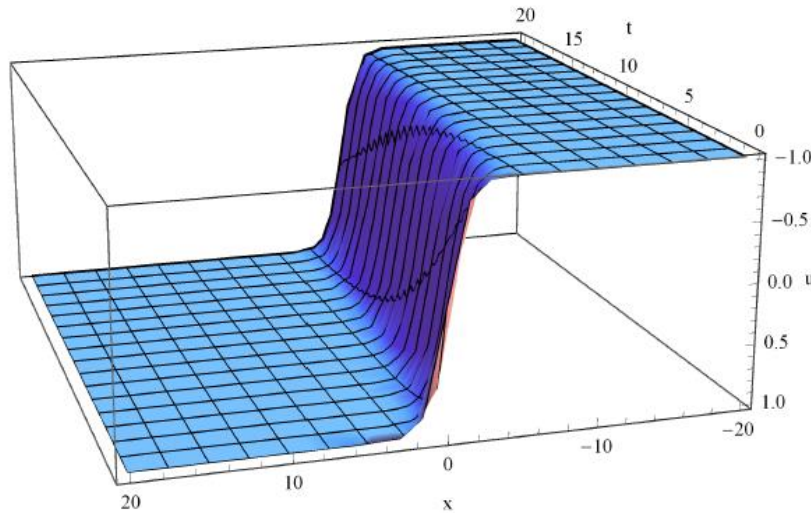


**Figure 1.** 3D plot of solution  $u(x, t) = \tanh(\sqrt{t} + (\sqrt{3}/2)x)$

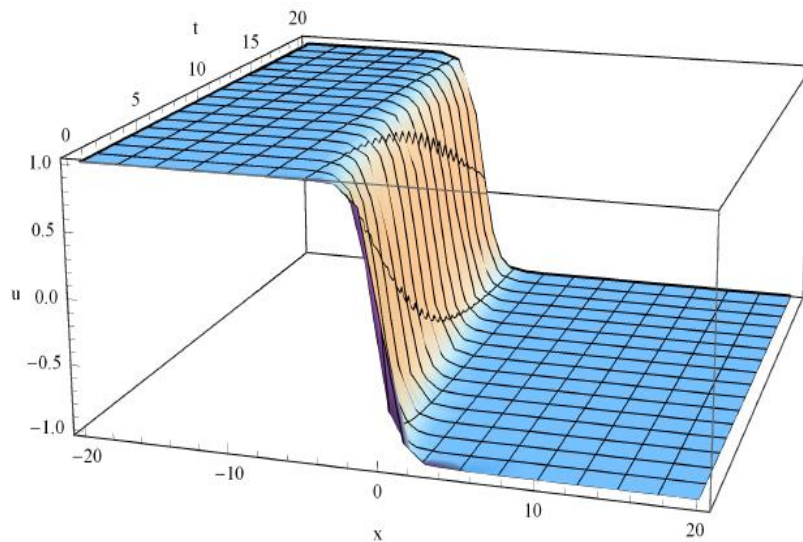


**Figure 2.** 3D plot of solution  $u(x, t) = -\tanh(\sqrt{t} + (\sqrt{3}/2)x)$

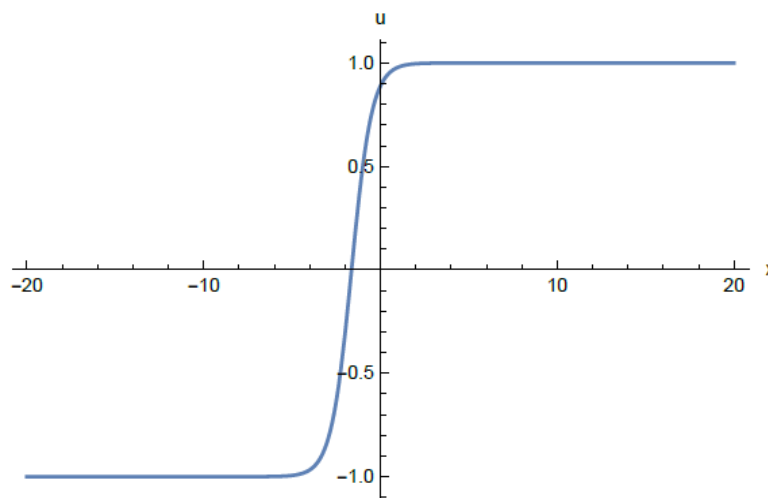


**Figure 3.** 2D plot of  $u(x, t) = \tanh(\sqrt{2} + (\sqrt{3}/2)x)$

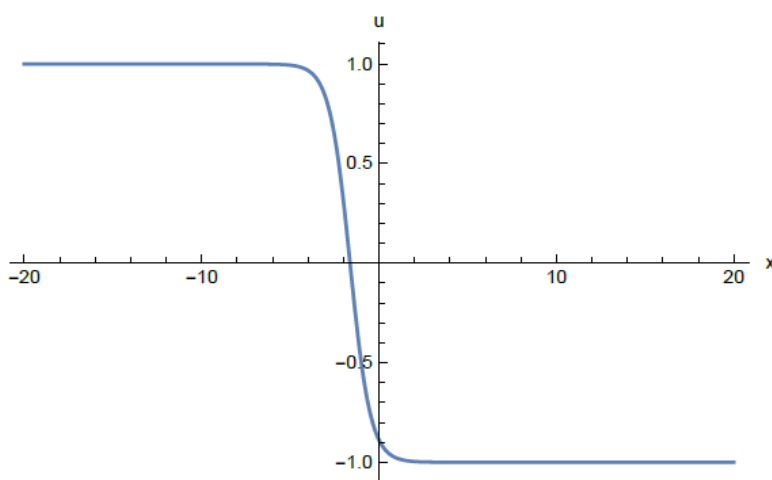


**Figure 4.** 2D plot of  $u(x, t) = -\tanh(\sqrt{2} + (\sqrt{3}/2)x)$

**Example 2.** Consider the conformable space-time fractional Phi-4 Eq. (1) for  $a = 5, b = -2, \lambda = 2$  and  $\alpha = 0.5, \beta = 1$ ; that is

$$D_t^{1/2} D_t^{1/2} u - 5u_{xx} + 2u + 2u^3 = 0. \tag{7}$$

This equation is called the time fractional Phi-4 equation. The solutions of Eq. (7) are

$$u = \pm i \sqrt{\frac{-2P}{Q}} F, \quad u = \pm i$$

such that  $A = i$ . When  $m = 0$ , condition (5) is satisfied for  $k = l = 1$ , then transformation becomes  $\xi = x + 2\sqrt{t}$ . In Table 4, when  $m = 0$ , the solutions in case 17 and 19 become  $u = \mp (\csc(x + 2\sqrt{t}) \pm \cot(x + 2\sqrt{t}))$ . Here, there are four different solutions, but we only consider two of them. Figure 5 and Figure 6 demonstrate the following solutions

$$u = \mp (\csc(x + 2\sqrt{t}) + \cot(x + 2\sqrt{t}))$$

in the region  $-10 \leq x \leq 10$  and  $1 \leq t \leq 2$ . Figure 5 represents the kink type travelling wave solution, while Figure 6 represents the antikink type travelling wave solution. Besides, Figure 7 and Figure 8 illustrate the same solutions with a 2D plot for  $-10 \leq x \leq 10$  at  $t = 2$ . Furthermore, the graphics of the solutions  $u = -\csc(x + 2\sqrt{t}) + \cot(x + 2\sqrt{t})$  and  $u = \csc(x + 2\sqrt{t}) - \cot(x + 2\sqrt{t})$  are similar to  $u = \csc(x + 2\sqrt{t}) + \cot(x + 2\sqrt{t})$  and  $u = -\csc(x + 2\sqrt{t}) - \cot(x + 2\sqrt{t})$ , the only difference between the graphics is that 3.5 units are shifted to the right. Therefore,

$$u = \mp \csc(x + 2\sqrt{t}) - \cot(x + 2\sqrt{t})$$

are called antikink type solutions while

$$u = \mp \csc(x + 2\sqrt{t}) + \cot(x + 2\sqrt{t})$$

are called kink type solutions.

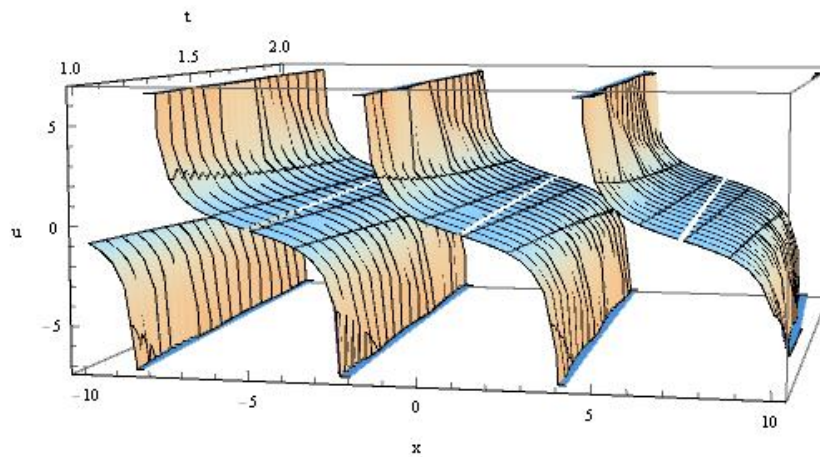


**Figure 5.** 3D plot of solution  $u(x, t) = \csc(x + 2\sqrt{t}) + \cot(x + 2\sqrt{t})$

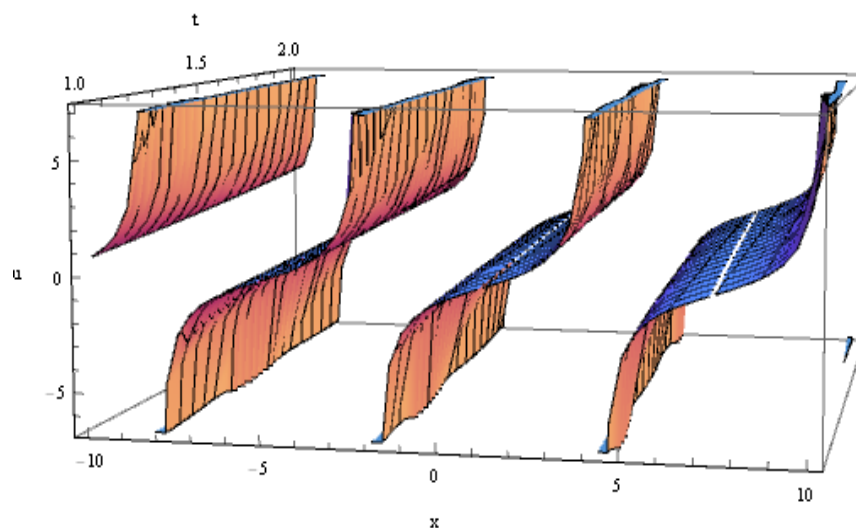


**Figure 6.** 3D plot of solution  $u(x, t) = -\csc(x + 2\sqrt{t}) - \cot(x + 2\sqrt{t})$

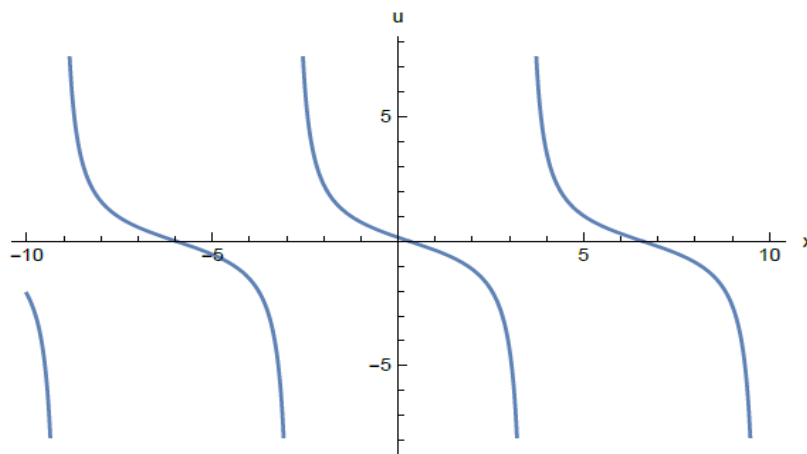


**Figure 7.** 2D plot of  $u(x, t) = \csc(x + 2\sqrt{2}) + \cot(x + 2\sqrt{2})$

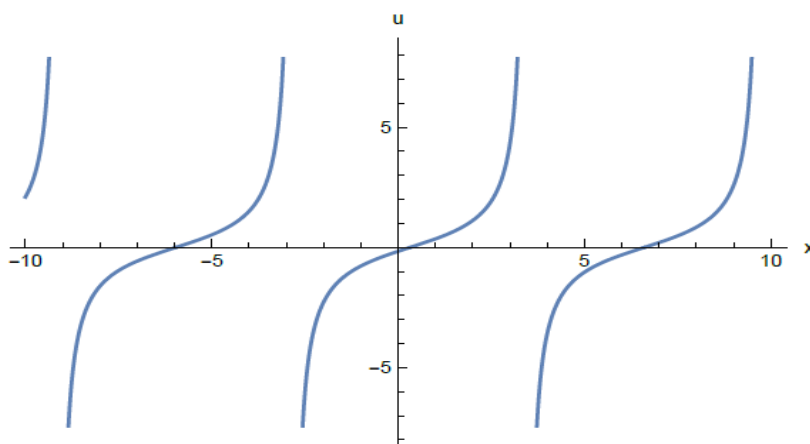


**Figure 8.** 2D plot of  $u(x, t) = -\csc(x + 2\sqrt{2}) - \cot(x + 2\sqrt{2})$

**Example 3.** Consider the conformable space-time fractional Phi-4 Eq. (1) for  $a = -3, b = 4, \lambda = 2$  and  $\alpha = 1, \beta = 0.5$ ; that is

$$u_{tt} + 3D_x^{1/2}D_x^{1/2}u - 4u + 2u^3 = 0. \tag{8}$$

This equation is called the space fractional Phi-4 equation. The solutions of Eq. (8) are

$$u = \pm \sqrt{\frac{-4P}{Q}}F, \quad u = \pm\sqrt{2}$$

such that  $A = \sqrt{2}$ . When  $m = 1$ , condition (5) is satisfied for  $k = l = 1$ , then transformation becomes  $\xi = t + 2\sqrt{x}$ . In Table 4, when  $m = 1$ , the solutions in case 10, 12, 14 and 16 become  $u = \pm 2\operatorname{sech}(t + 2\sqrt{x})$ . These solutions are illustrated for  $5 \leq x \leq 10$  and  $0 \leq t \leq 20$  in Figure 9 and Figure 10. Furthermore, Figure 11 and Figure 12 demonstrate the same solutions with the two-dimensional plot for  $0 \leq x \leq 20$  at  $t = 3$ .

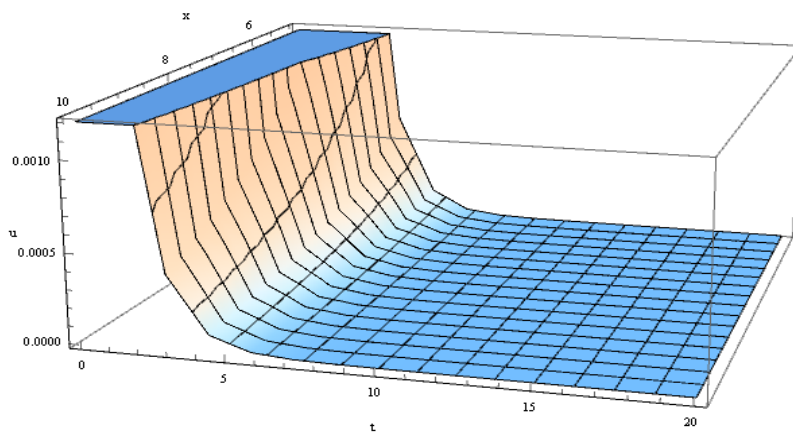


**Figure 9.** 3D plot of solution  $u(x, t) = 2\text{sech}(t + 2\sqrt{x})$

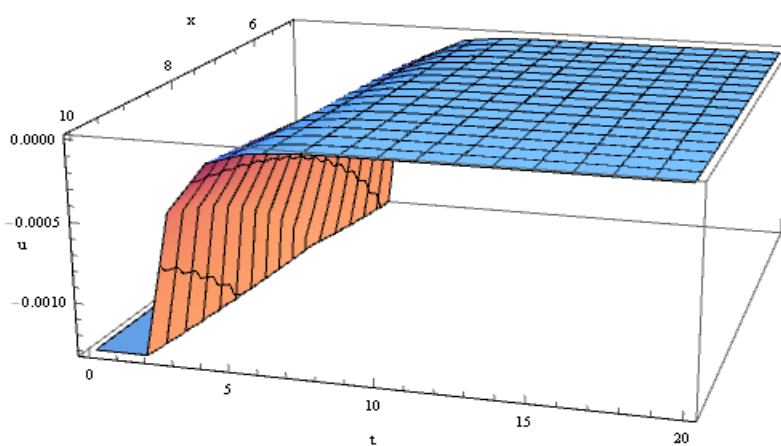


**Figure 10.** 3D plot of solution  $u(x, t) = -2\text{sech}(t + 2\sqrt{x})$

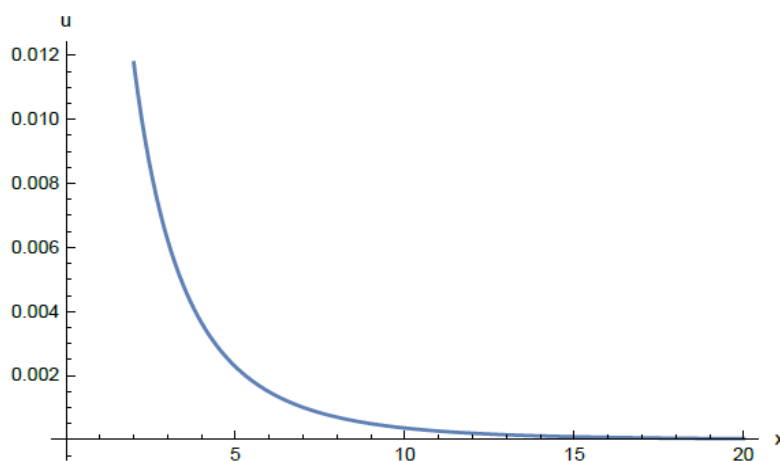


**Figure 11.** 2D plot of  $u(x, t) = 2\text{sech}(3 + 2\sqrt{x})$

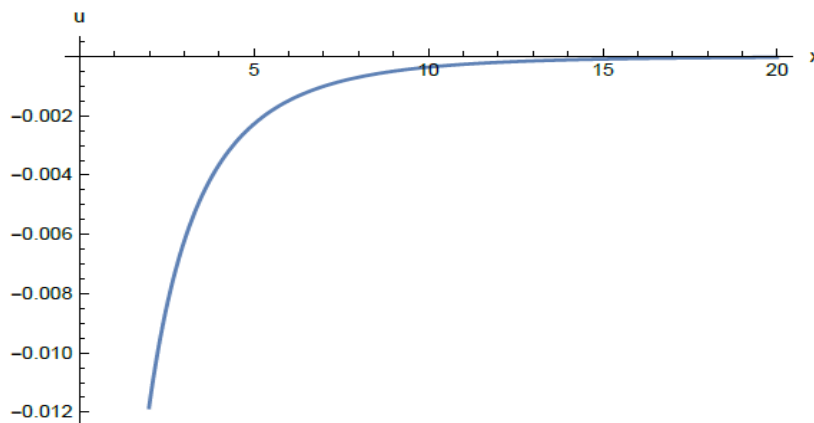


**Figure 12.** 2D plot of  $u(x, t) = -2\text{sech}(3 + 2\sqrt{x})$

**Example 4.** Consider the conformable space-time fractional Phi-4 Eq. (1) for  $a = 1$ ,  $b = 16$ ,  $\lambda = -16$  and  $\alpha = 0.2$ ,  $\beta = 0.2$ ; that is

$$D_t^{1/5} D_t^{1/5} u - D_x^{1/5} D_x^{1/5} u - 16u - 16u^3 = 0. \tag{9}$$

This equation is called the space-time fractional Phi-4 equation. The solutions of Eq. (9) are

$$u = \pm i \sqrt{\frac{-2P}{Q}} F, \quad u = \pm i$$

such that  $A = i$ . When  $m = 0$ , condition (5) is satisfied for  $k = 3$  and  $l = 1$ , then transformation becomes  $\xi = 15^5 \sqrt[5]{t} + 5^5 \sqrt[5]{x}$ . In Table 4, when  $m = 0$ , the solutions in case 6 and 8 become  $u = \mp \tan(15^5 \sqrt[5]{t} + 5^5 \sqrt[5]{x})$ . These solutions are illustrated for  $0 \leq x \leq 20$  and  $0 \leq t \leq 10$  in Figure 13 and Figure 14. Moreover, Figure 15 and Figure 16 demonstrate the same solutions with 2D plot for  $0 \leq x \leq 50000$  at  $t = 5$ . From Figure 15 and Figure 16, we can see that the wave frequency increases as  $x$  approaches to zero.

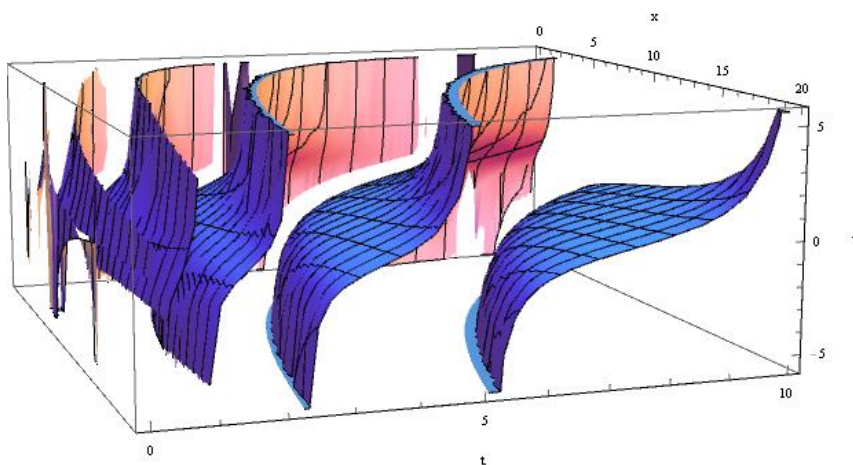


**Figure 13.** 3D plot of solution  $u(x, t) = \tan(15^5 \sqrt[5]{t} + 5^5 \sqrt[5]{x})$

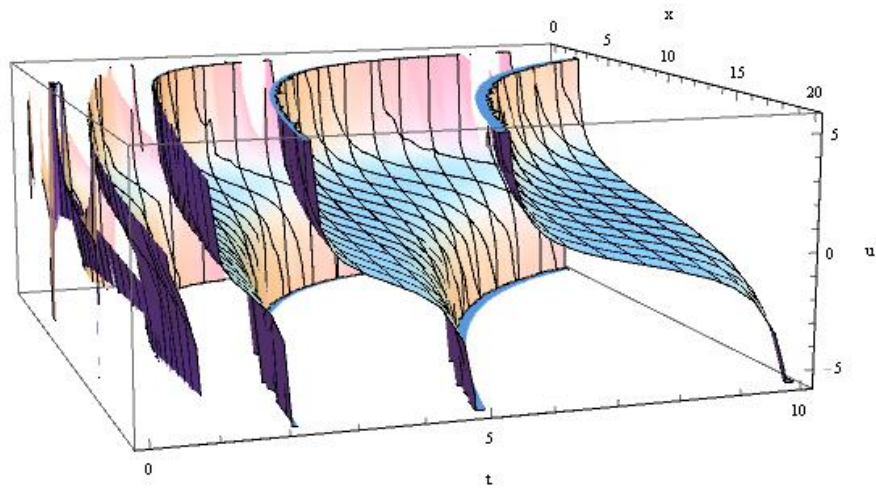


**Figure 14.** 3D plot of solution  $u(x, t) = -\tan(15^5\sqrt{t} + 5^5\sqrt{x})$

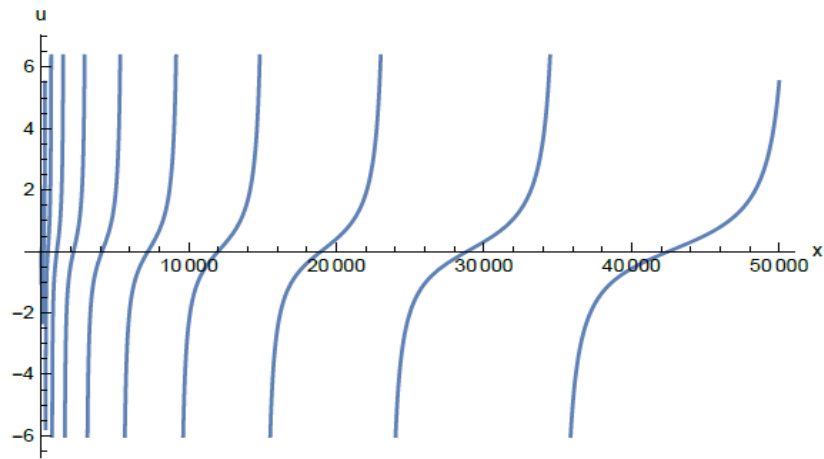


**Figure 15.** 2D plot of  $u(x, t) = \tan(15^5\sqrt{5} + 5^5\sqrt{x})$

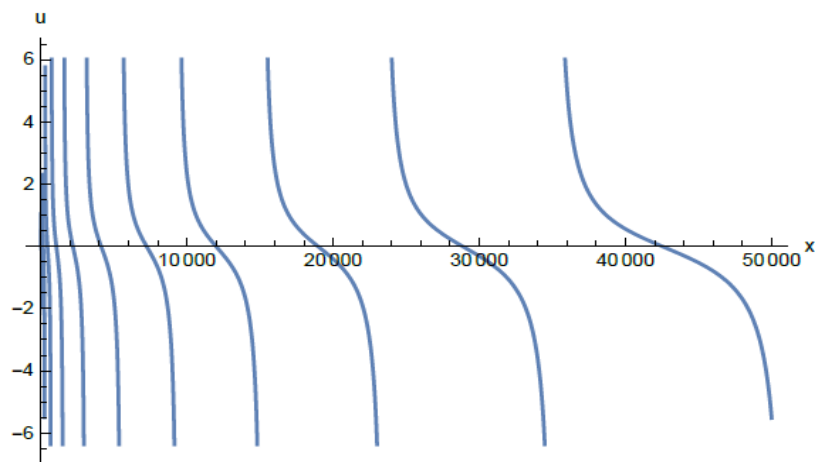


**Figure 16.** 2D plot of  $u(x, t) = -\tan(15^5\sqrt{5} + 5^5\sqrt{x})$

## 5. CONCLUSIONS

In this study, the exact solutions of the all of the time, space and space-time conformable fractional Phi-four equations, an analytic method has been developed using the Jacobi elliptic functions. This method is the first method in the literature and also this method is direct, quick and simple. The suggested method does not also need perturbation, linearization, boundary and initial conditions. Besides, by this method the solutions are found in a general form containing the hyperbolic, complex, rational and trigonometric functions, since the solutions include twelve Jacobi elliptic functions. Some of these solutions are solitary waves, such as kink like solutions illustrated in figures. Moreover, the solutions of the various methods such as sine-cosine ansatz and tanh methods are covered by this method.

In the literature, the modified Kudryashov [19], exponential function [19], extended direct algebraic [20], mapping [21], modified mapping [21] and generalized Kudryashov [23] methods include the conformable derivatives with respect to time, while the  $(G'/G, 1/G)$ -expansion method [24] contains the conformable derivatives with respect to space and time. When compared with these methods, it is seen that more solutions are obtained by our method. Because 10 solutions containing rational, trigonometric and hyperbolic functions with the exponential function method, 4 solutions containing logarithmic function with the modified Kudryashov method, 33 solutions containing rational, trigonometric and hyperbolic functions with the extended direct algebraic method, 13 solutions containing trigonometric, hyperbolic functions with the mapping methods, 4 solutions containing rational function with the generalized Kudryashov method and 10 solutions aining rational, trigonometric and hyperbolic functions with the  $(G'/G, 1/G)$ -expansion method are obtained. However, there exist 192 type solutions for 30 different cases in our suggested method and also infinitely many solutions can be determined depending on the parameters  $P, Q, R$  and  $m$ .

## REFERENCES

- [1] Lundquist, S., March, N. H. and Tosi, M. P., (1988), Order and Chaos in Nonlinear Physical Systems, Springer, New York.
- [2] Calogero, F. and Degasperis, A., (1982), Spectral Transform and Solitons: Tools to Solve and Investigate Nonlinear Evolution Equations, New York: North-Holland.
- [3] Wazwaz, A. M., (2007), Analytic study on nonlinear variants of the RLW and the PHI-four equations, Communications in Nonlinear Science and Numerical Simulation 12, 314–327.
- [4] Wazwaz, A. M., (2005), Generalized forms of the phi-four equation with compactons, solitons and periodic solutions, Mathematics and Computers in Simulation, 69, 580–588.
- [5] Alofi, A. S., (2013), Exact and Explicit Travelling Wave Solutions for the Nonlinear Partial Differential Equations, World Applied Sciences Journal, 21, 62-67.
- [6] Soliman, A. A., (2007), Exact travelling wave solution of nonlinear variants of the RLW and the PHI-four equations, Physics Letters A, 368, 383–390.
- [7] Deng, X., Zhao, M. and Li, X., (2009), Travelling wave solutions for a nonlinear variant of the PHI-four equation, Mathematical and Computer Modelling, 49, 617–622.
- [8] Xiang, C., (2012), A note on exact travelling wave solutions for nonlinear PHI-four equation, Applied Mechanics and Materials, 4569-4572.
- [9] Najafi, M., (2012), Using He's Variational Method to Seek the Travelling Wave Solution of PHI-Four Equation, International Journal of Applied Mathematical Research, 1 (4), 659-665.

- [10] Younis, M. and Zafar, A., (2013), The modified simple equation method for solving nonlinear Phi-Four equation, *International Journal of Innovation and Applied Studies*, 2, 661-664.
- [11] Akter, J. and Akbar, M. A., (2015), Exact solutions to the Benney–Luke equation and the Phi-4 equations by using modified simple equation method, *Results in Physics*, 5, 125-130.
- [12] Ehsani, F., Ehsani, F., Hadi, A. and Hadi, A., (2013), Analytical Solution of Phi-Four Equation, *Technical Journal of Engineering and Applied Sciences*, 3 (14), 1378-1388.
- [13] Akbulut, A., Kaplan, M. and Tascan, F., (2016), Conservation laws and Exact Solutions of Phi-Four (Phi-4) Equation via the  $(G'^G, 1/G)$ -Expansion Method, *Naturforsch*, 71 (5), 439-446.
- [14] Zahra, W. K., (2017), Trigonometric B-Spline Collocation Method for Solving PHI-Four and Allen–Cahn Equations, *Mediterranean Journal of Mathematics*, 14, 122-141.
- [15] Mahmud, F., Samsuzzoha, M. and Akbar, M. A., (2017), A generalized Kudrashov method to obtain exact travelling wave solutions of the PHI-four equation and the Fisher equation, *Results in Physics*, 7, 4296-4302.
- [16] Islam, M. S., Khan, K. and Akbar, M. A., (2017), Application of the improved F-expansion method with Riccati equation to find the exact solution of the nonlinear evolution equations, *Journal of the Egyptian Mathematical Society*, 25, 13–18.
- [17] Tariq, H. and Akram, G., (2017), New approach for exact solutions of time fractional Cahn–Allen equation and time fractional Phi-4 equation, *Physica A*, 473, 352–362.
- [18] Alquran, M., Jaradat, H. M. and Syam, M. I., (2017), Analytical solution of the time-fractional Phi-4 equation by using modified residual power series method, *Nonlinear Dyn*, 90:2525–2529.
- [19] Akram, G., Batool, F. and Riaz, A., (2018), Two reliable techniques for the analytical study of conformable time-fractional Phi-4 equation, *Opt Quant Electron*, 50:22.
- [20] Rezazadeh, H., Tariq, H., Eslami, M., Mirzazadeh, M., and Zhou, Q., (2018), New exact solutions of nonlinear conformable time-fractional Phi-4 equation, *Chinese Journal of Physics*, 2, in press.
- [21] Korpınar, Z., (2019), Some analytical solutions by mapping methods for non-linear conformable time-fractional Phi-4 equation, *Thermal Science*, 23.
- [22] Gao, W., Veerasha, P., Prakasha D. G., Baskonus, H. M. and Yel, G., (2020), New Numerical Results for the Time-Fractional Phi-Four Equation Using a Novel Analytical Approach, *Symmetry*, 12 (3), 478.
- [23] Rahman, A., Alam, N. and Roshid, H., (2020), The generalized Kudryshov method implemented to the nonlinear conformable time-fractional PHI-Four equation, *Annals of Pure and Appl. Mathematics* 21 (1), 69-76.
- [24] Sirisubtawee, S., Koonprasert, S., Sungnul, S. and Leekparn, T., (2019), Exact travelling wave solutions of the space–time fractional complex Ginzburg–Landau equation and the space-time fractional Phi-4 equation using reliable methods, *Advances in Difference Equations*, Doi: 10.1186/s13662-019-2154-9.
- [25] Feng, Q., (2018), A new approach for seeking coefficient function solutions of conformable fractional partial differential equations based on the Jacobi elliptic equation, *Chinese Journal of Physics*, 56(6), 2817-2828.
- [26] Tasbozan, O., Çenesiz, Y. and Kurt, A., (2016), New solutions for conformable fractional Boussinesq and combined KdV-mKdV equations using Jacobi elliptic function expansion method, *The European Physical Journal Plus*, 131(7), 244.
- [27] Kurt, A., (2019), New periodic wave solutions of a time fractional integrable shallow water equation, *Applied Ocean Research*, 85, 128-135.
- [28] El-Ganaini, S. and Al-Amr, M. O., (2019), New abundant wave solutions of the conformable space–time fractional  $(4+ 1)$ -dimensional Fokas equation in water waves, *Computers & Mathematics with Applications*, 78(6), 2094-2106.
- [29] Zayed, E. M. E. and Shohib, R. M. A., (2018), The unified sub-equation method and its applications to conformable space-time fractional fourth-order pochhammer-chree equation, *Physics & Astronomy International Journal*, 2, 452-463.

- [30] Kumar, V. S., Rezazadeh, H., Eslami, M., Izadi, F. and Osman, M. S., (2019), Jacobi elliptic function expansion method for solving KdV equation with conformable derivative and dual-power law nonlinearity, *International Journal of Applied and Computational Mathematics*, 5(5), 127.
- [31] Dascioglu, A., Culha, S., and Varol Bayram, D., (2017), New analytical solutions of the space fractional KdV equation in terms of Jacobi elliptic functions, *New Trends in Mathematical Sciences*, 5, No. 4, 232-241.
- [32] ulha, S. and Daşcıođlu, A., (2019), Analytic solutions of the space–time conformable fractional Klein–Gordon equation in general form, *Waves in Random and complex Media*, 29, No. 4, 775-790.
- [33] ulha Őnal, S., Daşcıođlu, A. and Varol Bayram, D., (2020), New exact solutions of space and time fractional modified Kawahara equation, *Physica A: Statistical Mechanics and its Applications*, 551, 124550.
- [34] Ali, A. T., (2011), New generalized Jacobi elliptic function rational expansion method, *Journal of Computational and Applied Mathematics*, 235, 4117–4127.
- [35] Khalil, R., Horani, M. A., Yousef, A. and Sababheh, M., (2014), A new definition of fractional derivative, *Journal of Computational and Applied Mathematics*, 264, 65–70.
- [36] Abdeljawad, T., (2015), On conformable fractional calculus, *Journal of Computational and Applied Mathematics*, 279, 57–66.
- [37] Erdelyi, A., Magnus, W., Oberhettinger, F. and Tricomi, F. G., (1993), *Higher Transcendental Functions*, vol. 2, McGraw-Hill: New York.
- [38] Abramowitz, M. and Stegun, I. A., (1972), *Handbook of Mathematical Functions with Formulas, Graphs, and Mathematical Tables*, U.S. Government Printing Office: Washington, D.C.
- [39] Remoissenet, M., (1993), *Waves Called Solitons: Concepts and Experiments*, Springer-Verlag, Berlin.



## Synthesis of New Bisbenzimidazole Salts and Determination Their Ligand Activities in C-C Coupling Reactions

Ülkü YILMAZ<sup>1\*</sup>, Hasan KÜÇÜKBAY<sup>2</sup>

<sup>1</sup> Department of Engineering Basic Sciences, Faculty of Engineering and Natural Sciences, Malatya Turgut Özal University, Malatya, Turkey.

<sup>2</sup> Department of Chemistry, Faculty Science and Arts, İnönü University, Malatya, Turkey.

(Received: 04.05.2020; Accepted: 18.05.2020)

**ABSTRACT:** New bisbenzimidazole salts were synthesized with 1,4-bis(1*H*-benzo[d]imidazol-1-yl)butane and benzyl halides. These new ligands carried out in Suzuki-Miyaura and Mizoroki-Heck C-C coupling reaction in the presence of palladium(II) acetate. It was observed that remarkable ligand activities of benzimidazolium halides (**L**<sub>1</sub>, **L**<sub>2</sub>, **L**<sub>3</sub>).

**Keywords:** Bisbenzimidazole, C-C coupling, Suzuki-Miyaura, Mizoroki-Heck, biphenyl, stilbene.

### 1. INTRODUCTION

Due to various bioactivities of biphenyl and stilbene cored molecules, their synthetic methods always attract attention [1-4].

The Suzuki-Miyaura (SM) cross-coupling reaction is one of the most excellent tools for the synthesis of symmetrical or unsymmetrical biphenyl derivatives derived from aryl halides and arylboronic acids [5-10]. The Mizoroki-Heck (MH) reaction is also one of the best methods for the synthesis of stilbenes from alkenes and aryl halides [11-15].

Doubtless, the center of the catalytic systems applied for the carbon-carbon bond formation reaction is palladium metal [16-18]. Moreover, because of their superior properties such as low toxicity, high electron-donating, and easy *in situ* preparation, N-Heterocyclic carbenes (NHCs) are preferred to other ligands in presence of palladium in coupling reactions [19-21]. On the other hand, because of the time of the coupling reaction is significantly shortened, microwave irradiation is preferred to conventional heating [22-26].

As mentioned above, due to the excellent properties of NHC ligands, in this study, three new benzimidazole salts were synthesized as NHC precursors and their ligand activities were investigated in the Suzuki-Miyaura and Mizoroki-Heck reactions.

\*Corresponding Author: ulku.yilmaz@ozal.edu.tr

ORCID number of authors: <sup>1</sup> 0000-0002-2806-4781, <sup>2</sup> 0000-0002-7180-9486

## 2. MATERIAL AND METHODS

In first, the chemicals were determined required for the experiments and all of them were bought from Acros, Aldrich, Merck, and Fluka Chemical Co. All structural characterization of the new compounds were implemented via NMR, IR, microanalysis. <sup>1</sup>H-NMR (400 MHz) and <sup>13</sup>C-NMR (100 MHz) spectra were recorded using Bruker Avanced III 400 UltraShield high-performance digital FT NMR spectrometer. Infrared spectra were recorded as KBr pellets in the range 4000-400 cm<sup>-1</sup> on a Perkin-Elmer Spectrum One FT-IR spectrometer. Elemental analysis was performed by LECO CHNS-932 elemental analyzer. Melting points were identified using an electrothermal melting point apparatus, Electrothermal 9200. All catalytic activity experiments were carried out in a microwave oven system manufactured by Milestone (Milestone Start S Microwave Labstation for Synthesis) under aerobic conditions.

### 2.1. Synthesis of 1,1'-(butane-1,4-diyl)bis(3-benzyl-1H-benzo[d]imidazol-3-ium) dichloride

A mixture of 1,4-bis(1H-benzo[d]imidazol-1-yl)butane (0.50 g, 1.73 mmol), benzyl chloride (0.44 g, 3.46 mmol) and DMF (5 mL) was refluxed in water bath. Then all volatiles were removed in vacuo and crude product was crystallised from ethanol. Yield: 80 %, 0.75 g, m.p.: 220-221 °C. <sup>1</sup>H-NMR (DMSO<sub>d</sub><sub>6</sub>-400 MHz): δ 10.56 (s, 2H, NCHN), 8.19-7.36 (m, 18H, Ar-H), 5.87 (s, 4H, CH<sub>2</sub>-C<sub>6</sub>H<sub>5</sub>), 4.68 (bs, 4H, N-CH<sub>2</sub>), 2.11 (bs, 4H, -CH<sub>2</sub>-) ppm. <sup>13</sup>C-NMR (DMSO<sub>d</sub><sub>6</sub>-100 MHz): δ 143.2 (NCHN), 134.6, 131.8, 131.6, 129.5, 129.4, 129.1, 127.2, 127.1, 114.5, 114.4 (Ar-C), 50.3 (CH<sub>2</sub>-C<sub>6</sub>H<sub>5</sub>), 46.5 (N-CH<sub>2</sub>), 25.8 (-CH<sub>2</sub>-) ppm. IR: ν<sub>(C=N)</sub>: 1561 cm<sup>-1</sup>. Anal. Calcd. for C<sub>32</sub>H<sub>32</sub>Cl<sub>2</sub>N<sub>4</sub> (543.54): C, 70.71; H, 5.93; N, 10.31. Found: C, 70.42; H, 5.80; N, 10.18. **L**<sub>2</sub> and **L**<sub>3</sub> were synthesized similar method.

### 2.2. 1,1'-(butane-1,4-diyl)bis(3-(4-methoxybenzyl)-1H-benzo[d]imidazol-3-ium) dibromide

Yield :78 %, 0.93 g, m.p.: 225-227 °C. <sup>1</sup>H-NMR (DMSO<sub>d</sub><sub>6</sub>-400 MHz): δ 10.48 (s, 2H, NCHN), 8.18-6.93 (m, 16H, Ar-H), 5.76 (s, 4H, CH<sub>2</sub>-C<sub>6</sub>H<sub>5</sub>), 4.65 (bs, 4H, N-CH<sub>2</sub>), 3.73 (s, 6H, OCH<sub>3</sub>), 2.08 (bs, 4H, -CH<sub>2</sub>-) ppm. <sup>13</sup>C-NMR (DMSO<sub>d</sub><sub>6</sub>-100 MHz): δ 142.9 (NCHN), 159.9, 131.8, 131.2, 130.6, 127.1, 127.0, 126.4, 114.7, 114.4 (Ar-C), 55.7 (OCH<sub>3</sub>), 49.9 (CH<sub>2</sub>-C<sub>6</sub>H<sub>5</sub>), 46.6 (N-CH<sub>2</sub>), 25.8 (-CH<sub>2</sub>-) ppm. IR: ν<sub>(C=N)</sub>: 1561 cm<sup>-1</sup>. Anal. Calcd. for C<sub>34</sub>H<sub>36</sub>Br<sub>2</sub>N<sub>4</sub>O<sub>2</sub> (692.50): C, 58.97; H, 5.24; N, 8.09. Found: C, 58.52; H, 5.12; N, 8.00.

### 2.3. 1,1'-(butane-1,4-diyl)bis(3-(4-nitrobenzyl)-1H-benzo[d]imidazol-3-ium) dibromide

Yield :75 %, 0.94 g, m.p.: 229-231 °C. <sup>1</sup>H-NMR (DMSO<sub>d</sub><sub>6</sub>-400 MHz): δ 10.21 (s, 2H, NCHN), 8.26-7.66 (m, 16H, Ar-H), 6.02 (s, 4H, CH<sub>2</sub>-C<sub>6</sub>H<sub>5</sub>), 4.66 (bs, 4H, N-CH<sub>2</sub>), 2.12 (bs, 4H, -CH<sub>2</sub>-) ppm. <sup>13</sup>C-NMR (DMSO<sub>d</sub><sub>6</sub>-100 MHz): δ 143.4 (NCHN), 148.0, 141.8, 131.8, 131.3, 129.9, 127.4, 127.2, 124.4, 114.5, 114.2 (Ar-C), 49.5 (CH<sub>2</sub>-C<sub>6</sub>H<sub>5</sub>), 46.9 (N-CH<sub>2</sub>), 25.9 (-CH<sub>2</sub>-) ppm. IR: ν<sub>(C=N)</sub>: 1562 cm<sup>-1</sup>. Anal. Calcd. for C<sub>32</sub>H<sub>30</sub>Br<sub>2</sub>N<sub>6</sub>O<sub>4</sub> (722.44): C, 53.20; H, 4.19; N, 11.63. Found: C, 53.00; H, 4.12; N, 11.30.

### 2.4. General methode for C-C coupling reaction

A mixture of aryl halide (1 mmol), phenylboronic acid or styrene (1mmol), K<sub>2</sub>CO<sub>3</sub> (2 mmol), Pd(OAc)<sub>2</sub> (0.01 mmol), ligand (0.01 mmol) and solvent (DMF:H<sub>2</sub>O (1:1), 6 mL) was added in an apparatus of microwave equipment. The mixture was stirred and heated at 100 °C by microwave irradiation (300 W) for 10 min. Then, it was cooled and extracted with ethyl acetate. The purification was done by crystallization from ethyl acetate/n-hexane (1:1). The isolated yield was calculated. The product structures were determined by <sup>1</sup>H-NMR and a comparison of the melting point.

### 3. RESULTS AND DISCUSSION

All ligands were synthesized by reaction of 1,4-bis(1*H*-benzo[d]imidazol-1-yl)butane and benzyl halides (Figure 1). The structures of NHC precursor ligands were characterized by <sup>1</sup>H NMR, <sup>13</sup>C NMR, IR and elemental analysis. The <sup>1</sup>H NMR and <sup>13</sup>C NMR spectra of **L**<sub>1</sub>, **L**<sub>2</sub> and **L**<sub>3</sub> ligands were viewed respectively. The decisive salt peaks for benzimidazolium salts were observed at 10.56, 10.48 and 10.21 ppm; 143.2, 142.9 and 143.4 ppm. IR spectra of ligands showed a stretching band of the C=N bonds at 1561, 1561 and 1562 cm<sup>-1</sup>. These results are coherent with the literature [27, 28].

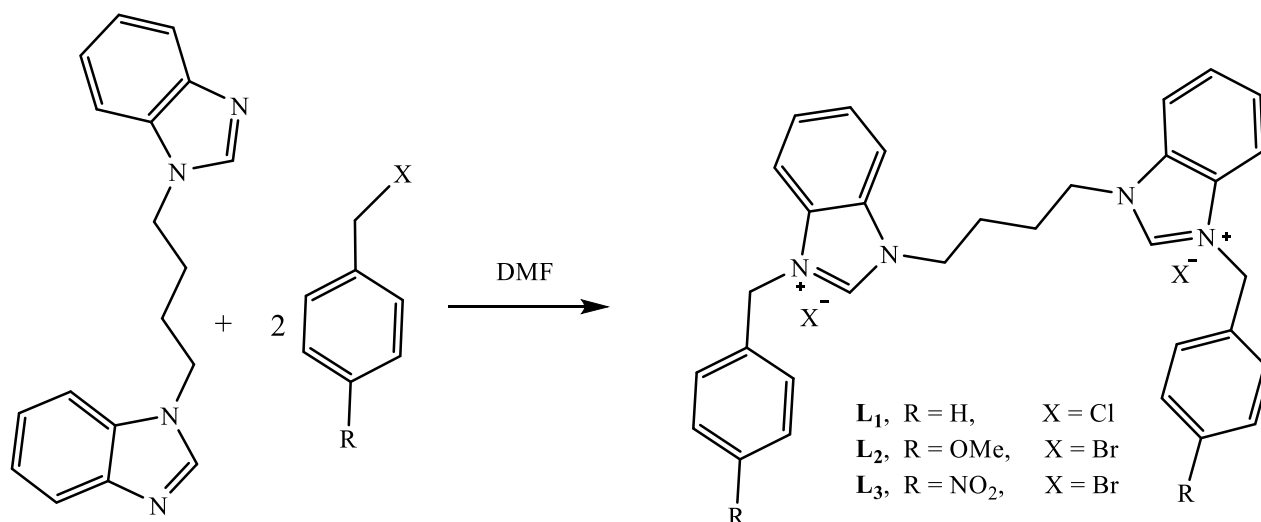


**Figure 1.** Synthesis procedure of bisbenzimidazolium halides

The effects of ligands derived from the new benzimidazolium halides were investigated on the Suzuki-Miyaura and Mizoroki-Heck C-C coupling reactions. Iodobenzene, bromobenzene, 4-iodoanisole, 4-bromoanisole, phenylboronic acid and styrene were used as reactants for the coupling reactions. A series of experiments were carried out to determine the optimization conditions (Table 1, entries 1-11). The results showed that the best reaction conditions were provided when using a catalytic system consist of K<sub>2</sub>CO<sub>3</sub> (2 mmol), DMF:H<sub>2</sub>O (6 mL), Pd(OAc)<sub>2</sub> and ligand (0,01 mmol) at 100 °C (Table 1, entry 4). When the activities of all ligands in the catalytic system were examined according to optimized conditions, it was observed that **L**<sub>2</sub> gave the best results. This is caused by the electron-donating methoxy group of **L**<sub>2</sub> compared to the other ligands.

**Table 1.** Effects of ligand-changing on the Suzuki-Miyaura reaction

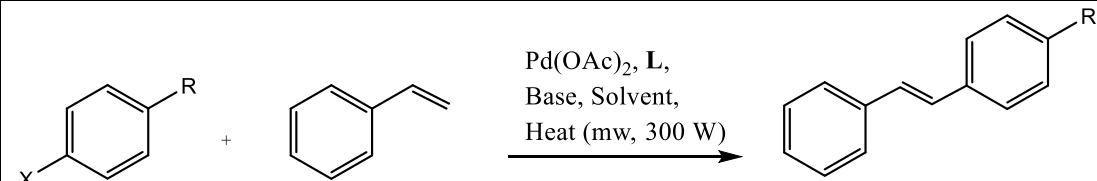
Entry	X	R	L	Base	Solvent	Time (min)	Heat (°C)	<sup>a</sup> Yield %
1	I	H	<b>L</b> <sub>2</sub>	K <sub>2</sub> CO <sub>3</sub>	DMF:H <sub>2</sub> O (1:1)	5	60	58
2	I	H	<b>L</b> <sub>2</sub>	K <sub>2</sub> CO <sub>3</sub>	DMF:H <sub>2</sub> O	5	80	71
3	I	H	<b>L</b> <sub>2</sub>	K <sub>2</sub> CO <sub>3</sub>	DMF:H <sub>2</sub> O	5	100	89

4	I	H	L <sub>2</sub>	K <sub>2</sub> CO <sub>3</sub>	DMF:H <sub>2</sub> O	10	100	99
5	I	H	L <sub>2</sub>	K <sub>2</sub> CO <sub>3</sub>	EtOH	10	100	80
6	I	H	L <sub>2</sub>	K <sub>2</sub> CO <sub>3</sub>	H <sub>2</sub> O	10	100	38
7	I	H	L <sub>2</sub>	K <sub>2</sub> CO <sub>3</sub>	DMF:H <sub>2</sub> O	10	100	<sup>b</sup> np
8	I	H	L <sub>2</sub>	K <sub>2</sub> CO <sub>3</sub>	DMF:H <sub>2</sub> O	10	100	<sup>c</sup> 50
9	I	H	L <sub>2</sub>	KOH	DMF:H <sub>2</sub> O	10	100	60
10	I	H	L <sub>2</sub>	NaOH	DMF:H <sub>2</sub> O	10	100	57
11	I	H	L <sub>2</sub>	K <sub>2</sub> CO <sub>3</sub>	DMF:H <sub>2</sub> O	10	100	<sup>d</sup> 75
12	I	H	L <sub>1</sub>	K <sub>2</sub> CO <sub>3</sub>	DMF:H <sub>2</sub> O	10	100	98
13	I	H	L <sub>3</sub>	K <sub>2</sub> CO <sub>3</sub>	DMF:H <sub>2</sub> O	10	100	95
14	I	OCH <sub>3</sub>	L <sub>1</sub>	K <sub>2</sub> CO <sub>3</sub>	DMF:H <sub>2</sub> O	10	100	96
15	I	OCH <sub>3</sub>	L <sub>2</sub>	K <sub>2</sub> CO <sub>3</sub>	DMF:H <sub>2</sub> O	10	100	98
16	I	OCH <sub>3</sub>	L <sub>3</sub>	K <sub>2</sub> CO <sub>3</sub>	DMF:H <sub>2</sub> O	10	100	92
17	Br	H	L <sub>1</sub>	K <sub>2</sub> CO <sub>3</sub>	DMF:H <sub>2</sub> O	10	100	90
18	Br	H	L <sub>2</sub>	K <sub>2</sub> CO <sub>3</sub>	DMF:H <sub>2</sub> O	10	100	95
19	Br	H	L <sub>3</sub>	K <sub>2</sub> CO <sub>3</sub>	DMF:H <sub>2</sub> O	10	100	86
20	Br	OCH <sub>3</sub>	L <sub>1</sub>	K <sub>2</sub> CO <sub>3</sub>	DMF:H <sub>2</sub> O	10	100	87
21	Br	OCH <sub>3</sub>	L <sub>2</sub>	K <sub>2</sub> CO <sub>3</sub>	DMF:H <sub>2</sub> O	10	100	90
22	Br	OCH <sub>3</sub>	L <sub>3</sub>	K <sub>2</sub> CO <sub>3</sub>	DMF:H <sub>2</sub> O	10	100	80

Reaction conditions: aryl halide (1 mmol), benzenboronic acid (1 mmol), solvent (6 mL, DMF:H<sub>2</sub>O (1:1)), base (2 mmol), Pd(OAc)<sub>2</sub> (0,01 mmol), L (0,01 mmol), <sup>a</sup>isolated yield, <sup>b</sup> no product, without Pd(OAc)<sub>2</sub>, <sup>c</sup>without L, <sup>d</sup>amount of 0.005 mmol Pd(OAc)<sub>2</sub>/L.

The effects of ligands were also investigated for the Mizoroki Heck reaction under similar conditions. The best results were also obtained by L<sub>2</sub> ligand (Table 2, entries 4, 15, 18 and 21). In addition to the ligand change, the change of alkyl halides was also observed to affect yields. Iodoaryls provided more good yields because of the nature of halogen.

**Table 2.** Effects of ligand-changing on the Mizoroki-Heck reaction

								
Entry	X	R	L	Base	Solvent	Time (min)	Heat (°C)	<sup>a</sup> Yield %
1	I	H	L <sub>2</sub>	K <sub>2</sub> CO <sub>3</sub>	DMF:H <sub>2</sub> O	5	60	25
2	I	H	L <sub>2</sub>	K <sub>2</sub> CO <sub>3</sub>	DMF:H <sub>2</sub> O	5	80	56
3	I	H	L <sub>2</sub>	K <sub>2</sub> CO <sub>3</sub>	DMF:H <sub>2</sub> O	5	100	80
4	I	H	L <sub>2</sub>	K <sub>2</sub> CO <sub>3</sub>	DMF:H <sub>2</sub> O	10	100	97
5	I	H	L <sub>2</sub>	K <sub>2</sub> CO <sub>3</sub>	EtOH	10	100	70
6	I	H	L <sub>2</sub>	K <sub>2</sub> CO <sub>3</sub>	H <sub>2</sub> O	10	100	18
7	I	H	L <sub>2</sub>	K <sub>2</sub> CO <sub>3</sub>	DMF:H <sub>2</sub> O	10	100	<sup>b</sup> np
8	I	H	L <sub>2</sub>	K <sub>2</sub> CO <sub>3</sub>	DMF:H <sub>2</sub> O	10	100	<sup>c</sup> 48
9	I	H	L <sub>2</sub>	KOH	DMF:H <sub>2</sub> O	10	100	51
10	I	H	L <sub>2</sub>	NaOH	DMF:H <sub>2</sub> O	10	100	44
11	I	H	L <sub>2</sub>	K <sub>2</sub> CO <sub>3</sub>	DMF:H <sub>2</sub> O	10	100	<sup>d</sup> 65
12	I	H	L <sub>1</sub>	K <sub>2</sub> CO <sub>3</sub>	DMF:H <sub>2</sub> O	10	100	92
13	I	H	L <sub>3</sub>	K <sub>2</sub> CO <sub>3</sub>	DMF:H <sub>2</sub> O	10	100	80
14	I	OCH <sub>3</sub>	L <sub>1</sub>	K <sub>2</sub> CO <sub>3</sub>	DMF:H <sub>2</sub> O	10	100	88
15	I	OCH <sub>3</sub>	L <sub>2</sub>	K <sub>2</sub> CO <sub>3</sub>	DMF:H <sub>2</sub> O	10	100	91
16	I	OCH <sub>3</sub>	L <sub>3</sub>	K <sub>2</sub> CO <sub>3</sub>	DMF:H <sub>2</sub> O	10	100	80
17	Br	H	L <sub>1</sub>	K <sub>2</sub> CO <sub>3</sub>	DMF:H <sub>2</sub> O	10	100	77
18	Br	H	L <sub>2</sub>	K <sub>2</sub> CO <sub>3</sub>	DMF:H <sub>2</sub> O	10	100	80
19	Br	H	L <sub>3</sub>	K <sub>2</sub> CO <sub>3</sub>	DMF:H <sub>2</sub> O	10	100	69

<b>20</b>	Br	OCH <sub>3</sub>	<b>L<sub>1</sub></b>	K <sub>2</sub> CO <sub>3</sub>	DMF:H <sub>2</sub> O	10	100	76
<b>21</b>	Br	OCH <sub>3</sub>	<b>L<sub>2</sub></b>	K <sub>2</sub> CO <sub>3</sub>	DMF:H <sub>2</sub> O	10	100	78
<b>22</b>	Br	OCH <sub>3</sub>	<b>L<sub>3</sub></b>	K <sub>2</sub> CO <sub>3</sub>	DMF:H <sub>2</sub> O	10	100	67

Reaction conditions: aryl halide (1 mmol), styrene (1 mmol), solvent (6 mL, DMF:H<sub>2</sub>O (1:1)), base (2 mmol), Pd(OAc)<sub>2</sub> (0,01 mmol), L (0,01 mmol), <sup>a</sup>isolated yield, <sup>b</sup> no product, without Pd(OAc)<sub>2</sub>, <sup>c</sup>without L, <sup>d</sup>amount of 0.005 mmol Pd(OAc)<sub>2</sub>/L.

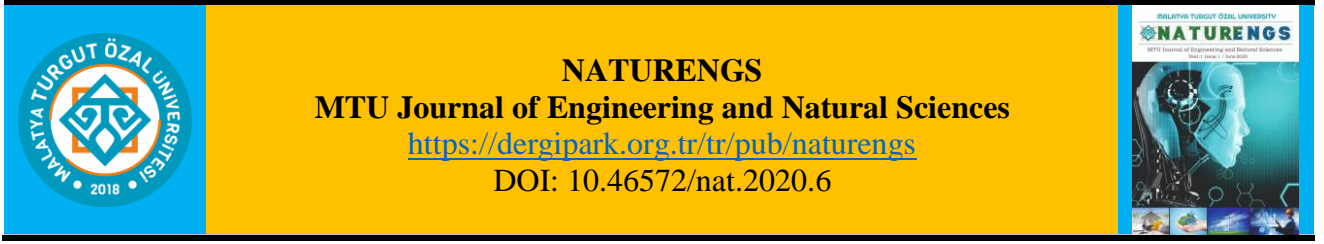
#### 4. CONCLUSIONS

A group of benzimidazole salts was synthesized including electron-withdrawing and electron-donating groups (**L<sub>1</sub>**, **L<sub>2</sub>**, **L<sub>3</sub>**). The structural analysis of these ligands was via spectroscopic techniques. These benzimidazolium halides were used as NHC precursor ligands in the catalytic systems for C-C coupling (SM, MH) reactions. All ligands were showed excellent activities with isolated yields between 67-99 % in the catalytic systems including K<sub>2</sub>CO<sub>3</sub> (2 mmol), DMF:H<sub>2</sub>O (1:1) (6 mL), Pd(OAc)<sub>2</sub> and ligand (0,01 mmol) at 100 °C for coupling reactions. Nevertheless the best activities were obtained by **L<sub>2</sub>** because of its electron-donating methoxy group.

#### REFERENCES

- [1] De Filippis, B., Ammazzalorso, A., Fantacuzzi, M., Giampietro, L., Maccallini, C. and Amoroso, R. (2018). Anticancer activity of stilbene-based derivatives, *Chem. Med. Chem.*, 12: 558-570.
- [2] Shen, T., Wang, X.N. and Lou, H.X. (2009). Natural stilbenes: an overview, *Nat. Prod. Rep.*, 26: 916-935.
- [3] Kozłowski, M.C., Morgan, B.J. and Linton, E.C. (2009), Total synthesis of chiral biaryl natural products by asymmetric biaryl coupling, *Chem. Soc. Rev.*, 38(11): 3193-3207.
- [4] Littke, A.F. and Fu, G.C. (2002). Palladium-Catalyzed Coupling Reactions of Aryl Chlorides, *Angew. Chem. Int. Ed.*, 41: 4176 -4211.
- [5] N. Miyaura and A. Suzuki, A. (1995). Palladium-Catalyzed Cross-Coupling Reactions of Organoboron Compounds, *Chem. Rev.*, 95(7): 2457-2483.
- [6] Aktaş, A., Akkoç, S. and Gök, Y. (2013). Palladium catalyzed Mizoroki–Heck and Suzuki–Miyaura reactions using naphthalenomethyl-substituted imidazolidin-2-ylidene ligands in aqueous media, *J. Coord. Chem.*, 66(16): 2901-2909.
- [7] Sajith, A.M. and Muralidharan, A. (2012). Microwave enhanced Suzuki coupling: a diversity-oriented approach to the synthesis of highly functionalised 3-substituted-2-aryl/heteroarylimidazo[4,5-b]pyridines, *Tetrahedron Letters*, 53:1036–1041.
- [8] Brenner, E., Matt, D., Henrion, M., Teci, M. and Toupet, L. (2011). Calix[4]arenes with one and two *N*-linked imidazolium units as precursors of *N*-heterocyclic carbene complexes. Coordination chemistry and use in Suzuki–Miyaura cross-coupling, *Dalton Trans.*, 40: 9889–9898.
- [9] Liu, T., Zhao, X., Shen, Q. And Lu L. (2012). General and highly efficient fluorinated-N-heterocyclic carbenebased catalysts for the palladium-catalyzed Suzuki-Miyaura reaction, *Tetrahedron*, 68: 6535-6547.
- [10] Wan, J-P., Wang, C., Zhou, R. and Liu, Y. (2012). Sustainable H<sub>2</sub>O/ethyl lactate system for ligand-free Suzuki–Miyaura reaction, *RSC Advances*, 2: 8789–8792.
- [11] Heck, R. F. and Nolley, J. P. (1972). Palladium-catalyzed vinylic hydrogen substitution reactions with aryl, benzyl, and styryl halides, *J. Org. Chem.*, 37: 2320–2322.
- [12] Mizoroki, T., Mori, K., and Ozaki A. (1971). Arylation of olefin with aryl iodine catalyzed by palladium. *Bull Chem Soc Jpn.*, 44: 581.

- [13] Demir, S., Zengin, R. and Özdemir, İ. (2012). Potential N-Heterocyclic carbene precursors in the palladium catalyzed Heck reaction, *Heteroatom Chem.*, 24(1): 77-83.
- [14] Botella, L. and Najera, C. (2004). Synthesis of methylated resveratrol and analogues by Heck reactions in organic and aqueous solvents, *Tetrahedron*, 60: 5563–5570.
- [15] Du, L-H. and Wang, Y-G. (2007). Microwave-Promoted Heck Reaction Using Pd(OAc)<sub>2</sub> as Catalyst under Ligand-Free and Solvent-Free Conditions, *Synth. Commun.*, 37: 217–222.
- [16] Fortea-Perez, F.R., Julve, M., Dikarev, E.V., Filatov, A.S. and Stiriba, S-E. (2018). Synthesis and structural characterization of well-defined bis (oxamato)palladate(II) precatalysts for Suzuki and Heck reactions, *Inorg. Chim. Acta*, 471: 788–796.
- [17] Saikia, B., Boruah, P.R., Ali, A.A. and Sarma, D. (2015). Simple and efficient phosphine-free Pd(OAc)<sub>2</sub> catalyzed urea accelerated Suzuki–Miyaura cross-coupling reactions in iPrOH–H<sub>2</sub>O at room temperature, *Tetrahedron Letters*, 56: 633–635.
- [18] Milde, B., Schaarschmidt, D., Ruffer, T. and Lang, H. (2012). Phosphino imidazoles and imidazolium salts for Suzuki C–C coupling reactions, *Dalton Trans.*, 41: 5377–5390.
- [19] Delaude, L. (2009). Betaine Adducts of N-Heterocyclic Carbenes: Synthesis, Properties, and Reactivity. *Eur. J. Inorg. Chem.* 2009: 1681–1699.
- [20] Valente, C., Çalimsiz, S., Hoi, K.H., Malli, D., Sayah, M. and Organ, M.G. (2012). The development of bulky palladium NHC complexes for the most-challenging cross-coupling reactions, *Angew. Chem. Int. Ed.*, 51: 3314 – 3332.
- [21] Türkmen, H., Pelit, L. and Çetinkaya, B. (2011). Water-soluble cis-[(NHC)PdBr<sub>2</sub>(TPPTS)] catalysts and their applications in Suzuki–Miyaura coupling of aryl chlorides, *J. Mol. Cat. A: Chem.*, 348: 88– 93.
- [22] Kappe, C.O., Pieber, B. and Dallinger, D. (2013). Microwave Effects in Organic Synthesis: Myth or Reality?, *Angew. Chem. Int. Ed.*, 52: 1088 -1094.
- [23] Yılmaz, Ü., Küçükbay, H., Şireci, N., Akkurt, M., Günal, S., Durmaz, R. and Tahir, M.N. (2011). Synthesis, microwave-promoted catalytic activity in Suzuki–Miyaura cross-coupling reactions and antimicrobial properties of novel benzimidazole salts bearing trimethylsilyl group, *Appl. Organometal. Chem.*, 25(5): 366-373.
- [24] Yılmaz, Ü., Deniz, S., Küçükbay, H. and Şireci, N. (2013). Microwave assisted Suzuki-Miyaura and Ullmann type homocoupling reactions of 2- and 3-halopyridines using a Pd(OAc)<sub>2</sub>/benzimidazolium salt and base catalyst System, *Molecules*, 18(4): 3712-3724.
- [25] Yılmaz, Ü., Şireci, N., Deniz, S. and Küçükbay, H. (2010). Synthesis and microwave-assisted catalytic activity of novel bis-benzimidazole salts bearing furfuryl and thenyl moieties in Heck and Suzuki cross-coupling reactions, *Appl. Organometal. Chem.*, 24(5): 414-420.
- [26] Yılmaz, Ü., Küçükbay, H., Çelikesir, S.T., Akkurt, M. and Büyükgüngör, O. (2013). Synthesis of novel benzimidazole salts and microwave-assisted catalytic activity of in situ generated Pd nanoparticles from a catalyst system consisting of benzimidazol salt, Pd(OAc)<sub>2</sub>, and base in a Suzuki-Miyaura reaction, *Turk. J. Chem.*, 37: 721-733.
- [27] Yılmaz, Ü. and Küçükbay, H. (2018). The catalytic effects of in situ prepared N-heterocyclic carbenes from benzimidazole salts in Suzuki–Miyaura cross-coupling reaction and uses in catalytic preparation of 1,3,5-triphenyl-1,3,5-triazinane-2,4,6-trione from phenyl isocyanate, *Turk. J. Chem.*, 42: 1706-1719.
- [28] Küçükbay, H., Yılmaz, Ü., Şireci, N. and Güvenç, N. (2011). Synthesis and antimicrobial activities of some bridged bis-benzimidazole derivatives, *Turk. J. Chem.*, 35: 561-571.



## Evaluation of Noise Emission in a Textile Plant

Zekeriya DURAN<sup>1</sup>, Mehmet GENÇ<sup>2\*</sup>, Tuğba DOĞAN<sup>3</sup>, Bülent ERDEM<sup>4</sup>

<sup>1</sup>Department of Drilling Program, Sivas Technical Sciences Vocational School, Sivas Cumhuriyet University, Sivas, Turkey.

<sup>2</sup>Department of Drilling Program, Hekimhan Mehmet Emin Sungur Vocational School, Malatya Turgut Özal University, Malatya, Turkey.

<sup>3</sup>Department of Industrial Engineering, Engineering Faculty, Sivas Cumhuriyet University, Sivas, Turkey.

<sup>4</sup>Mining Engineering Department, Engineering Faculty, Sivas Cumhuriyet University, Sivas, Turkey.

(Received: 13.05.2020; Accepted: 27.05.2020)

**ABSTRACT:** The textile industry is characterized by the use of complicated machinery in mass production methods in order to meet increased consumption demands. This situation brings with it some issues for the employees. Many of the machines used in the textile industry are operating at high noise levels. In this study, noise measurements taken from dyeing/finishing and weaving divisions in an integrated textile plant in Malatya city, Turkey were evaluated. Frequency distribution of dominant noise is also examined. Workers in the weaving division were exposed to higher levels of noise than those in dyeing/finishing. Accordingly, the noise level in weaving ranged from 99.2 to 101.1 dBA, while that in dyeing/finishing ranged from 77.1 to 79.3 dBA. It is also outside the 4000 Hz frequency zone, where the dominant frequencies of the maximum noise levels exposed by those working in the measured divisions fall in the middle frequency range to which the ear is most sensitive. Considering the frequency distribution, noise levels in the 4000 Hz region are calculated to be between 84.2 and 86.8 dBA in the weaving division and 60.0 to 61.9 dBA in the dyeing/finishing division. A noise histogram showed that noise in the weaving division had spread over a wider range than the dyeing/finishing division.

**Keywords:** Noise exposure, 1/3 octave band frequency, spectral analysis, frequency-noise relationship, textile plant.

### 1. INTRODUCTION

A negative working environment can lead to physical and mental health problems. Today, despite technological achievements, noise in the workplace stands up before us as a health problem. The textile industry is one of the most important locomotives of employment and foreign trade in Turkey. Production in the textile sector is based largely on human power. Workers employed in this sector may be exposed to significant noise in their workplaces.

Health is defined by the World Health Organization (WHO) "*a state of complete physical, mental and social well-being and not merely the absence of disease or infirmity*" The purpose of occupational health is that of employees; maximizing and maintaining physical, mental, and

\*Corresponding Author: mehmet.genc@ozal.edu.tr

ORCID number of authors: <sup>1</sup> 0000-0002-9327-8567, <sup>2</sup> 0000-0002-9950-0720

<sup>3</sup> 0000-0002-2628-4238, <sup>4</sup> 0000-0002-1226-9248

social well-being situations, placing them in jobs appropriate to their characteristics and risk factors in the workplace environment, ensuring protection from the risk factors harmful to health caused by working conditions and work environment. The working time of the employee in the workplace, the wage he received, the ways of paying wages, leave, etc. matters constitute the working conditions. The factors that are the sources of physical, chemical, biological, ergonomic and psychosocial factors that affect the health of the employee directly or indirectly, instantly or after a certain period in the production process constitute the working environment.

Sound can be measured and is an objective concept whose existence does not change depending on the person. Noise is a subjective concept. Noise can be defined as “unpleasant, unwanted, disturbing sound” [1]. Not every vibration in the ear is perceived as sound. Sound levels a human ear can detect are between 20 Hz and 20 kHz frequency limits [2, 3]. The human ear is not equally sensitive to all sound frequencies in this range, but is generally more sensitive to high frequency sound than low frequency sound. This sensitivity is greatest for sound frequencies between 2000 Hz - 5000 Hz. The frequency of sound to which the ear is most sensitive is 4000 Hz [4, 5].

A normal conversation is in the frequency range of 200 Hz - 10000 Hz. As can be seen, the frequency range to be examined is very wide and the use of fixed width bands is quite time-consuming in many cases. For this reason, the frequency range that should be examined in sound analysis is divided into sections called octave bands. 1/1 octave range is sufficient for analysis [6, 7]. There are different approaches in the literature to define the frequency ranges that the human ear can hear as low, medium and high. Frequencies below 200 Hz are low frequency sound, frequencies from 200 Hz to 2000 Hz are medium frequency sound and >2000 Hz frequency, high frequency sound [8]. Some researchers called sounds less than 200 Hz as low frequency sound [9-11]. Effective in personal protection, the noise intensity of the headphones; 30 dBA at low frequencies and 50 dBA at high frequencies. Similarly, polyurethane plugs placed in the outer ear canal are known to reduce by 25 dBA at low frequencies and 40 dBA at high frequencies [12].

Noise may cause hearing loss, nervous system and circulatory system disorders and disturbed hormonal balance. Another common negative effect of noise is sleep loss. It has also been stated that if one is exposed to noise for a prolonged time, it causes changes (dilatation) in heartbeat, blood pressure and respiration and it affects uric acid and lipid levels in the blood [13]. The potential negative effects of noise on human health are listed in Table 1.

**Table 1.** Noise levels and disturbances caused [14, 15]

Noise level	Sound pressure (dBA)	Effects on human health
1	30–65	Discomfort, anger, passion, sleep disturbance and concentration disorder, feeling of boredom
2	65–90	Physiological reactions; increased blood pressure, blood circulation disturbance, increased heart rate and breathing, decreased pressure in brain fluid, sudden reflexes, stress
3	90–120	Physiological reactions and headaches
4	120–140	Continuous damage to the inner ear, disruption of balance
5	>140	Serious brain damage, burst eardrum

The Occupational Safety and Health Administration of the USA (OSHA) sets the permissible exposure limit (PEL) of 90 dBA for all workers for an 8-hour day. But, where workers are exposed to a time-weighted average noise level of 85 dBA or higher over an 8-hour work shift,

OSHA mandates employers to implement a hearing conservation program in order to protect all workers in general industry. The “*Directive 2003/10/EC of the European Parliament and of the Council on the Minimum Health and Safety Requirements Regarding the Exposure of Workers to the Risks Arising from Physical Agents (Noise)*” [16] and the “*Regulation on the Protection of Workers from Risks Related to Noise*” issued by the Ministry of Labor and Social Security (MoLSS) both set the legal limits on noise exposure in the workplace, as follows [17]. It should be noted that the values are based on a worker's time-weighted average over an 8-hour day.

- a) Lower exposure action values: ( $L_{EX,8h}$ ) = 80 dBA or ( $P_{Peak}$ ) = 112 Pa (135 dBC in relation to 20  $\mu$ Pa).
- b) Higher exposure action values: ( $L_{EX,8h}$ ) = 85 dBA or ( $P_{Peak}$ ) = 140 Pa (137 dBC in relation to 20  $\mu$ Pa).
- c) Exposure limit values: ( $L_{EX,8h}$ ) = 87 dBA or ( $P_{Peak}$ ) = 200 Pa (140 dBC in relation to 20  $\mu$ Pa)

In a study conducted to determine the noise level of the weaving and yarn divisions in three textile factories in the Çukurova Region, the relationships between noise and frequency were examined. It is stated that the sound pressure level emitted by weaving machines is 78.3 to 100.8 dB, and 74.7 to 90.3 for spinning machines. It was also stated that the sound pressure level emitted by weaving machines ranged from 87.7 to 98.1 dB at the frequency of 4000 Hz, which the human ear was most sensitive, and 81.2 to 88.8 dB in spinning machines. It was stated that while the equivalent noise levels emitted by weaving machines ranged from 97.1 to 105.5 dBA, these values were between 89.7 and 93.9 dBA for spinning machines [18]. In another study, the sound level in the environment where the looms were located varied between 86 - 96 dBA indicating to high noise levels. It was commented that 35 % of the employees working for 20 years in the current 96 dBA sound environment would be deaf, unless necessary and correct measures were taken [19].

The study of Talukdar where one-minute exposure to sound levels above 100 dBA was emphasized, provided supportive results. It was concluded that noise exposure could cause permanent hearing loss. Besides, it was emphasized that textile workers, particularly weavers, suffered from occupational hearing loss [20]. In another study, it was stated that with the technological development, the noise level in the textile industry became a serious issue and an important occupational hazard. In some textile factories the maximum noise level has increased up to 95 dB, and the noise level has increased by an additional 5 dB with the combination of many machines. In another study the noise level inside the coating facility of a textile factory was measured experimentally and a noise emission model was developed [21]. Noise measurements were taken by ISO 9612 standard from various units in a textile plant and isobaric noise curves were drawn in the SURFER package.

The sound pressure level in the cotton beating unit was 79 dBA to 87 dBA, the average sound pressure level of the carding machines was 86 dBA at the frequency of 1000 Hz. It was also stated that the highest sound pressure level and dominant frequency in mixing were between 80 dBA and 250 Hz, and 86 dBA to 95 dBA in the cotton spinning unit, respectively [22]. Noise level was measured and analyzed with the MATLAB package at a textile factory in Ethiopia. It was concluded that spinning and weaving divisions were potential sources of noise [23]. In a textile company operating in the city of Uşak, noise measurements were taken and a questionnaire was applied to the employees. After examining the data the noise level was determined as 97.08 dBA. Supported with the survey results it was concluded that high noise

level reached could lead to permanent hearing losses, poor performance and low productivity in the workplace [24].

This study aimed to evaluate the noise exposure of workers in a textile plant in Malatya City. For this purpose, noise measurements were taken at different divisions and  $\frac{1}{3}$  octave frequency analysis was performed. The study also entails corrective measure suggestions in the case of excessive personal exposure to noise.

## 2. MATERIAL AND METHODS

In the textile plant, noise measurements were carried out following TS EN ISO 9612-2009 “Acoustics - Determination of acoustic-occupational noise exposure - Engineering method” and TS 2607 ISO 1999 “Acoustics - Determination of occupational noise exposure and estimation of noise-induced hearing impairment”. However, following the permit agreement with the workplace management upon taking noise measurements, the physical details of the workplace layout can only be given in a simple sketch (Figure 1). In the layout of the plant, the weaving division and the dyeing/finishing division were separated into insulated sections. Thus, the noise generated in each unit did not affect the other division.

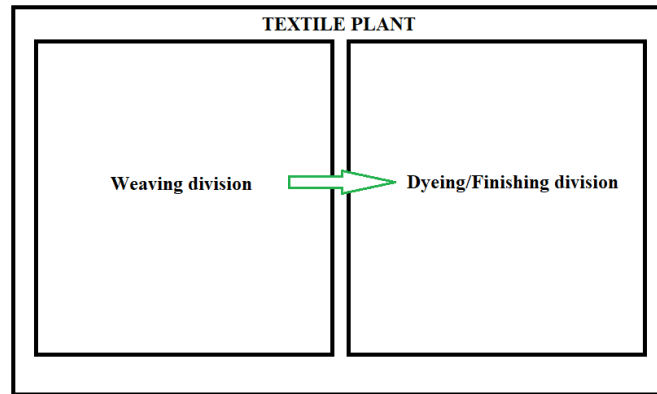


**Figure 1.** The textile plant layout.

The daily exposure level of employees ( $L_{EX-8h}$ ) was calculated based on noise measurements taken in accordance with these standards. The root mean square (RMS) of the frequency-weighted sound pressure values was defined. The frequency-noise relationship was derived.

Noise measurements were carried out using a high-precision noise level measuring device suitable for all noise measurements included in the “Regulation on the Assessment and Management of Environmental Noise” by the Ministry of Environment and Urbanization [25]. The noise meter also meets the requirements stipulated in the IEC 61672-1: 2002 Standard and has an internal  $\frac{1}{3}$  octave band filter for frequency analysis (Figure 2). Noise measurements were made with A, C and Z (linear) frequency weighting by defining three different profiles.



**Figure 2.** Noise level measuring device used in studies [25].

### 3. RESULTS AND DISCUSSION

Noise measurements were taken in the dyeing/finishing division and weaving division of a textile plant, located in Malatya City. The sound pressure employees were exposed to was measured using A, C (peak) and Z-weighted filters. The noise parameters measured and calculated in accordance with the relevant standards are given in Table 2. The equivalent continuous sound level ( $L_{Aeq}$ ) and the daily personal noise exposure ( $L_{EP,d}$ ,  $L_{EX,8hr}$ ) are given in Figure 3, where the minimum and maximum exposure action values and the exposure limit value are indicated. Evaluation of noise data has shown the following results.

- a) A-weighted, C-weighted and Z-weighted  $L_{EX,8h}$  in weaving division ranged from 99.2 dBA to 101.1 dBA, 100.4 dBC to 102.8 dBC and 100.6 dBZ to 103.1 dBZ, respectively.
- b)  $L_{EX,8h}$  in the weaving division is above the 85 dBA of the highest exposure action value specified in the relevant regulation.
- c) There is a maximum of 1 dB difference between A-weighted, C-weighted and Z-weighted noise levels in the weaving division.
- d) The dominant frequency of noise generated in the weaving division is around 1000 Hz.
- e) There is a potential for workers in the weaving department to experience increased physiological reactions and headaches as a result of noise exposure.
- f) A-weighted, C-weighted and Z-weighted  $L_{EX,8h}$  in dyeing/finishing division ranged from 77.1 dBA to 79.3 dBA, 82.4 dBC to 84.6 dBC and 83.1 dBZ to 85.2 dBZ, respectively. Figure 3 illustrates noise levels during operations in various divisions of the textile plant.
- g)  $L_{EX,8h}$  in dyeing/finishing division is below the 85 dBA of the highest exposure action value specified in the relevant regulation.
- h) Considering the  $L_{EX,8h}$  in dyeing/finishing division, the sound pressure difference between A-weighted, C-weighted and Z-weighted exposures is 5 dB at maximum, while the difference between C-weighted and Z-weighted exposures is around 1 dB.
- i) The  $L_{EX,8h}$  in dyeing/finishing division is approximately 20 dBA higher than that in the weaving division.
- j) The dominant frequency of noise generated in the dyeing/finishing division ranges between 400 Hz and 1200 Hz.
- k) There is a potential for workers in the dyeing/finishing division to experience exaggeration of reflexes (hyperreflexia), physiological reactions, increased blood pressure, increased heart rate, increased breathing and low cerebrospinal fluid (CSF) pressure as a result of noise exposure.
- l) Weaving division and dyeing/finishing division and noise histograms are given in Figure 4a and Figure 4b. The noise range in the dyeing/finishing division area is wider than the weaving division.
- m) Considering the frequency-noise relationship given in Figure 5, it is revealed that the dominant noise levels are in the middle frequency range. Therefore, the noise levels in the 4000 Hz frequency region, where the human ear is most sensitive, range between 84.2 dBA to 86.8 dBA in the weaving division and 60.0 dBA to 61.9 dBA in the dyeing/finishing division.

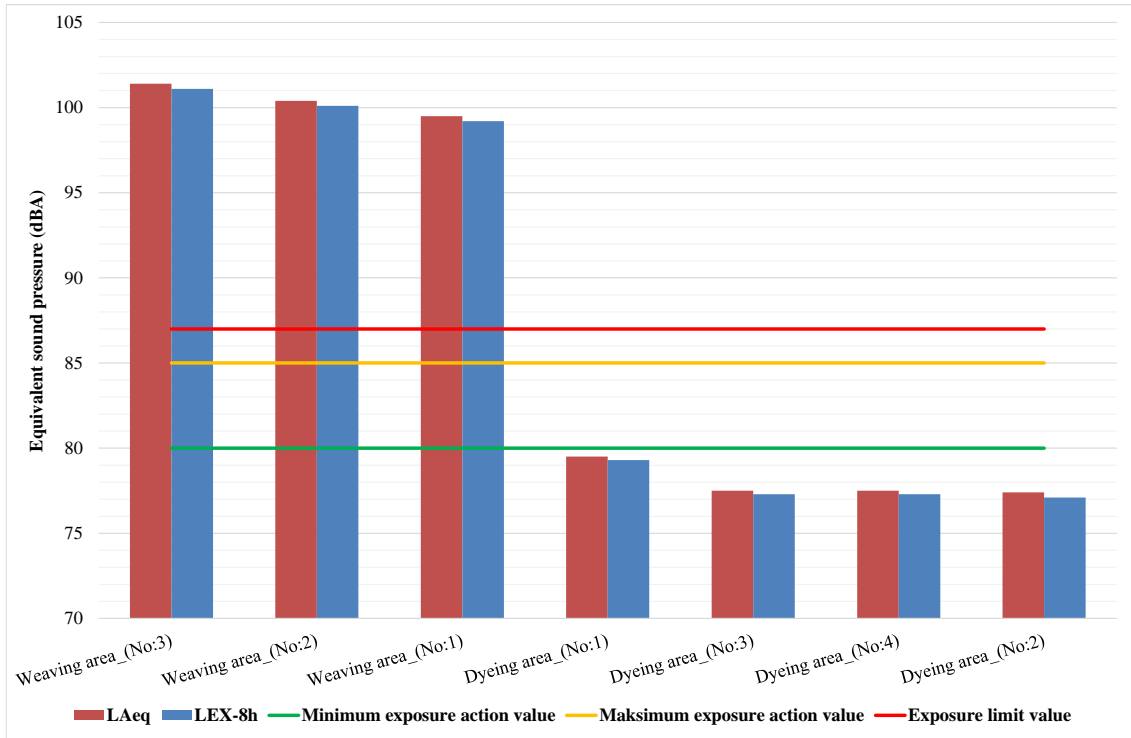


Figure 3. Noise levels during operations in the textile plant.

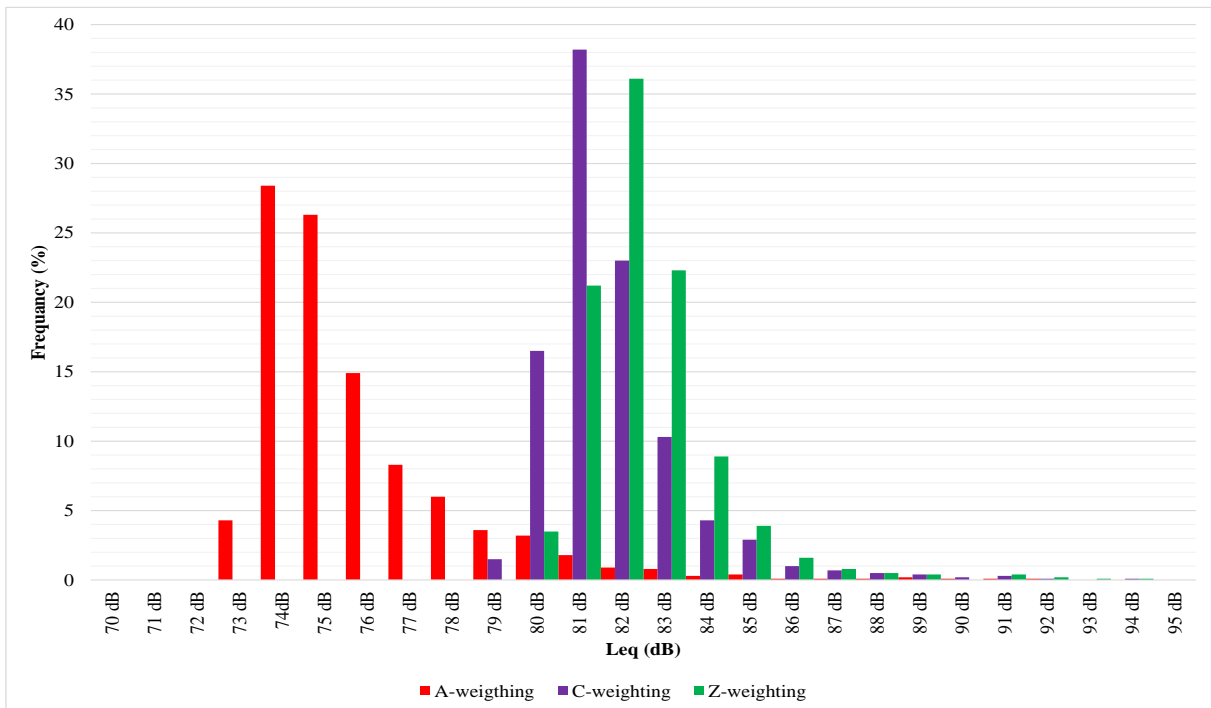


Figure 4a. Weaving division noise histogram

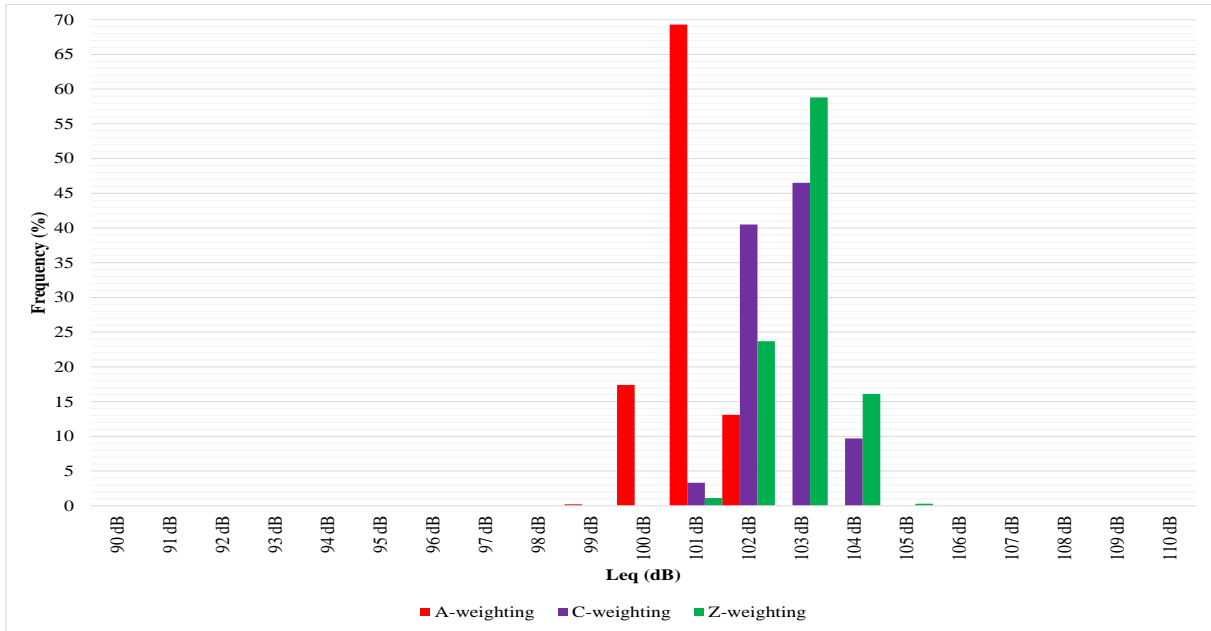


Figure 4b. Dyeing/finishing division noise histogram

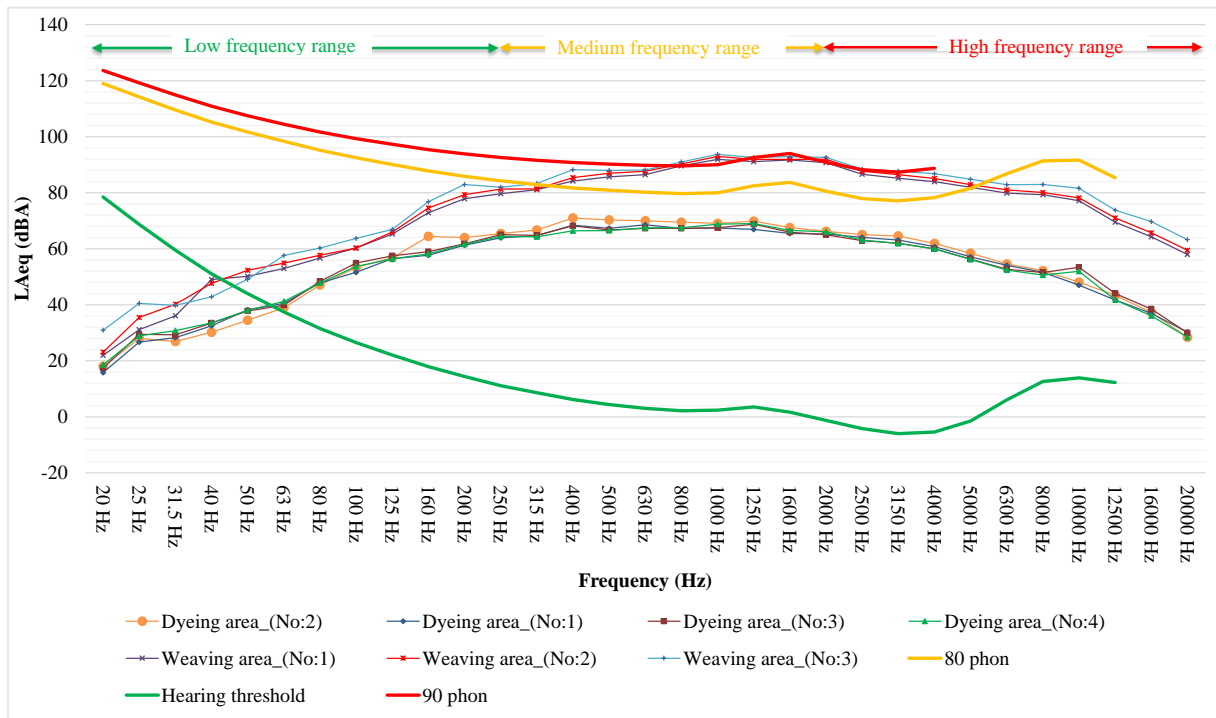


Figure 5. Frequency distribution of noise levels during operations of the textile plant.

#### 4. CONCLUSIONS

In this study, noise measurements taken from the weaving division and dyeing/finishing division in a textile plant were evaluated. In the light of the evaluations, the following conclusions were reached.

- a) The noise levels ranged from 99.2 dBA to 101.1 dBA in the weaving division, while in the dyeing/finishing division it ranged from 77.1 dBA to 79.3 dBA.
- b) Personnel working in the dyeing/finishing division are not required to use personal protective equipment.
- c) Personnel working in the weaving division, on the other hand, can only work for a maximum of 12 minutes without ear protectors in accordance with the relevant regulation. After this period, they should wear hearing protectors.
- d) The dominant frequencies of noise to which the staff working in the textile plant are exposed to are lower than 4000 Hz, which the ear is the most sensitive.
- e) Every effort should be made to reduce the noise level at its source in the weaving division. But, all ways to separate people from potentially damaging causes of noise are exhausted, workers must be provided with the correct personal hearing protectors. It must be noted that this equipment can be used as a temporary measure or the last resort.
- f) The noise level in the weaving division is higher than 85 dBA, which is the highest exposure action value specified in the relevant regulation. Employees may experience hearing loss, hearing-related health problems and loss of productivity at work.

**Table 2.** Noise parameters for the textile plant

Division	Round of measurement	Average time mm:ss	Filter detector	L <sub>peak</sub> (dB)	L <sub>max</sub> (dB)	L <sub>min</sub> (dB)	SPL (dB)	L <sub>eq</sub> (dB)	SEL (dB)	L <sub>10</sub> (dBA)	L <sub>50</sub> (dBA)	L <sub>90</sub> (dBA)	L <sub>EX,8h</sub> (dBA)	Working time (h)	Dominant frequency range (Hz)
<b>Dyeing/finishing</b>	1	05:04	A, Fast	102.2	88.4	77.2	79.2	79.5	104.4	81.4	78.5	77.6	<b>79.3</b>	<24.0	400-1250
			C, Fast	103.0	91.5	82.6	84.0	84.9	109.7	86.3	84.4	83.2	84.6		
			Z, Fast	102.8	91.6	83.2	84.6	85.4	110.3	86.8	85.0	83.9	85.2		
	2	05:27	A, Fast	103.5	92.4	73.5	75.5	77.4	102.5	79.5	75.6	74.2	<b>77.1</b>		
			C, Fast	106.2	94.5	79.6	81.8	82.7	107.8	84.1	81.8	80.5	82.4		
			Z, Fast	106.9	94.7	80.3	82.3	83.4	108.5	84.7	82.7	81.3	83.1		
	3	05:06	A, Fast	99.3	86.7	74.8	76.8	77.5	102.3	79.4	76.6	75.4	<b>77.3</b>		
			C, Fast	102.9	90.6	80.9	83.0	83.4	108.3	84.8	83.1	82.0	83.2		
			Z, Fast	104.0	91.1	81.7	83.9	84.3	109.2	85.7	84.0	82.8	84.1		
	4	05:04	A, Fast	106.0	93.3	74.8	76.7	77.5	102.3	78.2	76.9	76.0	<b>77.2</b>		
			C, Fast	108.0	94.9	80.9	83.0	83.0	107.8	83.9	82.7	81.6	82.7		
			Z, Fast	108.0	95.0	81.6	84.3	84.0	108.8	85.2	83.7	82.4	83.7		
<b>Weaving</b>	1	05:05	A, Fast	114.7	100.3	98.5	99.5	99.5	124.3	99.9	99.5	99.0	<b>99.2</b>	0.3	
			C, Fast	115.3	101.6	99.8	100.7	100.7	125.5	101.4	100.6	100.0	100.4		
			Z, Fast	115.7	101.8	100.0	100.9	100.9	125.8	101.7	100.8	100.1	100.6		
	2	05:06	A, Fast	114.7	101.3	99.6	100.8	100.4	125.3	100.9	100.4	100.0	<b>100.1</b>		
			C, Fast	115.7	102.8	100.6	102.0	101.7	126.6	102.5	101.6	101.0	101.4		
			Z, Fast	116.1	103.0	100.8	102.2	101.9	126.8	102.7	101.8	101.1	101.6		
	3	05:04	A, Fast	116.9	102.8	100.0	101.1	101.4	126.3	102.2	101.4	100.5	<b>101.1</b>		
			C, Fast	117.7	105.0	101.4	102.6	103.1	127.9	103.9	103.1	102.1	102.8		
			Z, Fast	118.4	105.2	101.7	102.9	103.4	128.2	104.3	103.4	102.3	103.1		

## NOMENCLATURE

- dB** : A relative unit of measure widely used in acoustics, electronics and communications.
- dBA** : A voice evaluation unit in which the human ear is particularly sensitive to medium and high frequencies.
- dBC** : A voice evaluation unit that correlates better with the human response to high noise levels.
- dBZ** : A voice evaluation unit implying no weighting (zero-frequency weighting) across the audio spectrum.
- $L_{EX, 8h}$**  : The sound exposure averaged over 8 hours ( $L_{EP,d}$ )
- $L_{max}$**  : Maximum sound level
- $L_{min}$**  : Minimum sound level
- $L_{peak}$**  : Peak sound pressure
- SPL** : Sound pressure level
- $L_{eq}$**  : Equivalent sound level
- SEL** : Sound exposure level
- $L_{10}$**  : The noise level just exceeded for 10% of the measurement period
- $L_{50}$**  : The noise level just exceeded for 50% of the measurement period
- $L_{90}$**  : The noise level just exceeded for 90% of the measurement period

## REFERENCES

- [1] Seçkiner, S.U., & Kurt, M. (2004). Ofis Güvenliğinin Değerlendirilmesi İçin Geliştirilmiş Ergonomi Teknolojisi: Kairos, Örnek Uygulama. Gazi Üniv. Müh. Mim. Fak. Der, 19(1), 37-38.
- [2] Broch, J.T., (1973). Application of B & K Equipment to Mechanical Vibration and Shock Measurement. Copenhagen.
- [3] Wereski, M., (2015). The Threshold of Hearing, The STEAM Journal: <http://scholarship.claremont.edu/steam/vol2/iss1/20>, 1-6.
- [4] Alberti, W., (2001). *The anatomy and physiology of the ear and hearing*, in Occupational Exposure to Noise: Evaluation, Prevention and Control, 53-63.
- [5] Heather, S., (2014). *The science of hearing*, [http://www.simonheather.co.uk/pages/articles/science\\_hearing.pdf](http://www.simonheather.co.uk/pages/articles/science_hearing.pdf).
- [6] Grandjean, E., (1988). Fitting the Task to the Man A Text Book of Occupational Ergonomics, Taylor & Francis Ltd, London.
- [7] Sanders, M.S., McCormick, E.J., (1992). Human Factors in Engineering and Design. McGraw-Hill international Editions, Psychology Series, Singapore.
- [8] WEB1, (2020). [https://www1.health.gov.au/internet/main/publishing.nsf/content/A12B57E41EC9F326CA257BF0001F9E7D/\\$FILE/health-effects-Environmental-Noise-2018.pdf](https://www1.health.gov.au/internet/main/publishing.nsf/content/A12B57E41EC9F326CA257BF0001F9E7D/$FILE/health-effects-Environmental-Noise-2018.pdf)
- [9] Leventhall, H.G., (2004). Low frequency noise and annoyance, Noise & Health, 6;23, 59-72.

- [10] Brodin, K., Bluhm, G., Eriksson, G., Nilsson, M. E., (2011). Infrasound and Low Frequency Noise From Wind Turbines: Exposure and Health Effects, *Environmental Research Letters*, 035103, 6.
- [11] Alves, J.A., Silva, L.T., Remoaldo, P.C., (2015). The Influence of Low-frequency Noise Pollution on the Quality of Life and Place in Sustainable Cities: A Case Study from Northern Portugal, *Sustainability*, 7(10), 13920-13946.
- [12] Güler, Ç., Çobanoğlu, Z., (2001). *Gürültü*, Çevre sağlığı temel kaynak dizisi No: 19, 43.
- [13] Ekerbiçer, H.Ç., Saltık A., (2008). Endüstriyel Gürültünün İnsan Sağlığı Üzerine Etkileri ve Korunma Yöntemleri, *TAF Prev. Med Bull*, 7(3), 261-264.
- [14] Fişne, A. (2008). Türkiye Taşkömürü Kurumu ocaklarında gürültü koşullarının incelenmesi, etkilenme düzeylerinin istatistiksel analizi ve risk değerlendirmesi. İstanbul Teknik Üniversitesi Fen Bilimleri Enstitüsü (Doktora Tezi), 217s, İstanbul.
- [15] Bilgili, S., Gürtepe, E., Türkel, E., Altınoluk, H. M., Hüsmen, N., Bütün, A., Ertorun, H. (2011). Çevresel gürültü ölçüm ve değerlendirme kılavuzu. Çevre ve Orman Bakanlığı Çevre Yönetimi Genel Müdürlüğü, Hava Yönetimi Dairesi Başkanlığı, 106s, Ankara.
- [16] EU. (2003). Directive 2003/10/EC of the European Parliament and of the Council on the Minimum Health and Safety Requirements Regarding the Exposure of Workers to the Risks Arising from Physical Agents (Noise). European Parliament, <https://eur-lex.europa.eu/legal-content/EN/TXT/?uri=CELEX:02003L0010-20081211#E0011>, Last accessed: 21.05.2020.
- [17] MoLSS. (2013). Regulation on the Protection of Workers from Risks Related to Noise. The Ministry of Labor and Social Security, [www.mevzuat.gov.tr](http://www.mevzuat.gov.tr); Last accessed: 21.05.2020.
- [18] Ege, F., Sümer, S.K., Sabancı, A., (2003). Tekstil Fabrikalarında Gürültü Düzeyi ve Etkileri, *Türk Tabipler Birliği Mesleki Sağlık ve Güvenlik Dergisi*, 30-39.
- [19] Babalık, F., (2003). İş yerlerinde gürültü ve sağrlık olasılığı, II. İş Sağlığı ve Güvenliği Kongresi, Adana.
- [20] Talukdar, M.K., (2001). Noise pollution and its control in textile industry, *Indian Journal of Fibre and Textile Research* 26(1):44-49.
- [21] Jayawardana, T.S.S., Perera, M.Y.A., Wijesena G.H.D., (2014). Analysis and control of noise in a textile factory, *International Journal of Scientific and Research Publications*, 4(12), ISSN 2250-3153, 1-7.
- [22] Golmohammadi, R., Monazzam, M.R., Zahra Hashemi, Z., Fard S.M.B., (2014). Pattern Evaluation of Noise Propagation at Various Units of a Textile Industry, *Caspian Journal of Applied Sciences Research*, 3(6), 1-8.
- [23] Ejigu, M.A., (2020). Excessive Sound Noise Risk Assessment in Textile Mills of an Ethiopian Kombolcha Textile Industry Share Company, *Int. J. Res. Ind. Eng. Vol. 8, No. 2*; 105–114.
- [24] Ulukaya, F., Çögenli, M.Z., (2020). Gürültülü Çalışma Ortamının Çalışanlar Üzerindeki Psikososyal Etkilerinin İncelenmesi: Tekstil Sektöründe Ampirik Bir Çalışma, *Anadolu Akademi Sosyal Bilimler Dergisi*, 131-140.
- [25] Svantek, (2013). Svan 971 Pocket-size Sound Level Meter&Analyser User Manual, SVANTEK SP. Z O.O., 57 pp, Warsaw, Poland.